

**Treating supersymmetric systems using the functional
renormalization group**

Dissertation

**zur Erlangung des akademischen Grades
"‘doctor rerum naturalium"’ (Dr. rer. nat.)**

**vorgelegt dem Rat der Physikalisch-Astronomischen-Fakultät
der Friedrich-Schiller- Universität Jena**

von M.Sc. Tobias Hellwig

geboren am 03.12.1986 in Lutherstadt Eisleben

Gutachter

1. Prof. Andreas Wipf, Jena
2. Prof. Jan Pawlowski, Heidelberg
3. Prof. Gian Paolo Vacca, Bologna

Tag der Disputation: 20.12.2016

Contents

| | |
|--|-----------|
| 1. Introduction | 9 |
| 2. Technical Introduction | 14 |
| 2.1. Notes on the FRG | 14 |
| 2.2. Notes on Supersymmetry | 16 |
| 2.3. Introduction to the shooting method | 17 |
| 2.4. The spectrum of perturbations | 22 |
| 2.4.1. Another shooting method | 23 |
| 3. Supersymmetric Quantum Mechanics | 25 |
| 3.1. Introduction | 25 |
| 3.2. The Model | 26 |
| 3.2.1. The flow equations | 27 |
| 3.3. Unbroken Supersymmetry | 28 |
| 3.4. Broken supersymmetry | 33 |
| 3.5. Summary | 35 |
| 4. The Wess-Zumino model | 36 |
| 4.1. The model in $d = 2, 3$ | 36 |
| 4.1.1. Special fluctuations | 39 |
| 4.1.2. $d = 3$ | 40 |
| 4.1.3. $d = 2$ | 42 |
| 4.2. Critical dimensions | 44 |
| 4.3. Spikes from polynomials | 47 |
| 4.4. Critical exponents from different methods | 51 |
| 4.5. Summary | 56 |

| | |
|---|-----------|
| 5. Emergent supersymmetry | 57 |
| 5.1. Introduction | 57 |
| 5.2. Rewriting the Yukawa model | 58 |
| 5.3. Setting V_0 to a constant | 60 |
| 5.4. Neglecting h | 61 |
| 5.5. Adaptive flow F_k | 63 |
| 5.5.1. Not one loop exact | 64 |
| 5.5.2. One loop exact | 66 |
| 5.6. Summary | 69 |
| 6. The $O(N)$ model | 71 |
| 6.1. Formulation of the theory | 71 |
| 6.2. The large N results | 73 |
| 6.3. Polynomial expansions around the minimum | 73 |
| 6.3.1. The case of LPA | 74 |
| 6.3.2. The case of LPA' | 77 |
| 6.3.3. NLO truncation | 78 |
| 6.4. The shooting method | 79 |
| 6.4.1. Starting at $\rho = 0$ | 79 |
| 6.4.2. Starting at $\rho > 0$ | 80 |
| 6.5. N close to one | 81 |
| 6.6. $d < 3$ | 84 |
| 6.7. summary | 86 |
| 7. Conclusion | 89 |
| A. Appendix | 91 |
| A.1. Shooting Example | 91 |
| A.2. Superspace formulation | 91 |

Summary

As supersymmetry is a theory with very interesting properties, we want to approach it using an FRG formulation. Therefore, we deal with supersymmetric flow equations in the scope of this work. This thesis is organized in two main parts.

In the first few chapters we apply techniques well known from bosonic models in the framework of our supersymmetric formulation of the FRG. By doing so we establish the means to discuss physically more relevant models. We start with supersymmetric quantum mechanics and use those as a testing ground for the derivative expansion. In passing we also investigate the flow equations in the spontaneously broken phase and highlight the difference to the unbroken ones. In a next step we use the shooting method to calculate the fixed-point solution in LPA' of the $\mathcal{N} = 1$ Wess-Zumino model in two and three spacetime dimensions. We discuss the polynomial expansion around zero and how the Ising fixed point can be found using this technique. The spectra of the fixed points is given and the different implementations of a variation of the anomalous dimension along those fluctuations is discussed.

In the second part of this work we turn toward phenomenologically more relevant topics. The first is emergent supersymmetry. We study a Yukawa theory and show how employing the supersymmetric techniques and flows the emergence of supersymmetry shows up. We find that the spectrum of a fixed point of such a theory should decompose into a supersymmetric part and an explicitly supersymmetry breaking part. This is true as long as the fixed-point couplings are supersymmetric. The last part of this work is dedicated to the investigation of the supersymmetric $O(N)$ model in three spacetime dimensions. A lack of a global fixed-point solution emerges. In order to see this we employ a polynomial expansion as well as the shooting method. We present the results up to order LPA'. We shed some light on the results by discussing the critical dimension of the model.

Zusammenfassung

Supersymmetrie ist eine Theorie die fortwährendes Interesse auf sich zieht. Aus diesem Grund wird im Rahmen dieser Arbeit die funktionale Renormierungsgruppe (FRG) verwendet um aus diesem Blickwinkel Einblicke zu gewinnen. Die Arbeit ist zweigeteilt:

Im ersten Abschnitt diskutieren wir technische Aspekte und untersuchen die Anwendbarkeit von Techniken bekannt aus bosonischen Theorien. Wir befassen uns mit supersymmetrischer Quantenmechanik und diskutieren in diesem Rahmen die Ableitungsentwicklung. Des Weiteren wird der Unterschied zwischen supersymmetrischen Flussgleichungen in der symmetrischen und spontan gebrochenen Phasen herausgearbeitet. Danach wenden wir uns den Wess-Zumino Modellen in zwei und drei Raumzeit Dimensionen zu. Wir verwenden ein Schießverfahren um die Fixpunktlösungen zu bestimmen. Zusätzlich beschreiben wir, wie eine polynomielle Entwicklung um den Ursprung es erlaubt, den Ising Fixpunkt zu finden. Wir geben die Spektren der Fixpunkte und untersuchen den Einfluss verschiedener Implementierungen der Variation der anomalen Dimension.

Im zweiten Abschnitt wenden wir uns experimentell physikalisch relevanteren Themen zu. Wir starten mit emergenter Supersymmetrie. Eine Yukawa Theorie wird umformuliert und, mittels der Techniken bekannt von den supersymmetrischen Theorien, das Auftauchen der Supersymmetrie gezeigt. Es zeigt sich, dass das Spektrum der Theorie aus einem supersymmetrischen und einem explizit Supersymmetrie brechenden Teil besteht. Wir sehen dies, so lange der Fixpunkt Kopplungen aufweist, die Supersymmetrie erlauben. Abschließend betrachten wir das supersymmetrische $O(N)$ Model in drei Raumzeit Dimensionen. Wir zeigen mittels polynomieller und Schieß-Verfahren, dass kein globaler Fixpunkt existiert. Die Ergebnisse werden bis zur LPA' (lokale Potenzial Approximation) Trunkierung gegeben. Wir beleuchten diese Ergebnisse mit Hinblick auf die kritische Dimension des Models.

1. Introduction

With the emergence of today's picture of elementary particle physics and the fundamental forces of nature it remained unclear how or if gravity can be non-trivially combined with these forces [1]. In [2] and most strongly [3] no-go theorems were formulated that a bosonic symmetry will not be able to provide us with such a generalization.

In order to circumvent this problem fermionic symmetry operators were necessary [4]. This was the birth of supersymmetry [5, 6]. A symmetry that connects bosonic and fermionic degrees of freedom. Over the years a lot of useful applications of supersymmetry in works to enhance our understanding of fundamental processes of nature were found. String theory [7, 8], as an approach to formulate a fundamental UV complete theory, needs supersymmetry in most formulations to avoid, e.g., tachyonic states [9]. These arise for example if one formulates a purely bosonic string theory. One reason for the need of supersymmetry is the property that fermionic loops contribute with an opposite sign as bosonic ones and therefore a cancellation can occur [10, 11]. The latter work inspired the construction of the Wess-Zumino model [5]. These cancellations do also occur for the ground state energy calculation in supersymmetric models. This helps reducing the result for the cosmological constant from an QFT point of view and less fine tuning is necessary to match the observed one.

As complete as the standard model looks like from high energy collision experiments [12–17] we have indications of physics beyond the standard model. Planck data as well as astrophysical observations show that our current understanding of cosmology needs additional candidates for dark matter [18–25] as well as an explanation for dark energy [26]. Minimal supersymmetric theories provide a natural candidate for dark matter [27–29] if R parity is implemented. R parity [30–32] does not allow a decay of a superpartner into purely SM matter and therefore provides us with a stable particle that may fulfill the role of dark matter. Also for models of gauge unification, that is the standard model $SU(3)_c \times SU(2)_L \times U(1)_Y$ can be unified into one

gauge group, e.g. an $SU(5)$ [31, 33, 34] or $SO(10)$ [35–38]¹, supersymmetry is of relevance. A minimal extended standard model shows a running of the gauge couplings of the mentioned sectors in such a way that they meet at approximately one point. There the breaking of the higher symmetry could have taken place.

There are a lot of exclusion plots as given before but the unknown mechanism of a possible supersymmetry breaking provides a lot of free parameters which make it hard to make any falsifying statement [42–44]. The models of supersymmetry breaking are typically perturbative ones and it could be insightful to gather means in order to deal with strongly coupled supersymmetric systems. One problem is that supersymmetry on the lattice is in principle broken as no infinitesimal distance is present anymore due to the lattice spacing. It was shown that one can try to stick with a subset of supercharges and this seems to allow for keeping supersymmetry present in the thermodynamical limit [45–48]. Nonetheless, this is limited to systems with sufficient supercharges.

The case of supersymmetry has not to be limited to $d \geq 4$. It is possible to construct optical systems so that the wave equation is supersymmetric[49]. Therefore a supersymmetric theory is realized.

Also in lower dimensions supersymmetry is a valid symmetry that could show up in solid-state physics. In $d = 2$ there is a family of superconformal models. Especially the tricritical-Ising model, the second unitary minimal model, is isomorph to the first unitary minimal superconformal model [50, 51]. There supersymmetry is present in a physically relevant system.

Furthermore such a realization of supersymmetry at criticality has not to be limited to $d = 2$. In this work we look at $d = 3$ and confront ourselves with the possibility of a general Yukawa theory showing signs of supersymmetry²[52–56]. The inclusion of such a additional symmetry in calculations can prove helpful and provide a better understanding of the occurring phase transitions.

In order to do so we resort to a by now well established method, the functional renormalization group (FRG) in the form we are using firstly formulated by Wetterich [57] and shortly thereafter by Morris [58]. Over the last two decades a lot of time and work was spent on this method to treat strongly coupled non perturbative systems. There are other functional methods available for the treatment of such systems, e.g. Schwinger-Dyson equation ([59, 60, 60] or more recent

¹Although both $SU(5)$ (very strongly) and $SO(10)$ are constrained by proton decay results and measurements of its lifetime [39–41].

²As long as the field content allows in principal for supersymmetry.

[61]) or Polchinski equation [62, 63]. These methods do not have to compete with each other but may profit from the virtues each has in different situations. So it is possible to use results of one method as an input for another one [64].

The particular approach using the FRG equation in its one loop formulation we use has proven itself very successful. Problems in QCD [65–70], the Higgs-mass, and solid-state physics, were dealt with. Furthermore, it provided us with a efficient tool to study a new approach to quantum gravity, i.e. asymptotic safety [71–79]. The last even provided us with an approach how to understand the seemingly necessary dark energy from a different point of view [80, 81]. Higgs studies within the FRG approach provided us with a new explanation for the mass limits and elucidate the vacuum stability problem [82, 83].

In solid-state physics the common believe about the phase diagram in a honeycomb lattice was improved on and the phase structure clarified [84].

As we can see the method is flexible enough to treat a broad range of models. In general one can also treat problems that are within the range of perturbation theory but the numerical results are typically not comparable. The flexibility given by the method is often bought with the price that other methods can provide more significant digits in concrete calculations. But these methods are typically more specialized.

One can also treat supersymmetric theories with the FRG [85]. This is even possible for supersymmetric gauge theories as was shown in [86]. The trade-off in this case was between the number of degrees of freedom and the linear realization of the symmetries³. This work concentrates on the more easy case of mostly $O(1)$ and at the end also $O(N)$ theories in dimensions two and three. We always work at zero temperature and use an uniform field approximation. In [88] non-zero temperatures were taken into account.

Why should we be interested in these kind of systems? As mentioned before there is still a search for supersymmetry going on. An approach that can also deal with strongly coupled systems may come in handy when one is describing the breaking of supersymmetry. Especially it would allow us to reexamine some statements that were made from a perturbative point of view. In order to do so we feel that it is necessary to gain a better understanding of supersymmetric FRG formulations. Especially some work that has been done for bosonic models should be reinvestigated in the supersymmetric case.

³Note that the common Wess-Zumino gauge is not supersymmetry invariant. A gauge transformation is necessary to reestablish it [87].

How to formulate a converging derivative expansion [89–92]? How well are polynomial expansions and shooting methods doing [93, 94]? How do they compare with each other? Are these methods sufficient to compute the interesting part of the spectrum?

We do not only validate these tools but also obtain some new insights. Let us look at the scope of the work. We start with the introduction of some technical aspects that is used throughout this work. This consists of some words regarding the FRG. Here we point out some of the aspects we have to take care of and what we can expect from the used method.

As a next step aspects of supersymmetry are presented. This cannot be complete in any way but there is a lot of literature available to cover this subject. As we are only using a small subset of the general theory of supersymmetry we hope the small part given may prove sufficient.

As a last part we provide a technical explanation on the calculation of the later on introduced fixed points and the spectrum of their perturbations θ_i . We provide it as part of this work and not the appendix as it explains some differences noted in a previous work on Yukawa theories [56].

In the second chapter we think about a formulation of the derivative expansion in the case of a supersymmetric theory. We use a quantum mechanical toy model for the implementation in order to be able to compare our results with exact ones. We provide a way how to improve on a truncation in a systematic way and show that our ansatz does converge. As a second part we investigate some aspects of supersymmetry breaking. Especially a pitfall in possible calculations is pointed out.

After these initial steps we finally turn toward $d = 2, 3$ and study the Wess-Zumino model. We compute the fixed points in those models using the formerly described method. Some additional discussions on the spectrum of perturbations as well as other means to find fixed points are also presented. Also some insight into the critical dimensions for some couplings is provided.

Continuing from the knowledge we gained from examining the $d = 3$ Wess-Zumino model we deal with a more general Yukawa theory. We show that if the field content of the Yukawa theory is the same as the one of the Wess-Zumino model we can use the supersymmetric formulation of the flow equations to deal with it. We see the influence of supersymmetry on such a model. To do so we use a technique that was previously used in the context of four Fermi theories [64, 95] and is known there as dynamic bosonization.

After dealing for some prolonged time with $O(1)$ models we finally turn to the case of the

$O(N)$ models in $d = 3$. While extensive studies of the large N case can be found in the literature [96–98] little seems to be known for the finite N case. We try to close this gap. To understand our results we rely on the work on critical dimensions done before.

At the end of this work and each chapter we provide a summary of the results. Therefore, the summary at the end is quite short and does not pick up every detail that was already given at the end of the chapters. Instead we try to give a summary of the emergent picture and what can be learnt from the overall study. Also an outlook is presented at this point.

The compilation of this thesis is solely due to the author. However, a large part of the work presented here has been published in a number of articles and in collaboration with several authors. Chapter 2,4 and 5 rely on work done in collaboration with Andreas Wipf and Omar Zanusso. Chapter 3 is based on joined work with Marianne Heilmann, Benjamin Knorr, Andreas Wipf and Marcus Ansorg. Chapter 6 is founded on a collaboration with Marianne Heilmann and Andreas Wipf. The implemented Slac derivative formulation is using input provided by Andreas Wipf and Georg Bergner.

2. Technical Introduction

2.1. Notes on the FRG

As already mentioned we make use of an exact renormalization group method which is often called the Wetterich equation. Introduced in the early '90s, it has proven a quite powerful method to tackle different physical problems. The main idea goes back to Wilson [99] who introduced the Wilsonian renormalization group flow in 1971. The idea is to calculate quantum corrections step by step according to their energy or in other words the momentum they are carrying. This can be done in discrete or continuous steps, in the following we use the latter.

Let us make ourself familiar with the used equation. In Euclidean spacetimes it reads [57]

$$k\partial_k\Gamma_k[\Phi] = \frac{1}{2}\text{STr} \left(k\partial_k R_k (\Gamma_k^{(2)} + R_k)^{-1} \right). \quad (2.1.1)$$

On the left hand side we have the aforementioned parameter k that determines the energy scale which ranges typically from 0 to some UV cut-off scale Λ . Γ_k is the effective average action that is a functional of the averaged fields Φ and is changing with k according to above mentioned equation. At $k = 0$ we get the effective average action Γ_0 , which describes effectively interactions we may be interested in, after having integrated out every quantum fluctuation present in the system. On the right hand side we find the supertrace of a function of the second functional derivative of Γ_k with respect to the fields. The also found R_k is a regulator function that appears in the cut-off action $\Delta S_k = \frac{1}{2} \int \Phi R_k \Phi$ so that the denominator of (2.1.1) is the full 2-point function at the scale k modified by an Regulator, $\overset{\rightarrow}{\delta}_\Phi (\Gamma_k + \Delta S_k) \overset{\leftarrow}{\delta}_\Phi$. The choice of R_k is not unique as long as some requirements are matched. The reason that ΔS_k is quadratic in the fields goes back to the fact that one wants to obtain a one-loop exact equation as stated before.

In actual calculations one uses an effective action that only spans a subspace of the allowed theory space. The latter being determined by the field content and the symmetries. This is in order as in a generic scenario solving above equation is not possible from a practical point

of view. The procedure of limiting Γ_k is called choosing a truncation. There are different systematic truncation schemes one can use [100, 101]. Throughout this work we only deal with the so-called derivative expansion [89, 90]. The name stems from the fact that one is expanding in terms of derivatives. The leading order approximation is given by a potential plus a standard kinetic term. This could be expanded to the next level by allowing for a wavefunction renormalization and further more including also terms with more derivatives (e.g. ∂^4 in a bosonic theory [92]). Since we are lacking, in general, a systematic way of calculating the errors made by a truncation we can only try to estimate it. One way is to start with a low order truncation and go to higher truncation orders. Then monitor the changes. In an ideal case these quickly fall off and we may trust our results. This is similar to calculating a Taylor expansion of a function and trust the result when adding higher order terms does not change the result instead of calculating the preferred error estimate. In both cases there may also be a finite radius of convergence, limiting the range in which we may trust our results. A study of the convergence of the derivative expansion can be found in the chapter on supersymmetric quantum mechanics 3 .

As already pointed out the choice of R_k is not unique. A broad range of functions are allowed as long as they do respect some fundamental properties ¹ . This means without any truncation Γ_0 is only a function of Γ_Λ and independent of the choice of R_k . When we introduce a truncation this statement is not true as one can suspect. This implies that a reasonable choice of R_k probably improves the rate of convergence of the truncation scheme. One thing that comes to mind is to look at the internal symmetries of the given model. While it should be straightforward to implement the symmetry also in the effective average action at scales different from Λ this could be not the case for the cut-off action. Given a nonlinear symmetry the construction of an invariant quadratic term is generically impossible. But adding a term that does not respect the symmetry breaks the symmetry on the right hand side and therefore Γ_k for all $0 < k < \Lambda$. Thus, also very likely in an truncated scheme for $k = 0$ where we want to extract the informations about infrared physics. For this reason it is advisable to look out for a scheme in which the symmetry is realized in a linear way. This is how we proceed. If this is not possible one has to rely on more involved methods. For instance using a background field method [102–106] and using modified Ward-Takahashi identities [107–111] .

There are also other ways to optimize the regulator in some sense. [64, 112–115] But let us

¹These are in fact: $\lim_{k \rightarrow 0} R_k(q) \rightarrow 0$, $\lim_{k \rightarrow \Lambda \rightarrow \infty} R_k(q) \rightarrow \infty$, $\lim_{q \rightarrow 0} R_k(q) > 0$

turn a bit more to special points in theory space and their influence on flows as the change of Γ_k along k is named. Here going along the flow means going to smaller k . Due to the form of the flow equation (2.1.1) there are a lot of similarities with the theory of dynamical systems. There, attractive and repulsive orbits are of special interest. In the later part of this work we are interested in theories in two and three dimensions. Here, the interesting orbits can be turned into fixed points by a rescaling of the couplings in Γ_k and the field with some power of k . These fixed points play an important role for the observed infrared physics. One trivial fixed point is the Gaussian one where all couplings vanish (neglecting the vacuum energy). Obviously, there is no flow at all in this case. A second fixed point could be identified at infinite couplings, in a, in some sense, compactified theory space, since then the denominator of the right hand side of the flow equation vanishes. However, we are looking for a another type of fixed points. Those have non-trivial couplings and describe phase transitions [116]. They have a finite number of relevant or repulsive directions and are attractive in the other directions. Associated with each direction is a critical exponent θ_i that describes the behavior near the fixed point. At least the relevant ones can be related to the thermodynamical critical exponents of phase transitions. Therefore the most relevant information extracted is the existence of a fixed point and the relevant critical exponent and not the actual scheme dependent couplings at a fixed point.

2.2. Notes on Supersymmetry

Before we start to investigate certain supersymmetric models let us remind ourself of some general properties of supersymmetry. More technical aspects can be found in [117]. Supersymmetry relates fermions to bosons and vice versa by a fermionic symmetry. Fields combined in such a way are called multiplets. The couplings between the fields of such a multiplet are not independent anymore and in this sense the degrees of freedom of a theory are reduced. A prominent example is the fact that the masses of all particles within a supermultiplet have to be the same [118]. Also those fields have to transform under some internal symmetry in the same way. This, for instance, limits the possibilities to identify fermions and gauge bosons of the standard model of particle physics as part of one supermultiplet as they do transform under different representations.

Since this work focuses on lower dimensional models without gauge symmetries let us come back to the pieces of information we need in the further scope of this work. In supersymmetric

theories it is common to formulate the theory in two ways. One is called on-shell while the second one is called off-shell. The naming is related to the fact that the first one has to use the equation of motions to close the algebra while in the second formulation this is not necessary. This is achieved by an introduction of auxiliary fields. In this work we always denote them by F . A second advantage of the off-shell formulation is that the supersymmetry is linearly realized. This is of great importance for the FRG formulation as we want a regulator that respects the symmetry of the theory and is quadratic in the fields [57].

In the following we are concentrating on the off-shell formulation. In fact we use the superfield formalism [119]. As mentioned one has to introduce an auxiliary field which is purely algebraic and quadratic in the action ΔS_Λ describing the theory at the cut-off scale. This allows to easily integrate out the auxiliary field within a path integral formulation of quantum field theory. On the other hand one can solve the equation of motion (EOM) of F and end up with the same result. Taking quantum corrections into account while staying off-shell the auxiliary field obtains a kinetic part and becomes dynamical. So at intermediate scales $0 < k < \Lambda$ it is not straightforward to compare the on-shell with the off-shell formulation.

We are going to integrate out all quantum fluctuations in order to arrive at the effective average action. At an IR scale $k \approx 0$ we eliminate the auxiliary field in order to obtain the physical quantities of interest. If we are only interested in the ground state energy and the mass of the supermultiplet we may forget about the kinetic terms we obtained for F and solve again a algebraic EOM. When dealing with a supersymmetric quantum mechanical model we see how this procedure works.

It is noteworthy to point out that due to the above prescription to obtain the effective potential the auxiliary field still indicates whether supersymmetry is spontaneously broken or not. When F obtains a non zero vacuum expectation value the symmetry is broken. So the best way to look for supersymmetry breaking along the RG flows is to check whether F obtains an expectation value. This also has an influence on our construction of the flows which we discuss in the following chapter 3.

2.3. Introduction to the shooting method

As the shooting method combined with a spike plot [56, 120–123] is the main tool to find the fixed points within this work there are some comments in order. The fixed point equations, we

have to deal with, have the form

$$0 = S + u''(\phi)\mathcal{F}'(u'(\phi)) = S + \partial_\phi\mathcal{F}(u'(\phi)), \quad S = -\alpha u + \gamma u'\phi, \quad \alpha > \gamma. \quad (2.3.1)$$

Here S is the scaling part of u and \mathcal{F} is the dimensionless formulation of the right hand side of the dimensionful flow equation for the potential term u . Starting at $\phi = 0$ we integrate toward $\phi = \infty$. The fixed-point solutions are quantized and so we expect to stop at some ϕ_{\max} . At this point a singularity occurs in the numerical evaluation of the ODE. We keep track of the values ϕ_{\max} with respect to our initial conditions. Near the initial conditions that belong to a global solution we expect to see large values of ϕ_{\max} . In fact a rapid change in ϕ_{\max} is a better indication of a fixed-point solution. The shape of ϕ_{\max} as a function of the initial conditions is obviously model dependent. We investigate the quantization condition for a model similar to the Wess-Zumino model. Furthermore we give some technical details that are insightful but not essential to understand the following chapters. Therefore skipping to the next section is possible for the hasty reader.

As we see later on we end up with a \mathcal{F} that fulfills

$$\lim_{u'^2 \rightarrow \infty} \mathcal{F}' \rightarrow +0, \quad \mathcal{F}'(0) < 0, \quad \mathcal{F}'(u') = \mathcal{F}'(-u'). \quad (2.3.2)$$

$$\mathcal{F}''(u') < 0, \quad \mathcal{F}'''(u') > 0, \quad \text{for } u' > u'_0 \quad (2.3.3)$$

for some positive u'_0 . See Fig. 2.1 for an example and the appendix for the actual computation. We expect a convex effective potential $u^2/2$ for large ϕ . This means $|u| \rightarrow \infty$ for large $|\phi|$. In order to fulfill the above equation 2.3.1 we need $|u'| \rightarrow \infty$. Therefore \mathcal{F}' has a zero crossing at $\phi_0 \in (0, \infty)$. At this point the differential equation has a potential singularity. The only viable solution is $S(\phi_0) = 0$. This is one quantisation condition.

It was pointed out that in the scalar model the behavior at infinity provides a second quantization condition [90]. Since the general form of the fixed point equation is not too different in our case from the scalar one we would expect to encounter also this second one. Given η and fixed parity only one free parameter remains. Having two quantization conditions could easily overconstrain the system. We are looking at both constraints and investigate them in more detail to understand what is going on.

Let us assume that there exists a solution that is crossing the first possible singular point ϕ_0 in a regular way. Note that in this region we have $\mathcal{F}' > 0$,

$$u'' = (\alpha u - \gamma u'\phi)/\mathcal{F}' > 0 \Leftrightarrow (\alpha u - \gamma u'\phi) > 0. \quad (2.3.4)$$

For reasons of symmetry $u'' > 0$ can be chosen without loss of generality. We can imagine two possible ways for a singularity to arise. We leave the regime $u'' > 0$ and afterward the regime $u' \gg 1$ or $u'' \rightarrow \infty$ for finite ϕ . Let us examine these two cases closer. Assume $u''(\phi_1) = 0+$ then

$$\alpha u(\phi_1) - \gamma u'(\phi_1)\phi_1 = 0 \Rightarrow \alpha u(\phi_1 + \Delta\phi) - \gamma u'(\phi_1 + \Delta\phi)(\phi_1 + \Delta\phi) \quad (2.3.5)$$

$$= (\alpha - \gamma)u'(\phi_1)\Delta\phi + \mathcal{O}(\Delta\phi^2) > 0. \quad (2.3.6)$$

Therefore we never leave the considered regime. Now let us turn toward an explosion scenario for u'' . Keep in mind that $F'(\phi) > 0$ and $\partial_\phi F'(\phi) < 0$ is also true for positive u'' in the region of interest. Assume $u''(\phi_2) > \frac{u'(\phi_2)(\alpha - \gamma)}{\partial_\phi \mathcal{F}'(\phi_2) + \gamma\phi_2} > 0$. Then

$$\begin{aligned} u''(\phi_2 + \Delta\phi) &= (u(\phi_2 + \Delta\phi) - \gamma u'(\phi_2 + \Delta\phi)(\phi_2 + \Delta\phi)) / |\mathcal{F}'(\phi_2 + \Delta\phi)| \quad (2.3.7) \\ &= u''(\phi_2) + \frac{\Delta\phi}{|\mathcal{F}'(\phi_2)|} ((\alpha - \gamma)u'(\phi_2) + u''(\phi_2)(|\partial_\phi \mathcal{F}'(\phi_2)| - \gamma\phi_2)) + \mathcal{O}(\Delta\phi^2) < u''(\phi_2) \end{aligned}$$

So an explosion scenario does also not take place, at least as long as the denominator $\partial_\phi \mathcal{F}'(\phi_2) + \gamma\phi_2$ in the assumption is positive for some $\phi > \phi_0$. Note that the denominator is monotonously increasing in ϕ . In this way we are saved from any additional singularity. The behavior was induced by the fact that the scaling term changes its sign compared to the scalar case. Indeed, there an explosion scenario stops the further integration if some constraints are not met.

After being convinced that there are as many quantization criteria for global solutions as free parameters let us assume that there are indeed global solutions. As described in the beginning, we start to integrate a solution U at $\phi = 0$ for arbitrary parameters and ends at a singularity. This singularity is typically the zero of \mathcal{F}' . Assume we have chosen parameters close to a nontrivial global solution u_* . Close to ϕ_0 we can end up with overestimating or underestimating u'' compared to the values of the global solution.

Considering the first case we roughly find that u' increases too quickly. This increases S and decreases $|\mathcal{F}'|$. This gives a further boost in u'' . This pushes \mathcal{F}' toward zero and $u'' \rightarrow \infty$. Our solution terminates before reaching ϕ_0 .

Now let us turn to the other scenario. As u'' is too small S gets too small too quickly and \mathcal{F}' tends to stay finite. This provides a zero crossing of S without a zero crossing for \mathcal{F}' . While this does not terminate the integration the solution ends nonetheless at a finite ϕ : Now, we are stuck with a negative u'' . With a decreasing u' , \mathcal{F}' encounters its zero for negative u' at some point. This terminates again the integration as u'' blows up. Note that this process takes some

integration time. We therefore expect that the termination point is larger than ϕ_0 .

A remark is in order at this point. A negative u'' in the second scenario could obviously lead to another change of sign of the scalar part. This allows for a zero crossing of \mathcal{F}' . Such a case would then belong to a new fixed point solution. Exactly this mechanism allows for multicritical fixed points as sign changes in u'' are necessary for multiple minima of u and therefore u^2 . We expect only a discrete set of fixed points. If this is the case then one is able to choose initial conditions close enough to the first fixed point so that the second fixed point is not influencing the local analysis in parameter space.

We find that choosing parameters close to the ones belonging to global solutions gives us a

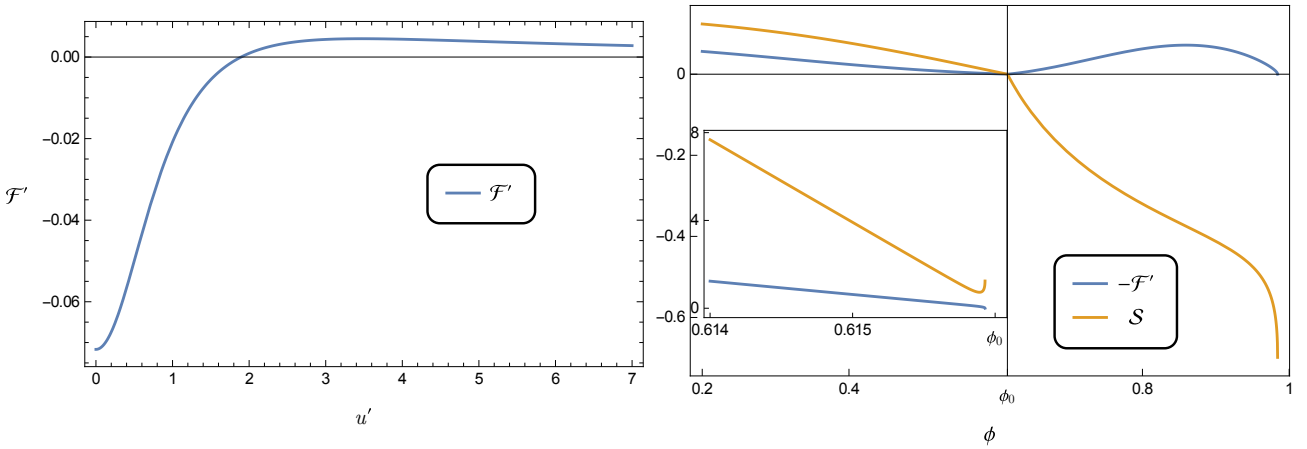


Figure 2.1.: We see the generic shape of $\mathcal{F}'(u')$ in a Wess-Zumino model on the left hand side. On the right hand side is a plot of $\mathcal{F}'(u'(\phi))$ and $S(\phi)$. We are giving two cases close to a global fixed point solution. ϕ_0 denotes the simultaneous zero crossing of S and \mathcal{F}' of the global solution. The plot is the case in which we underestimate u'' and only S has a zero crossing. The solution terminates at $\phi_{\max} > \phi_0$. The inlay shows a solution where we overestimate u'' and only \mathcal{F}' reaches zero giving a divergence of u'' with $\phi < \phi_0$. The plots are produced using the $d = 2$ Ising-class parameters.

quick change in the field value ϕ_{\max} at which the integration stops. In fact it should be a jump. In Fig. 2.1 we see a plot of both cases on the right hand side. Note that according to our analysis also the sign of S and \mathcal{F}' gives away the critical parameters. This may prove helpful when the spike plot provides no clear picture. A simple example is a non-moving singularity. A spike plot for such a case is provided in Fig. 2.2 Nonetheless one needs more information about the actual model as with the more generic shooting method keeping track of ϕ_{\max} .

In an L_2 norm we may be arbitrary close to the fixed point solution up to $\phi \approx \phi_0$ with our numerical method. Nonetheless we are not able to cross ϕ_0 and stay close to the correct fixed point solution. As the $\mathcal{F}' = 0$ property is important for the spectrum we pick up such a solution and take it as an approximation of the correct solution up to $\phi \approx \phi_0$. In other words we are taking the solutions on the side of the spike with $\phi_{\max} < \phi_0$ and disregard those on the side with $\phi_{\max} > \phi_0$. Afterwards we take the limit in parameter space to the position of the spike. In the present work we always consider the right hand side of the spike².

Finally, let us sum up what we have found. We have one constraint for one free parameter. This should lead to a quantization of global solutions. Monitoring the endpoint of an integration determines the critical parameters, i.e. the ones of global solutions, by a quick change in the value of ϕ_{\max} . We can use this knowledge as an input for a global solver or use it as an approximation to the solution up to $\phi \approx \phi_0$. We continue with the latter.

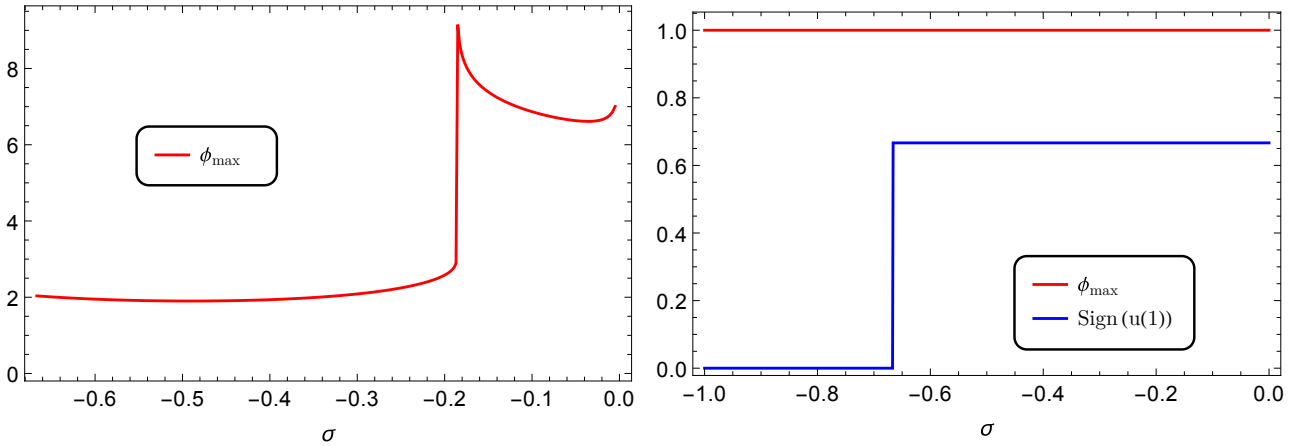


Figure 2.2.: On the left is the spike plot for $u'' = \frac{2}{6u-\phi u'} - 1$ and $u'(0) = 0$. This resembles the fixed point equation for $d = 3$ in a scalar $O(1)$ theory. We have a clear spike by plotting ϕ_{\max} over $\sigma = u''(0)$. On the right we take $u'' = \frac{u}{1-\phi^2} - 1$ and $u'(0) = 0$. The spike plot is governed by the non-moving singularity $\phi - 1$. Therefore ϕ_{\max} is giving away no spike while the sign change in u provides us with a good guess for the critical parameter. Here $\text{Sign}(u(1)) = (\text{sgn}(u) + 1)/3$.

²The one exception is the $O(N)$ model at $d < 3$. But more on this later on.

2.4. The spectrum of perturbations

Having found a fixed point solution one can expand in all couplings as fixed point solution plus a infinitesimal k dependent perturbation, e.g. for the potential $W^* + \epsilon\delta W$ up to the leading linear order in ϵ . The obtained PDE has the form of a generalized heat equation

$$\partial_k \delta u = H \delta u. \quad (2.4.1)$$

Here the Hamiltonian H is given by the right hand side of the dimensionless flow equation and the time derivative origins in the left hand side. It is useful to calculate the spectrum of the Hamilton operator in order to distinguish between relevant and irrelevant perturbations. As is well known the negative part of the spectrum of H leads to infrared relevant fluctuations. The eigenvalues of those are the relevant ones in which we have a special interest. Therefore asking for the critical exponents is equivalent to solve the static Schrödinger equation with the Hamiltonian H on the fixed-point background. There are several techniques to do so. In the frame of this work we use a pseudospectral method on the basis of sin and cos functions (the Slac derivative [124–126]) to calculate the discretized Hamiltonian. Then a simple matrix diagonalization of this discretized formulation gives us numerical results for the eigenvalues. This procedure requires some smoothness properties of H .

One can transform the eigenvalue equation

$$Hu = f(\phi)\partial_\phi^2 u(\phi) + g(\phi)\partial_\phi u(\phi) + h(\phi)u(\phi) = \theta u \quad (2.4.2)$$

into a more standard form

$$\tilde{H}v = f(\phi)\partial_\phi^2 v(\phi) + \tilde{h}(\phi)v(\phi) = \theta v(\phi), \quad v = e^{-\int_0^\phi \frac{g(\varphi)}{2f(\varphi)} d\varphi} u. \quad (2.4.3)$$

This transformation becomes singular at $\phi_0 > 0$ if $f(\phi_0) = 0$. So the spectrum of the operator H only depends on the shape in the inner region $(-\phi_0, \phi_0)$ if $\lim_{\phi \rightarrow \phi_0^-} g/f = +\infty$. As we see later on, this is the case in the Wess-Zumino model. This is especially helpful when using the shooting method. As we only obtain a fixed-point solution in a finite range, eq. 2.4.3 tells us that the fluctuations also only depend on the solution within a region given by f . If we can find the fixed point solution up to ϕ_0 we have all the information we need for the spectrum. Comparing eq. (2.3.1) with eq. (2.4.3) we observe that f coincides with \mathcal{F}' . So indeed, within a good approximation, we obtain the fixed point solution up to ϕ_0 and it is reasonable to use an approximate solution with the property $\mathcal{F}' \approx 0$.

Altogether we prefer to use the Slac derivative to compute the spectrum of linearized fluctuations when we take continuous contributions into account. Our finite range solutions are sufficient due to a special form of the operator H whose spectrum we are interested in.

2.4.1. Another shooting method

We want to give a second method [100, 127, 128] when we have to deal with a different set of problems. Given the eigenvalue problem

$$\theta u(\phi) = u''(\phi) + u(\phi) - u(\phi_0), \quad (2.4.4)$$

we have the corresponding integral operator

$$H(\phi, \tilde{\phi}) = (\delta''(\tilde{\phi} - \phi) + \delta(\tilde{\phi} - \phi) - \delta(\tilde{\phi} - \phi_0)), \text{ with } (Hu)(\phi) = \int d\tilde{\phi} H(\phi, \tilde{\phi})u(\tilde{\phi}). \quad (2.4.5)$$

As we cannot give a simple representation as in 2.4.2 we call this a non-continuous operator. In the upcoming scenarios ϕ_0 may or may not depend on the function u . As we do not have the means to solve this problem directly we do so in two steps.

The first step is to set $u(\phi_0)$ to be a constant c . Then for any given constants c and θ we can solve the differential equation

$$\theta u(\phi) = u''(\phi) + u(\phi) - c. \quad (2.4.6)$$

This is not an eigenvalue problem any more and therefore we cannot use the Slac method. As the eigenfunctions of the eigenvalue problem (2.4.4) and its generalizations shall belong to a Hilbert space with an at most polynomial weight function we know that u itself may at most behave polynomial. We also know that the solution for θ , that are no eigenvalues, tends to grow in an exponential way to $\pm\infty$ [100].

For most values of c we should find θ_+ for which the solution $u(\theta_+, c)$ grows quickly to ∞ and θ_- whose solution goes to $-\infty$. We can now make a bisection procedure to look for the limiting θ which approximately separates both cases. This is the eigenvalue θ for a given c .

The found solution does not guarantee that $u(\phi_0) = c$. Therefore we have to vary c until this is the case. This procedure may take a while and is necessary for every θ we are interested in.

We notice that if there is more than one eigenvalue in between the two initially chosen θ_+ and θ_- one has to choose those two closer together. A good starting point may be $c = 0$ and use the Slac derivative to calculate θ . Compute $u(\phi_0)$ and afterwards choose for c according to

the computed value of $u(\phi_0)$. Take θ_+ and θ_- close to the $\theta(c = 0)$. One gets a new value of $u(\phi_0) - c$. Go on up to a needed precision. We give an example in the appendix.

The described method obviously also works for more generalized forms of eq. (2.4.4), e.g. one can include functions in front of u and u'' or have a more involved function at $u(\phi_0)$. We are calculating a linear response of a system later on. Therefore, one should make sure to stay in this regime. In order to do so one has to work with small u compared to the background solution. In this way changes in ϕ_0 are also only taken on a linear level into account.

At last a word of caution. Eigenvalues present for $c = 0$ may disappear for inappropriately chosen c . For instance the function $\theta(c)$ could become complex. We provide an example of the method in the appendix A.1.

3. Supersymmetric Quantum Mechanics

3.1. Introduction

As a starting point we examine a well understood theory, i.e., $\mathcal{N} = 1$ quantum mechanics in one spatial dimension. This model can be solved to arbitrary precision by diagonalizing the Hamiltonian. [85] We may refer to these results as exact.

One can treat this model equivalently as a $0 + 1$ dimensional QFT with one scalar field and its supersymmetric fermionic partner. In this way all the methods available for treating a QFT can be applied to this model. In the further study we pick the exact functional renormalization group method (FRG) and compare the results obtained with this method with the ones we already know from the quantum mechanical point of view. As some work was done before [85, 129] we are mainly interested in the convergence of the derivative expansion for the supersymmetric model [130]. This chapter is mainly based on the paper mentioned last. Although a lot of work was also done in this direction before, e.g., for scalar field theories, we reexamine this due to the fact that we are using an off-shell formulation and thus our derivative expansion is not in powers of momentum but rather in momentum times auxiliary field. While investigating this expansion we also have a look at the mechanism of spontaneous symmetry breaking and the technical implications related to it.

Since this is a model originating in quantum mechanics, we expect that tunneling effects play a role when we examine a double well potential or one with even more minima [131]. This should give rise to some instanton effects in our effective field theory. Including non-local interactions into the effective action would be one way to treat these effects. On the other hand one can hope that a series of derivative operators converges to a non-local term like it was hinted in a previous work [132]. Therefore, we hope that our results improve by adding

additional derivative terms to our truncation in the coupling region in which the tunneling effect starts to show up significantly. Again, the analogy is the increasing convergence of a partial sum of a Taylor series within the radius of convergence.

In the following, we start with formulating the model and our truncations for the FRG treatment. Here we also set some conventions we are using throughout this work. Afterwards we compute some numerical results and get some insight into the mechanisms determining the quality of our results. As a last part we are summarizing our findings about the convergence of the derivative expansion before going on to other models.

3.2. The Model

Reformulating the quantum mechanical model as a QFT gives us the on shell action

$$S_{\text{on}} = \int d\tau \left[\frac{1}{2} \partial_\tau \phi(\tau) \partial_\tau \phi(\tau) - \frac{i}{2} \bar{\psi} \partial_\tau \psi + \frac{1}{2} W'(\phi)^2 - \bar{\psi} \psi W''(\phi) \right]. \quad (3.2.1)$$

with the Grassmann valued fermion field ψ and the real scalar field ϕ . Reformulating it using the purely imaginary auxiliary field F to linearize the supersymmetry, we obtain the off shell action

$$S_{\text{off}} = \int d\tau \left[\frac{1}{2} \partial_\tau \phi \partial_\tau \phi + \frac{1}{2} F^2 - \frac{i}{2} \bar{\psi} \partial_\tau \psi + i F W'(\phi) - \bar{\psi} \psi W''(\phi) \right] \quad (3.2.2)$$

$$= \int d\tau d\theta d\bar{\theta} \frac{1}{2} \Phi K \Phi + i W(\Phi) = \int dz \frac{1}{2} \Phi K \Phi + i W(\Phi) \quad (3.2.3)$$

where in the second line we introduced the superfield and the superspace coordinate,

$$\Phi = \phi + \bar{\theta} \psi + \bar{\psi} \theta + \bar{\theta} \theta F, \quad z = (\tau, \theta, \bar{\theta}). \quad (3.2.4)$$

and the superderivative

$$K = \bar{D} D - D \bar{D}, \quad \bar{D} = i \partial_\theta - \bar{\theta} \partial_\tau, \quad D = i \partial_{\bar{\theta}} - \theta \partial_\tau \quad (3.2.5)$$

using the auxiliary Grassmann variable θ . Our bare superpotential W is of polynomial form in the UV. Following the standard derivative expansion we count the number of superderivatives to determine the order of our truncation. So an operator of the type $K^2 = \partial_\tau^2$ is an NNLO operator although it is only a second derivative in time. We examine the theory up to NNLO order which gives rise to the effective Lagrangian

$$\mathcal{L} = \mathcal{L}_{\text{pot}} + \mathcal{L}_{\text{NLO}} + \mathcal{L}_{\text{NNLO}}. \quad (3.2.6)$$

We have used the abbreviations

$$\mathcal{L}_{\text{pot}} = iW(\Phi), \quad (3.2.7)$$

$$\mathcal{L}_{\text{NLO}} = -\frac{1}{2}Z(\Phi)\Phi K\Phi, \quad (3.2.8)$$

$$\mathcal{L}_{\text{NNLO}} = \frac{i}{4}Y_1(\Phi)K^2\Phi + \frac{i}{4}Y_2(\Phi)(K\Phi)(K\Phi). \quad (3.2.9)$$

Neglecting $\mathcal{L}_{\text{NNLO}}$ and putting Z to one yields the LPA truncation while allowing for a function $Z(\phi)$ gives NLO and also including $Y_i(\phi)$ is called NNLO. Since we are in 1 dimension we do not expect to see any non trivial fixed points and therefore not introduce dimensionless quantities. Instead we study the flow of the couplings. In order to extract physical meaningful quantities, we have to calculate the effective potential. This can be done by solving the EOM of the auxiliary field F

$$F = -\frac{2i}{3Y} \left(\sqrt{Z^2 + \frac{3}{4}(4W' - 2X\ddot{\phi} - (X' - Y)\dot{\phi}^2)Y - Z} \right), \quad Y = Y', \quad X = Y'_1 + Y_2. \quad (3.2.10)$$

One had to choose the solution of the quadratic EOM with the correct sign. Otherwise the solution would diverge in the NLO case, therefore especially in the UV with $\mathcal{L}_{\text{NNLO}} = 0$. The solution (3.2.10) is dynamical with time derivatives in contrast to the UV-case. Inserting the non dynamical part back into the Lagrangian \mathcal{L} yields the bosonic effective potential V_{Bos}

$$V_{\text{Bos}} = \frac{2}{27Y^2} \left(\sqrt{3W'Y + Z^2} - Z \right) \left(6W'Y + Z^2 - Z\sqrt{3W'Y + Z^2} \right),$$

$$V_{\text{Bos,NLO}} = \frac{W'^2}{2Z}. \quad (3.2.11)$$

A word of caution is in order at this point. Given the above formula, one could obtain an effective potential that is complex. This is not a breakdown of the theory but rather one of the truncation.

3.2.1. The flow equations

In order to obtain the flow equations we have to calculate the right hand side of the aforementioned eq.

$$\partial_t \Gamma_k = \frac{1}{2} \text{STr} \frac{\partial_t R_k}{\Gamma_k^{(2)} + R_k}, \quad t = \log(k/\Lambda). \quad (3.2.12)$$

For our effective average action we make the already introduced ansatz (3.2.6),

$$\Gamma_k = \int dz \mathcal{L}(k, z) \quad (3.2.13)$$

with \mathcal{L} as a function of the energy scale k according to equation (3.2.12). The actual computation can be found in appendix A.2. We just want to note that we expand around $F = 0$, the supersymmetric phase, and use a regulator

$$R_k = (ir_1) - Z(\Phi_0)r_2K \quad (3.2.14)$$

giving the cut-off function

$$\Delta S_k = \frac{1}{2} \int dz \Phi R_k \Phi. \quad (3.2.15)$$

r_1 is playing the role of a mass regulator which we use in the first part of this chapter. r_2 is a momentum regulator that is especially necessary in higher dimensions. Note that we spectrally adjust our regulator by including $Z(\Phi_0)$. $\Phi_0 = \phi_0$ is chosen as the minimum of the potential. We end up with the following flow of the effective potential at NNLO level

$$\partial_k W_k = \frac{1}{2} \int_{-\infty}^{\infty} \frac{dq}{2\pi} \left(\partial_k r_1 \frac{(Z'(A^2 - B^2 q^2) - 2BAA')}{(B^2 q^2 + A^2)^2} + \partial_k (r_2 Z_0) \frac{A'(A^2 - B^2 q^2) + 2Bq^2 AZ'}{(B^2 q^2 + A^2)^2} \right), \quad (3.2.16)$$

$$A = W'' + r_1 + q^2/2X, \quad B = Z + r_2 Z_0, \quad Z_0 = Z(\Phi_0). \quad (3.2.17)$$

Here we suppressed the dependencies of the functions for reasons of convenience.

3.3. Unbroken Supersymmetry

At the UV scale we choose the initial conditions $W_k = \phi^4/4 + g\phi^3/3 + \phi^2 + \phi$, $Z_k = 1$, $Y_{1,k} = 0$ and $Y_{2,k} = 0$. Choosing $g = 0$ gives a convex starting potential for which already a simple LPA truncation should give satisfying results. With increasing g the potential starts to develop a second minima see also Fig. 3.1 which following our argumentation at the beginning should lead to worse results. In this region we can test our derivative expansion and look for the convergence near the probable convergence radius in g . This should give us an impression how good our derivative expansion is doing. We want to point out that we have chosen a superpotential with the first derivative W' ranging from plus to minus infinity. Choosing such a potential leads to the case that at the infrared scale W' still ranges from plus to minus infinity and therefore still has a zero. Therefore the expectation value of F is also still zero and we can not break supersymmetry. Due to this fact it is sufficient to choose a mass regulator $r_1 = k$ and $r_2 = 0$. As supersymmetry is unbroken the ground state energy stays zero and is therefore

inadequate for a check of the convergence. For a comparison with the numerical results from diagonalizing the Hamiltonian we consider the effective mass of the particle given by the pole of the propagator at the minimum $W'(\phi_0) = 0$ at $k = 0$,

$$G_k|_{\bar{\theta}\theta\bar{\theta}'\theta'} = \frac{Zq^2}{Z^2q^2 + (W'' + \frac{1}{2}Xq^2)^2} \delta(q - q') \Rightarrow \quad (3.3.1)$$

$$m^2 = \lim_{k \rightarrow 0} \frac{2}{X^2} \left(Z^2 + XW'' - Z\sqrt{Z^2 + 2XW''} \right). \quad (3.3.2)$$

Note that also the pole of the propagator has two solution and the one describing the correct UV behavior ($\text{NNLO} = 0$) is chosen. In the simple LPA truncation this is just the curvature of the effective potential $V_{\text{Bos}} = W'^2/2$ at $\phi = \phi_0$. There are different ways to calculate the

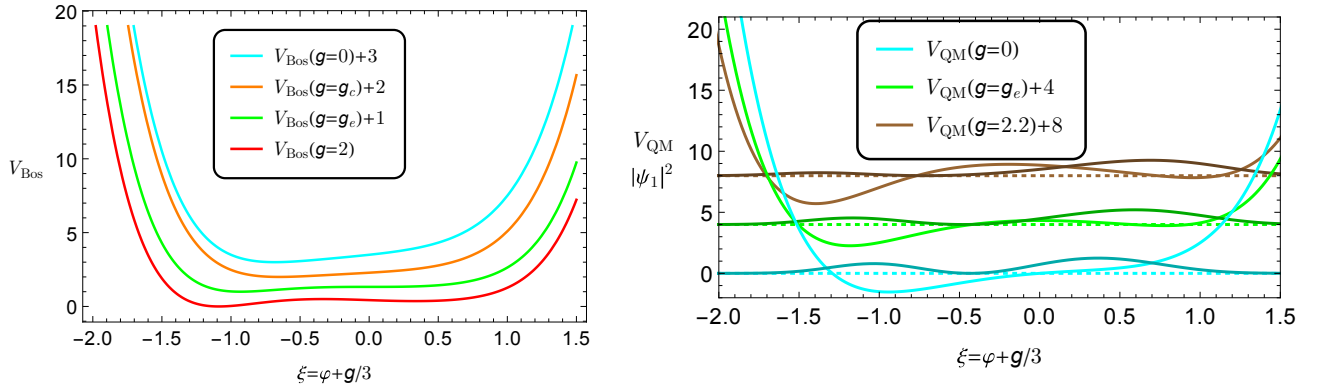


Figure 3.1.: On the left is the shape of different effective UV potentials $V_{\text{Bos}}|_k = \Lambda$ parametrized by the coupling g . Note the development of a non-convexity at $g_c \approx 0.897$ and thereafter a second minimum at $g_e = \sqrt{3}$. On the right are the squares of the real first-excited-state wavefunctions ψ_1 against their quantum mechanical potentials $V_{\text{QM}} = (W'^2 - W'')/2$ depicted in a slightly lighter color for a standard stationary Schrödinger equation $H = p^2/2 + V_{\text{QM}}$. Added is also a shifted baseline plotted as dots. Note the increasing shift of the squared wave function away from the first minimum into the second non-global one.

numerical flow; for instance finite differences in a finite region and fixed boundaries or global pseudospectral methods. Since the flow is negligible for large ϕ we end up in both cases with numerically coinciding results. Fig. 3.2 shows the results calculated with a finite difference method for the calculated masses for different truncations and couplings g . We have a good convergence as long as $g < g_c$ and a reasonable convergence for $g < g_e$ where g_c and g_e are the values at which a non-convexity and a second minimum of the effective potential respectively appear. It is noteworthy that g_e is also the value at which the superpotential W starts to show

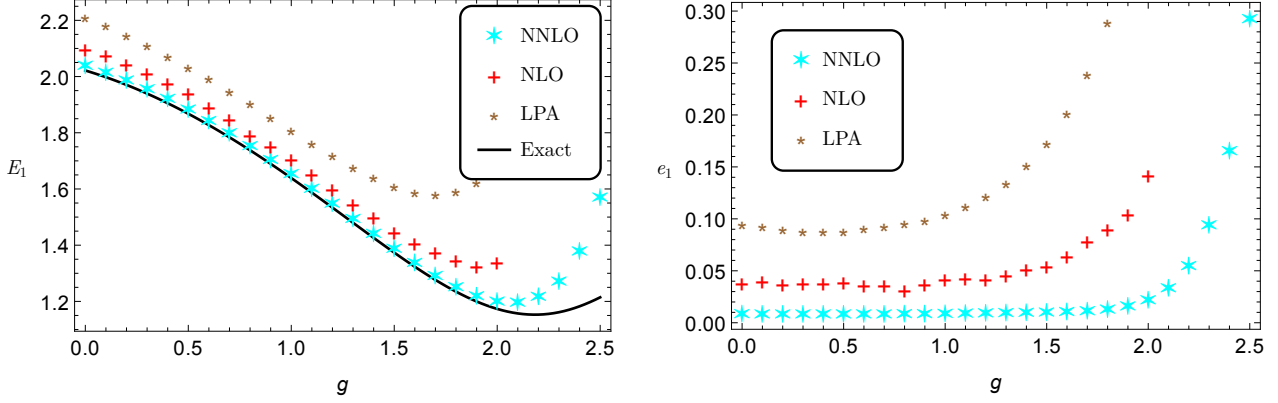


Figure 3.2.: Given are the results for the effective mass given by different truncations and compared to the numerical exact results using the Hamiltonian formulation of the quantum mechanical system. On the left are the numbers calculated while on the right the relative error $e_1 = E_{1,\text{truncation}}/E_{1,\text{exact}} - 1$. One sees a good convergence of the result for non convex starting potentials $g < g_c \approx 0.9$. The LPA truncation deviates as soon as a non-convexity builds up. With the establishing of the second minima also the NNLO truncation starts to give worse results and soon thereafter breaks down $g \gtrsim 2$.

a additional non-convexity in the intermediate region. This naturally coincides with the fact that a second minimum of W'^2 appears. A minimum that is merely separated from the global one at $g \approx g_e$ does not seem to put to much stress on the NNLO truncation. Beginning with $g = 2$ the second minimum together with its very broad shape do significantly contribute to the first excited state and the influence of the first minimum diminishes, see Fig. 3.1. This gives our ansatz a hard time to deal with it. As mentioned before we have a built-in check whether our NNLO truncation is still working fine. When the effective potential becomes complex valued for any field value we know that our truncation is insufficient. Indeed for large g this is the case.

A possible reason for this is the fact that our derivation of the flow equations has used an expansion around $F = 0$ instead of a more general $F = W'$. The former would obviously not be true for the second minimum. We examine the impact of considering an expansion around $F \neq 0$ in the following section dealing with spontaneous symmetry breaking. At this point we look at a class of non-convex superpotentials that do not start with a non supersymmetric minimum $W' = \phi^5 - g\phi^3 + \phi$. Within our truncations and a large range of g they do also not develop such a minimum e.g. for $g = 3$ all minima are supersymmetric. In Fig. 3.3 we give the

numerical results and compare them to the exact ones. Also we see the shape of the effective potential for $g = 2.3$ for different k in Fig.3.4.

We first note that our convergence in the truncations is not as good as it was before. More importantly the pattern we observe is quite similar to the one we had before. The LPA is the first one to fail for increasing g . With a further increment in g also the NLO case gives way. Shortly afterwards the NNLO breaks down. Note that in this scenario the build up of the tunneling barrier of the UV effective potential is quicker in g than it was before. This is probably the reason why NNLO is breaking down so shortly after NLO.

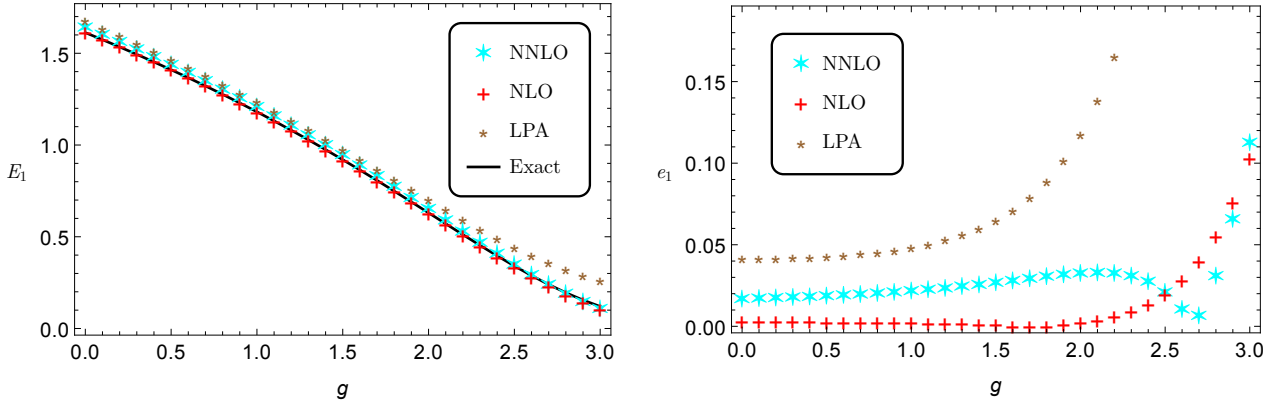


Figure 3.3.: We compare for an odd superpotential $W' = \phi^5 - g\phi^3 + \phi$ the results in different truncations for different $g \in [0, 3]$. We see again a failure of the different truncations for large g . Note that for $g = 3$ the effective potential never develops a non-supersymmetric minimum nonetheless all truncation break down. We observe that LPA starts to break down with the rise of the non-convexity at $g \approx 1$. NLO starts to deviate with the first additional minima ($g \approx 1.5$) and starts to break down as the last two additional minima appear ($g = 2$). NNLO is in this scenario not as good as NLO in absolute values but is again more stable against increasing g than NLO.

The absence of the non-supersymmetric minima as well as the large error indicate that indeed the non-convexities are the main reason for the error we observe. Since tunneling effects are strongly suppressed in higher dimensions we expect to be able to capture the qualitative physical aspects in our later on analysis.

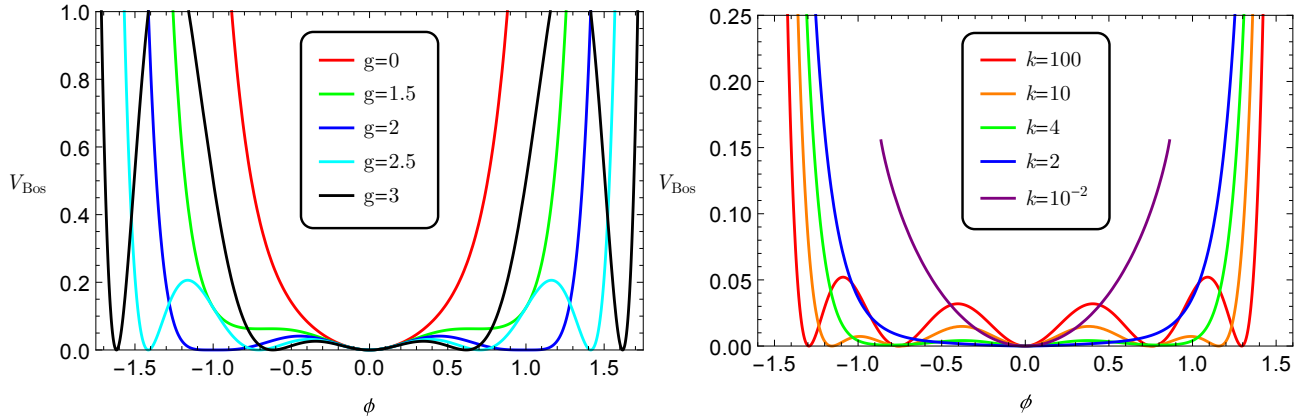


Figure 3.4.: On the left we see different effective potentials $V_{\text{Bos,UV}} = W'^2/2$ in the UV for different g with $W' = \phi^5 - g\phi^3 + \phi$. The potential $W'^2/2$ is non-convex for $g > 1.012$. Two additional minima exist for $2 > g > 2\sqrt{5}/3$. For larger g we start with 5 minima in the effective potential. Note the build up of the barrier isolating the outer two minima from the three inner ones for large g . On the right hand side the flow of the effective potential in NNLO truncation for $g = 2.3$ is depicted. For our later analysis it is important that the outermost minima are defining the curvature in the IR minimum. For this reason we identify them as the physical minima when we discuss the Wess-Zumino model. The plot of the effective potential for $g \approx 0$ is stopping for finite ϕ as it turns complex at this point. This indicates the breakdown of our truncation level.

3.4. Broken supersymmetry

As mentioned we are also interested in the spontaneous breaking of supersymmetry. To observe such a behavior we have to modify our starting potential. We choose a superpotential in such a way that W'_k is an even function and therefore a finite flow time might be sufficient to lift its minima above zero which is needed for the breaking of supersymmetry. When W'_0 is a positive function a minimum of W'_0 is also minimum of $W_0'^2$ and therefore in good approximation also the ones of the effective potential. So the propagator given in (3.2.12) has an infrared divergence at the physical minimum. This is due to the fact that we have so far expanded around $F = 0$. But in the broken phase this is no longer justified. Instead we should expand F around $W'_k(\phi)$ or $W'_k(\phi_0)$ where we prefer to use the first one. Note that the field F is still k independent only the expansion point is different at every scale.

An issue is the fact that the projection scheme using the Taylor series in F around $F_0 \neq 0$ is not unique. For instance, in the NLO case we have beside the old terms $(F - F_0)^1$ and $(F - F_0)^2$ also a term $(F - F_0)^0$ giving us three possible projections for the two functions Z and W' . We give results for different projections and the flow equations in full generality in the appendix . The flow equation in an NLO truncation for a field independent Z can be read of from

$$\begin{aligned} \text{lhs} &= iF\partial_k W' + \frac{1}{2}\partial_k Z F^2 + \mathcal{O}(F^3) \\ &= \left(\frac{W'\partial_k W'}{Z} - \frac{W'^2\partial_k Z}{Z^2} \right) (F - F_0)^0 + i \left(\partial_k W' - \frac{W'\partial_k Z}{Z} \right) (F - F_0)^1 + \frac{1}{2}\partial_k Z (F - F_0)^2 + \dots, \end{aligned} \quad (3.4.1)$$

$$\begin{aligned} \text{rhs} &= \frac{1}{2} \int_{-k}^k \frac{dq}{2\pi} (\partial_k(Zr_2)(W'' - B^2q^2)) \left[\frac{W'W'''}{\mathcal{N}(\mathcal{N}Z + BW'W'')} (F - F_0)^0 + \right. \\ &\quad \left. \frac{iW''''Z^2}{(\mathcal{N}Z + BW'W''')^2} (F - F_0)^1 + \frac{BW''''^2Z^3}{(\mathcal{N}Z + BW'W''')^3} (F - F_0)^2 + \dots \right] \\ \mathcal{N} &= B^2q^2 + W''^2, \quad B = Z(1 + r_2), \quad F_0 = -iW'/Z. \end{aligned} \quad (3.4.2)$$

We see that in the propagator the new term $W'W'''$ appears lifting the singularity at $W'' = 0$. This term is exactly the additional contribution to the mass of the bosons when supersymmetry is broken. Due to the complicated structure of the flow equations we have to limit ourselves to very basic truncations for our numerical approach. We follow the RG flow according to the old flow equation as long as we are in the unbroken phase and switch to eq. (3.4.2) as soon as we enter the broken phase ($W''^2 > 0$). This point coincides with the restoration of the \mathbb{Z}_2 symmetric phase. Further on we use a polynomial truncation of the potential and restrict ourselves in NLO to a field independent Z which is normally called an LPA' truncation. We

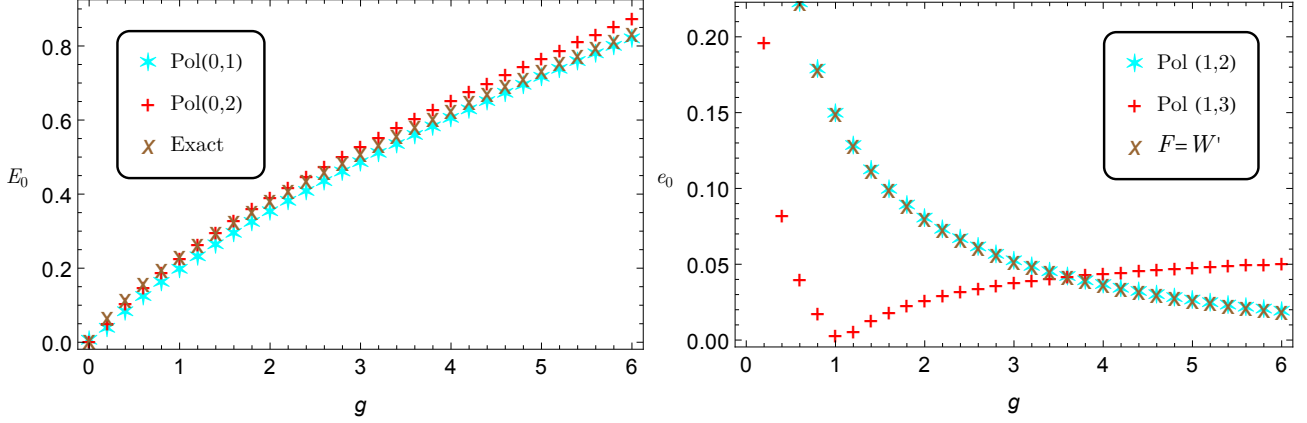


Figure 3.5.: On the left we see the results for the ground state energy of the system compared to exact results. The results are given for different truncations where we denoted in brackets the projection scheme on the powers of the Taylor expansion in $F - F_0$. On the right we depict the relative errors with respect to the exact values. There we also provide data points to compare results using the projection scheme with $F_0 = W'(\phi)$ along the whole flow and the case in which we start to use it as soon as breaking takes place as described in the main text.

are also using a momentum regulator $r_2 = (k^2/p^2 - 1)\theta(k^2 - p^2)$ instead of the mass regulator r_1 . As we see in Fig. 3.5 the results are quite good for the ground state energies although our starting potentials have two minimas. We can also see that the projection on $F = W'$ in the unbroken phase is not necessary as the results do not change significantly.

At this point we should elaborate a bit on this point. We mentioned in the introduction as well as in the discussion of the unbroken phase the possible difficulty to account for tunneling effects yet we are able to calculate a good estimate of the ground state energy. The reason is that the tunneling effect with two clearly separated minima provides an exponentially suppressed split of the energy levels of one minimum alone. Thus we can expect that as long as the influence of the tunneling effect is very small on the ground-state energy our estimates with only local terms should still be good. Indeed if we try to calculate the split with a simple truncation including W and $Z(0)$ we do not see it. This is immanently present in the fact that our obtained effective potential $W'^2(\phi)/(2Z(\phi_0))$ is always flat at $\phi = 0$ instead of having a small remaining curvature. This indicates that one needs at least a function $Z(\phi)$ to see this split. The parameter choice with the smallest barrier is the one with $g \approx 0$. Here we can also spot the largest relative error. This is another indication that large tunneling effects are indeed troublesome as we expected. Interestingly the two given NLO truncations obtained by different projection schemes do not

give a coherent picture on which one is better. The one using $(F - F_0)^0$ and $(F - F_0)^1$ (1,0) leads to more accurate results for large g while the one using $(F - F_0)^0$ and $(F - F_0)^2$ (0,2) is better performing for small g . The latter scheme picks up more contribution in the flow that would produce higher derivative terms, e.g. Y_1 and Y_2 in an extended truncation. This seems to be helpful in the strong tunneling regime with small g while in the weak tunneling regime it is misleading.

As we encounter the necessity to project onto $F_0 \neq 0$ in the broken phase we may ask ourselves what happens if we also use this projection scheme ($F_0 = W'(\phi)/Z$) while being in the symmetric phase. Doing so and comparing with the former results shows that this only leads to minor changes, see also Fig. (3.5). This very good agreement partially goes back to the fact that we are quickly entering the broken phase.

3.5. Summary

Let us summarize our findings before we go on. We have seen that our derivative expansion works fine and that as long as the first derivative of the superpotential shows no non-convexities a simple LPA scheme captures the qualitative behavior of the theory. For non-convex cases we could extend our truncation and obtain some good results.

We proceed in the following chapters using the more simple LPA and LPA' truncation to deal with our models. We can be assured that in the admissible regions for LPA the derivative expansion converges nicely and therefore a numerical improvement of our numbers is in principle always at hand. As we also await much less tunneling effects we think LPA' to be sufficient.

An important feature that we have uncovered is that the easy projection scheme around $F = 0$ cannot be used in the phase with broken supersymmetry. This may be worrisome from a numerical point of view but as we see later on is not so relevant for the physics near the fixed points we are discussing.

The reader more aware of the flow equation may have noticed that we used only one regulator. In [130] one finds some discussions about this topic. Our results are in reasonable agreement with the exact results. Therefore, we can expect that our regulator choice was not too bad for the used truncations.

4. The Wess-Zumino model

In the following section we are discussing the Wess-Zumino model in $2 \leq d \leq 3$ with a \mathbb{Z}_2 symmetry. Some previous FRG treatment of this model can be found in [88, 133, 134]. The first two sections of this chapter are based on [128]. The field content of the model is a real scalar field and a Majorana fermion. We expect to see a different number of non-trivial fixed points depending on the dimension. In $d = 2$ there should be an infinite number of fixed points which can be easily seen from a conformal field theory point of view. On the other hand we expect in $d = 3$ only the Wilson-Fisher fixed point belonging to the Ising universality class. Therefore we await to observe a branching of new fixed points at intermediate critical dimensions. In order to see these we employ the shooting method introduced earlier on 2.3. A different approach to the $d = 3$ case is the one of conformal bootstrap [135]. The $d = 2$ case is in principle solved via conformal field theories, e.g. [136]. Especially in the latter case we want to emphasize that we use this model to test our method and refer to those sources for exact numbers for the critical exponents.

We are giving results for the critical exponents of the models in an LPA' truncation using the Slac derivative and the ones obtained by a modified shooting method. A difference in the numbers is pointed out and an explanation given why this happens. We are also providing an alternative method to obtain the Ising class fixed points using a polynomial expansion of the potential around the origin. This was already described in [137] for a bosonic theory.

4.1. The model in $d = 2, 3$

The model has to be formulated in Minkowski spacetime since the Majorana property can only be fulfilled with this signature for $d = 3$. Therefore the flow equation for a Minkowski signature has to be used and after doing the algebra on the right hand side it is possible to do a Wick rotation giving us an Euclidean flow. Before doing so let us recapitulate the UV off-shell

formulation

$$\mathcal{L} = -\frac{1}{2}(\partial_\mu\phi)^2 + \frac{i}{2}\bar{\psi}\not{\partial}\psi - \frac{1}{2}F^2 + FW' - \frac{1}{4}W''\bar{\psi}\psi$$

We have the scalar field ϕ , the Majorana Fermion ψ , and the auxiliary field F . For our effective average action we make an LPA' Ansatz

$$\Gamma_k = \int d^d x \left[-\frac{Z(\phi_0)}{2} ((\partial_\mu\phi)^2 + i\bar{\psi}\not{\partial}\psi + F^2) + FW' - \frac{1}{4}W''\bar{\psi}\psi \right].$$

We have defined $Z(\phi_0)$ as the value of Z from an NLO truncation in the physical minimum ϕ_0 . As we have seen in the flow of the quantum mechanical model this is the outermost supersymmetric minimum of the effective potential

$$V_{\text{bos}} = \frac{W'^2}{2Z(\phi_0)}. \quad (4.1.1)$$

Note that therefore even and odd superpotentials lead to a \mathbb{Z}_2 symmetric effective potential. We already see that the model is quite similar to the quantum mechanical one with the same degrees of freedom: 2 real scalar ones from ϕ and F and 2 real Grassmanian ones from the Majorana Spinor ψ . We have the symmetry property $\bar{\chi}\psi = \bar{\psi}\chi$ for Majorana Fermions. We take this into account and change some prefactors in Γ_k compared to the QM model. The flow equations for W and Z are then formally the same as in the previous model. In $d = 3$ we can use a momentum regulator

$$r_{2,1} = Z(\phi_0)(k/|p| - 1)\theta(k^2 - p^2) \quad (4.1.2)$$

which is an analogue to the standard θ regulator, also called Litim regulator, of the bosonic model. It also eliminates the momentum dependence of the denominator on the right hand side of the flow equation and in this sense maximizes the gap. Note that this regulator is not valid for higher order truncation as divergences show up. Also in $d = 2$ already in LPA' the regulator does not give a convergent flow for the wavefunction renormalization. For this reason we also use a second regulator

$$r_{2,2} = Z(\phi_0)(k^2/p^2 - 1)\theta(k^2 - p^2), \quad (4.1.3)$$

obtaining a different set of momentum integrals in our flow equations. These resemble those used in the quantum mechanical setup when investigating supersymmetry breaking.

For the following analysis we use the second set of flow equations ($r_{2,2}$), but also provide results

for $r_{2,1}$ in $d = 3$. As mentioned in the introduction we can do a rescaling of fields and couplings in order to look for fixed points. In this model the rescaling is

$$\tilde{\phi} = k^{\frac{2-d}{2}} Z^{-\frac{1}{2}} \phi, \quad (4.1.4)$$

$$\tilde{\psi} = k^{\frac{1-d}{2}} Z^{-\frac{1}{2}} \psi, \quad (4.1.5)$$

$$u = k^{-d/2} Z^{-\frac{1}{2}} W', \quad (4.1.6)$$

$$\eta = -\partial_t \log(Z(\phi_0)). \quad (4.1.7)$$

Here we have introduced the anomalous dimension η that determines the anomalous scaling of the fields. As we have a supersymmetric theory the anomalous scaling of fields in one multiplet is the same. This gives us only one anomalous dimension in contrast to a general Yukawa model. In terms of the new fields and couplings we have the flow equations ($r_{2,2}$)

$$\partial_t u = S_{\eta,d}(u, u', \phi) + \partial_{u'} \mathcal{F}_{\eta,d}(u') u'', \quad (4.1.8)$$

where $S_{\eta,d}$ is the scaling part and $\mathcal{F}_{\eta,d}$ stems from the fluctuations,

$$\begin{aligned} S_{\eta,d}(u, u', \phi) &= -\frac{d-\eta}{2} u + \frac{d-2+\eta}{2} \phi u', \quad \mathcal{F}_{\eta,d}(u') = -\frac{c_d}{2} ((2-\eta) \mathcal{H}_{1,0}(u') + \frac{d\eta}{d+2} \mathcal{H}_{1,1}(u')) u', \\ \eta &= c_d \left[(2-\eta) \mathcal{H}_{3,0}(u') + \frac{d\eta}{2+d} \mathcal{H}_{3,1}(u') - \frac{d(2-\eta)}{d+2} \mathcal{H}_{3,1}(u') u'^2 u'' - \frac{d\eta}{d+4} \mathcal{H}_{3,2}(u') u'^2 \right] u''^2|_{\phi=\phi_0}, \\ \mathcal{H}_{l,m}(u') &= (m+d/2) \int_0^1 dt \frac{t^{m+d/2-1}}{(1+tu')^l}, \quad c_d^{-1} = (4\pi)^{d/2} \Gamma(1+d/2). \end{aligned} \quad (4.1.9)$$

We have dropped the $\tilde{}$ for the sake of an easier notation. In LPA' we are essentially left with one ODE and one constraint when we look for the fixed points of the model, i.e. $\partial_t u = 0$. Let us neglect the constraint, i.e. the η equation, for the moment.

We are interested in the global solutions to this ODE. As argued before there is a quantization of these solutions due to constraints present in the ODE. The solving method of our choice is the spike plot. We use as a parameter for it the first $\sigma' = u'(0)$ or second derivative $\sigma = u''(0)$ of the odd or even dimensionless potential u , respectively.

Now, we also want to include the η equation. We can only compute η once we have found a local solution that is close to the global one. Thus it is reasonable to compute the spike plot for a number of different input parameters η_{in} . From this result calculate each time η_{out} according to the formula given. Plot the difference $\eta_{\text{in}} - \eta_{\text{out}}$ over η_{in} and search for a zero. Refine the input set and do so until a desired precision is met. Following the described procedure we obtain the fixed-point solutions with consistent values of η .

One can also calculate a non-trivial η at $\phi = 0$ in the Wess-Zumino model for even u . Doing so means that we calculate η in the minimum of the superpotential. We refer to this truncation by η_0 . We note that for odd u $\eta_0 = 0$ as it scales with u''^2 . When we follow this approach we can determine η from the input parameter σ and do not have to follow the above described procedure to match the input η with the calculated one.

Having the fixed-point solution u_* we are able to linearize around this fixed point $u(t, \phi) = u_*(\phi) + e^{-\theta t} \epsilon \delta u(\phi)$ keeping η constant. This gives us a problem of the type

$$-\theta \delta u(\phi) = H(u, \partial_\phi) \delta u(\phi), \quad H = \partial_{u''}(\partial_t u) \partial_\phi^2 + \partial_{u'}(\partial_t u) \partial_\phi + \partial_u(\partial_t u). \quad (4.1.10)$$

$\partial_t u$ is given by equation (4.1.9). We discussed this kind of problem in Sec. 2.4 and proposed the Slac derivative as a tool for solving it. Doing so, we obtain the critical exponents θ . Positive θ belong to relevant directions since $t \rightarrow -\infty$ in the convention introduced before. In the next section we make some general statements on some fluctuations independent of d .

4.1.1. Special fluctuations

Before we present actual solutions we investigate the form of special fluctuations. To remind ourselves the equation for the fluctuations is given by 4.1.10

$$-\theta \delta u(\phi) = [\partial_{u''}(\partial_t u) \partial_\phi^2 + \partial_{u'}(\partial_t u) \partial_\phi + \partial_u(\partial_t u)] \delta u. \quad (4.1.11)$$

By making the special ansatz $\delta u = 1$ we get the equation $-\theta = \partial_u(\partial_t u) = -\frac{d-\eta}{2}$. Therefore one even fluctuation should always have the eigenvalue $\theta_1 = \frac{d-\eta}{2}$. For even potentials this is a relevant fluctuation belonging to the symmetry class. We have no vacuum energy fluctuation in the supersymmetric case. Thus, in the Ising class it must be related to the correlation length critical exponent ν . As it turns out

$$\nu_{\text{Ising}} = \frac{1}{\theta_1} = \frac{2}{d-\eta}. \quad (4.1.12)$$

This close relation was named superscaling in [133].

We want to point out two things at this point. Firstly although the fluctuation is a trivial constant in u it is not trivial in the on-shell formulation. As we have

$$V_{\text{Bos}} = \frac{W'^2}{2Z}, \quad \Rightarrow \quad \Delta V_{\text{Bos}} = \frac{W' \Delta W'}{Z}, \quad (4.1.13)$$

the discussed fluctuation in the on-shell formulation behaves as \sqrt{V} .

Secondly the critical exponents are also shifted between a formulation in $W' \sim u$ and $V_{\text{Bos}} \sim v$

by a constant value of η . This has to be taken into account when comparing results in both formulations. The reason is the way how the dimensionless quantities are defined. The standard dimensionless form of V_{Bos} would be $v_{\text{Bos}} = k^{-d}V_{\text{Bos}}$ instead of $v_{\text{Bos}} = k^{-d}(2Z)^{-1}W_{\text{Bos}}'^2$. We emphasize on the lack of Z in the rescaling leading to the difference of one η .

Another special fluctuation is $\delta u = u'$. Then we get

$$-\theta u' = \partial_{u''}(\partial_t u)u''' + \partial_{u'}(\partial_t u)u'' + \partial_u(\partial_t u)u' = \partial_\phi(\partial_t u) - \partial_\phi(\partial_t u)|_{u,u',u''} \quad (4.1.14)$$

$$= 0 - \frac{d-2+\eta}{2}u', \quad \Rightarrow \quad \theta = \frac{d-2+\eta}{2}. \quad (4.1.15)$$

Here, we used that the first derivative w.r.t. the dimensionless field ϕ of the fixed-point equation is also zero. This fluctuation does not share the symmetry of u . Therefore it never belongs to the symmetry respecting fluctuations. But it is a relevant fluctuation that can be used as a test for the stability of our numeric solutions.

After these quite general statements we turn toward the cases of $d = 2$ and $d = 3$.

4.1.2. $d = 3$

In this and the next section we want to show that the concepts introduced before can be realized in practical computations. We therefore give critical exponents up to quite a high precision as a proof of concept.

In $d = 3$ we expect to see only one nontrivial fixed point belonging to the Ising-class. This was already investigated before in [88]. In Fig. 4.1 is the spike plot with $\eta = 0$ and $\eta = 1/4$ of the $d = 3$ model for a broad range of initial data. As expected we see only one nontrivial spike with a pronounced peak at $\sigma_{\text{cr}} \approx 3.76$ and $\sigma_{\text{cr}} \approx 1.65$ respectively. We are also providing the sign of the scalar part at the endpoint depending on the initial data. We clearly see the change of the sign at the position of the spike. We identify $\sigma = u''(0)$ at the spike as the critical parameter belonging to the Wilson-Fisher fixed-point solution.

As mentioned, we use a σ that is a bit to the right of the spike to compute our approximation of the fixed-point solution. An example for $\eta = 1/4$ is given in Fig. 4.2. We see that the solution a bit to the left has an additional tail that does bend down. This is a behavior we do not expect and is unphysical. This can be understood, as the Ising solution should have an effective potential that is convex. We therefore discard this part of the solution by taking the one to the right of the spike.

We stated at the end of the last section that we compute η in the physical minimum. We also

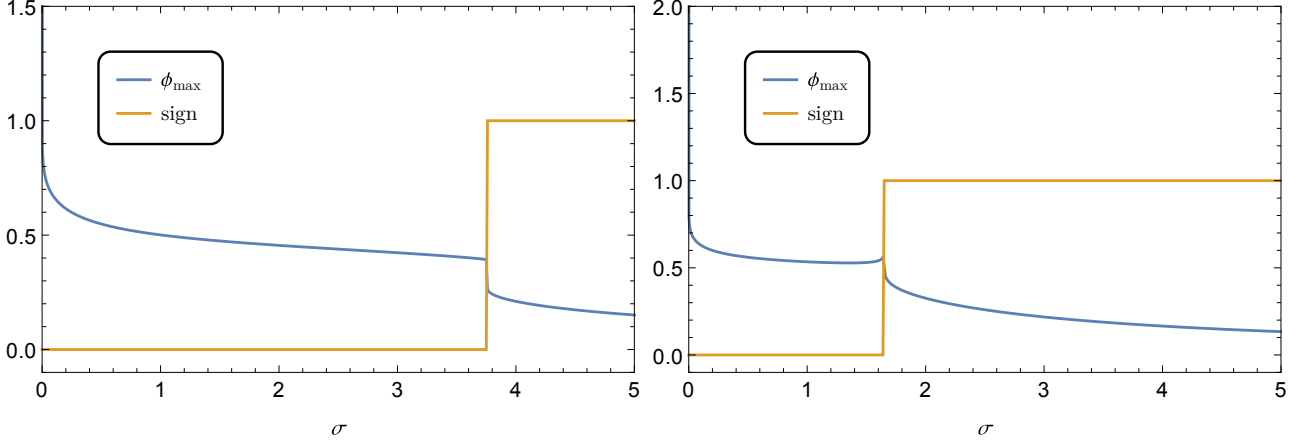


Figure 4.1.: We provide the spike plot for even superpotentials $\sigma = u''(0)$. On the left hand side is the one for $\eta = 0$. We see ϕ_{\max} and $(\text{sgn}(S_{\eta,d}) + 1)/2$. The near vertical lines are in fact jumps and not continuous parts. These jumps give away the critical value as we expect. On the right we have $\eta = 1/4$, where the spike is shifted to the left. The reason is presented in the discussion of general dimensions Sec. 4.2. At the moment it is important that we have only one spike for both values of η .

| | σ_{cr} | η_{in} | η_{out} | ν | | σ_{cr} | η_{in} | η_{out} | ν |
|---------------------------------|----------------------|--------------------|---------------------|--------|---------------------------------|----------------------|--------------------|---------------------|--------|
| LPA ⁰ _{n=1} | 2.0239 | 0.1880 | 0.1599 | 0.7112 | LPA ⁰ _{n=2} | 2.3558 | 0.1807 | 0.1531 | 0.7094 |
| LPA' _{n=1} | 2.1333 | 0.1736 | 0.1736 | 0.7076 | LPA' _{n=2} | 2.4794 | 0.1670 | 0.1670 | 0.7060 |

Table 4.1.: We see the critical parameters for different regulator $n = 1, 2$ and η schemes. LPA⁰ refers to η_0 .

introduced η_0 before. We provide the values of σ_{cr} for these two scenarios and the two regulator choices in Tab. 4.1. There, we also find the values for the critical exponent ν belonging to the correlation length. As we employ a pseudospectral method formulated in ϕ to calculate the critical exponents we are picking up even and odd fluctuations of the superpotential. We translate these into fluctuations of the dimensionless effective potential

$$v_{\text{bos}} + \Delta v \sim (u + \Delta u)^2/2|_{\Delta u^{0,1}} \sim v_{\text{bos}} + u\Delta u.$$

It shows that only fluctuations belonging to the symmetry class of the potential are respecting the symmetry of the effective potential. The eigenvalues θ^+ of those can be found in Tab. 4.2. The ones not respecting the symmetry (θ^-) are also listed there. They would belong to magnetic fluctuations in an Ising model. As argued before we can provide very accurate numbers for the critical exponents. This could be achieved by the fact that only a finite range

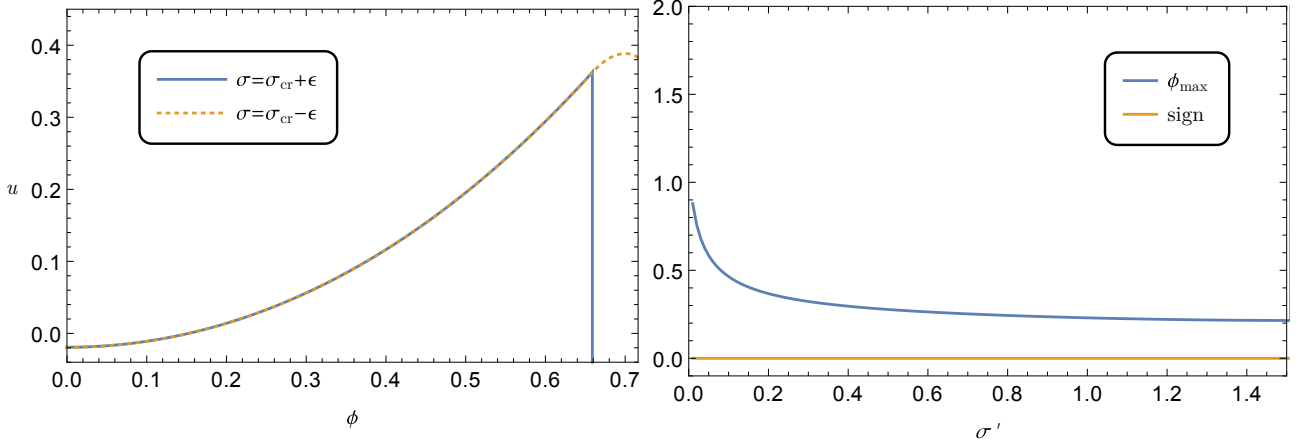


Figure 4.2.: To the left we see the two kind of numerical solutions we obtain near the global fixed-point solution. We used $\eta = 1/4$ and ϵ is of the order 10^{-15} . The blue vertical line indicates the singularity appearing for the blue curve. The yellow curve ends at the right border of the plot. Both solutions nearly coincide in their shared interval of existence. On the right we have a spike plot for an odd superpotential u with $\sigma' = u'(\phi_0)$. We have no spike for finite σ' . This indicates the absence of a fixed-point solution for odd superpotentials in $d = 3$.

of the solution is necessary to calculate the eigenvalues.

4.1.3. $d = 2$

We just discussed the Wess-Zumino model in $d = 3$ and now turn our attention toward the model in $d = 2$. Here we can compare our results with the ones from the conformal field theories. We expect to observe an infinite number of fixed points in our spike plots. At least this would be true if we adopt our anomalous dimension dynamically. When we choose one finite positive anomalous dimension we see only a finite number of spikes. In Fig. 4.3 we find some indication that this is true. We note that lowering η provides more spikes in the plot. We know from CFT that the higher critical models have a very small anomalous dimensions. In order to see these one has to go to ever smaller anomalous dimension.

We limit ourselves and only look at the first two critical models. This means the Ising class with two minima and the tri-Ising class with three minima. In order to find the tri-Ising class a spike plot for an odd superpotential u is in order Fig. 4.4.

The critical parameters of the Ising class can be found in Tab. 4.3. In Tab. 4.4 the critical exponents are given. We observe for the Ising class only one relevant direction respecting the

| | θ_1^+ | θ_2^+ | θ_3^+ | θ_4^+ | | θ_1^- | θ_2^- | θ_3^- | θ_4^- |
|----------------|--------------|--------------|--------------|--------------|----------------|--------------|--------------|--------------|--------------|
| LPA $^0_{n=1}$ | 1.4060 | -0.3510 | -2.5715 | -5.1730 | LPA $^0_{n=1}$ | 0.5940 | -1.4102 | -3.8274 | -6.6048 |
| LPA $'_{n=1}$ | 1.4130 | -0.3824 | -2.6813 | -5.4004 | LPA $'_{n=1}$ | 0.5868 | -1.4760 | -3.9916 | -6.9056 |
| LPA $^0_{n=2}$ | 1.4097 | -0.3500 | -2.5281 | -5.0357 | LPA $^0_{n=2}$ | 0.5903 | -1.3941 | -3.7438 | -6.3997 |
| LPA $'_{n=2}$ | 1.4165 | -0.3773 | -2.6200 | -5.2216 | LPA $'_{n=2}$ | 0.5835 | -1.4500 | -3.8791 | -6.6435 |

Table 4.2.: In the left table are the values for the even critical exponents in $d = 3$. They respect the symmetry of the model. The right table consist of the odd ones. The values are obtained with the Slac derivative for different flow equations as described in the text.

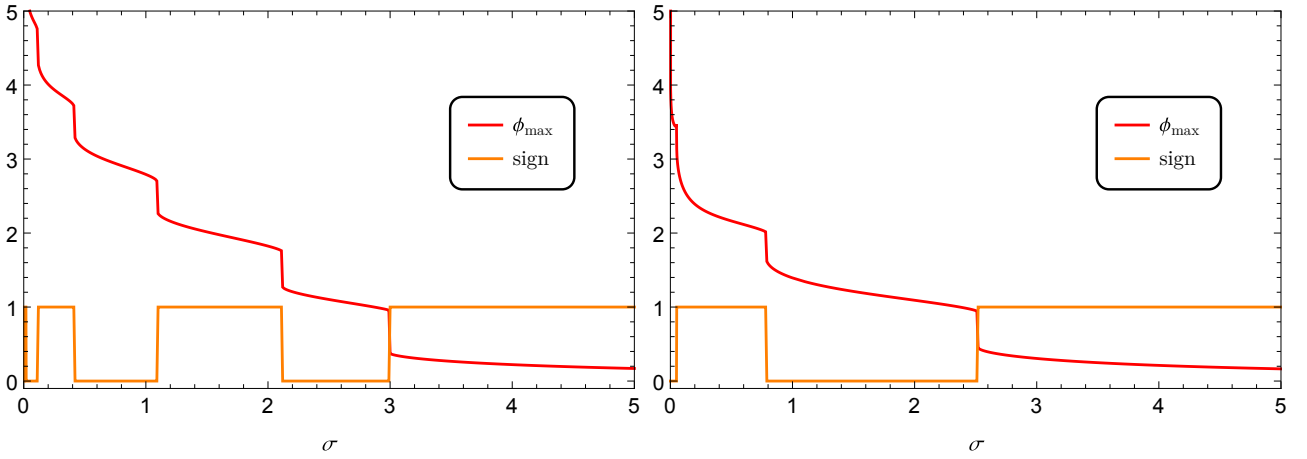


Figure 4.3.: On the left hand side is the spike plot for $\eta = 1/10$ with $\sigma = u''(0)$. We see ϕ_{\max} and $(\text{sgn}(S_{\eta,d}) + 1)/2$. Again both show us the same critical value. On the right we chose $\eta = 1/4$. We see that the number of spikes is changing with η . We also observe that the spikes are denser for smaller σ . The spike indicating the solution for the Ising fixed points is the rightmost.

symmetry of the model. This coincides with our expectations.

Now let us turn to the tri-Ising class solution. In Tab. 4.5 we give the critical parameters of this model. We find only one relevant direction that respects the symmetry as can be seen in Tab. 4.6. Again odd fluctuations are denoted with a minus sign and the wording is chosen w.r.t. the effective potential $u^2/2$. The interesting fact that there is only one relevant direction will be discussed in the following Sec. 4.2. This is in contrast to a bosonic model in which the number of relevant direction is increasing by one when one goes to the next universality class, e.g. Ising has one relevant direction and tri-Ising has two. We also still find two positive odd

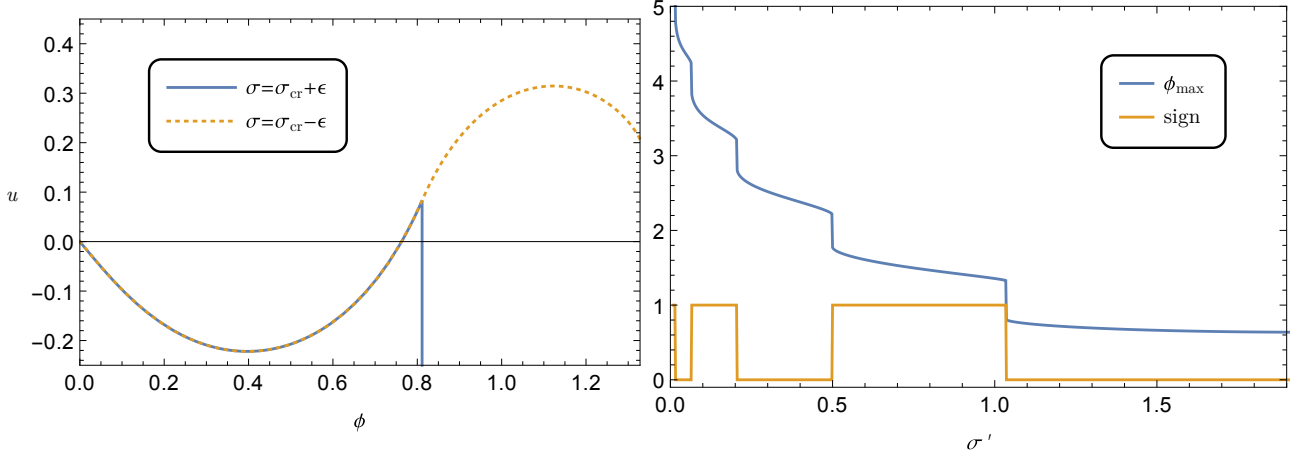


Figure 4.4.: On the left we are provided with a tri-Ising class numerical solutions for $\eta = 1/10$. On the right is the spike plot for the odd superpotentials. Note that we have several spikes. The critical parameter for the tri-Ising class is determined by the rightmost.

eigenvalues θ^- . We cannot provide the LPA⁰ case with η_0 as it is always zero for odd potentials.

The shape of the effective tri-Ising class fixed-point potential V_{Bos} has the interesting property that although the \mathbb{Z}_2 symmetry may be restored the supersymmetry can never be spontaneously broken. This is immanent in the fact that the potential is odd. This was already discussed in the quantum mechanics chapter 3.3.

Altogether, we have the quite general statement that even superpotentials u are supersymmetric if and only if the \mathbb{Z}_2 symmetry is broken. So we cannot restore both symmetries. The class of odd superpotentials u on the other hand can have a phase with restored \mathbb{Z}_2 symmetry and supersymmetry.

| | σ_{cr} | η_{in} | η_{out} | ν | $2\theta_1^-$ |
|--|----------------------|--------------------|---------------------|--------|---------------|
| LPA ⁰ _{$n=2$} | 1.7594 | 0.4386 | 0.3386 | 1.2809 | 0.4386 |
| LPA' _{$n=2$} | 1.9478 | 0.3971 | 0.3971 | 1.2478 | 0.3971 |

Table 4.3.: Critical parameters for the supersymmetric Ising class in $d = 2$.

4.2. Critical dimensions

In the following we want to work out a criteria how many nontrivial fixed points we expect for a given dimension. In order to do so we have to study the mass dimension of the couplings.

| | | | | | | | | | |
|----------------|--------------|--------------|--------------|--------------|----------------|--------------|--------------|--------------|--------------|
| Slac: | θ_1^+ | θ_2^+ | θ_3^+ | θ_4^+ | Slac: | θ_1^- | θ_2^- | θ_3^- | θ_4^- |
| LPA $^0_{n=2}$ | 0.7807 | -0.4383 | -2.2224 | -4.5711 | LPA $^0_{n=2}$ | 0.2193 | -1.2602 | -3.3268 | -5.9549 |
| LPA $'_{n=2}$ | 0.8014 | -0.5125 | -2.5416 | -5.3095 | LPA $'_{n=2}$ | 0.1986 | -1.4365 | -3.8335 | -6.9700 |

Table 4.4.: Even (left) and odd (right) critical exponents of the Ising class in $d = 2$.

| | | | | |
|---------------|-----------------------|--------------------|---------------------|--------|
| | σ'_{cr} | η_{in} | η_{out} | ν |
| LPA $'_{n=2}$ | 0.3794 | 0.3201 | 0.3201 | 1.6653 |

Table 4.5.: Critical parameters for the supersymmetric tricritical Ising class in $d = 2$.

| | | | | | | | | | |
|---------------|--------------|--------------|--------------|--------------|---------------|--------------|--------------|--------------|--------------|
| | θ_1^+ | θ_2^+ | θ_3^+ | θ_4^+ | | θ_1^- | θ_2^- | θ_3^- | θ_4^- |
| LPA $'_{n=2}$ | 0.6005 | -0.3129 | -1.5245 | -3.0465 | LPA $'_{n=2}$ | 0.8399 | 0.1601 | -0.8780 | -2.2473 |

Table 4.6.: Even (left) and odd (right) critical exponents of the tri-critical Ising class. The even ones are those belonging to the symmetry class of the model.

From a perturbative point of view one can easily determine how many relevant couplings do exist. Just read of the trivial scaling dimension from the Lagrangian. In the Wess-Zumino model the dimensions of the fields are given by

$$[\phi] = \frac{d-2+\eta}{2}, \quad [\psi] = \frac{d-1+\eta}{2}, \quad [F] = \frac{d+\eta}{2}. \quad (4.2.1)$$

We have already included the anomalous scaling as an improvement for our calculations. Looking at the terms that appear in the potential we gain the couplings and their mass dimension

$$g_{F,n} F \phi^n \Rightarrow [g_{F,n}] = -d + [F] + n[\phi] = (n-1)\frac{d}{2} - n + \frac{n+1}{2}\eta,$$

$$g_{\psi,n} \bar{\psi} \psi \phi^n \Rightarrow [g_{\psi,n}] = -d + 2[\psi] + n[\phi] = n\frac{d}{2} - (n+1) + \frac{n+2}{2}\eta.$$

The couplings $g_{F,n}$ are the ones showing up in FW' and the $g_{\psi,n}$ are the ones in $\bar{\psi}\psi W''$. As both are related also the mass dimensions are related by a shift in n by one. We therefore only discuss $g_{F,n}$ from here on. A coupling turns infrared relevant when its dimension becomes positive. A coupling is marginal if its mass dimension vanishes,

$$0 \stackrel{!}{=} [g_{F,n}] \Rightarrow d = \frac{2n - \eta(n+1)}{n-1}.$$

If we want a \mathbb{Z}_2 -symmetric potential we have to restrict ourselves to either odd or even n . Choosing odd ones we have

$$d = \frac{(1 - \eta) + m(2 - \eta)}{m} \stackrel{\eta=0}{=} 3, \frac{5}{2}, \frac{7}{3}, \dots \quad n = 2m + 1, \quad m \in \mathbb{N}.$$

The $m = 0$ coupling $g_{F,1}$ is just the mass always being relevant.

The first nontrivial fixed point of this class should therefore appear for $d = 3 - \epsilon$. In the even case we find

$$d = \frac{4m - \eta(2m + 1)}{2m - 1} \stackrel{\eta=0}{=} 4, \frac{8}{3}, \frac{12}{5}, \dots \quad n = 2m, \quad m \in \mathbb{N} \quad (4.2.2)$$

For $m = 0$ we find the vacuum energy which is also always relevant in a Yukawa model but here absent due to supersymmetry. In $d = 4 - \epsilon$ we should observe a non-trivial fixed point. We conclude that we should find just one Wilson-Fisher fixed point in $d = 3$ with an even superpotential W' . Indeed that was the case. We can see that for vanishing η the number of relevant couplings increases to ∞ as d goes to 2. This coincides with the CFT result.

Up to now we have only done an analysis that would be valid in perturbation theory. As we saw in the discussion of the model in $d = 2$ we still have fixed points with one, two, and three relevant directions. This can be understood as we are away from the Gaussian fixed point at which perturbation theory is valid.

What have we learnt from this analysis? In the spike plot the Gaussian fixed point is located at coupling $\sigma^{(\prime)} = 0$. For a dimension d just below a critical dimension determined by (4.2.2) we can hope that a near Gaussian fixed point is emerging which has as many relevant couplings as our analysis suggest. In Fig. 4.5 we give the spike plot for even and odd superpotentials W' using the dimensionless formulation (4.1.9). We can see that the dimensions at which the new critical models emerge are exactly the ones for $\eta = 0$. This can be understood as in the small coupling regime also η is quite small. While we use a fixed η for the odd superpotential W' we employ η_0 introduced before for the even ones. One can see how the number of spikes is limited for a fixed η in $d = 2$ while the dynamically chosen η_0 gives us an increasing frequency of sign changes as we approach $\sigma = 0$.

Now we can finally understand the shift of the position of the spike by varying η . Increasing η decreases the critical dimension. Therefore the fixed-point solutions are pushed toward the Gaussian solution in order to vanish for sufficient large η .

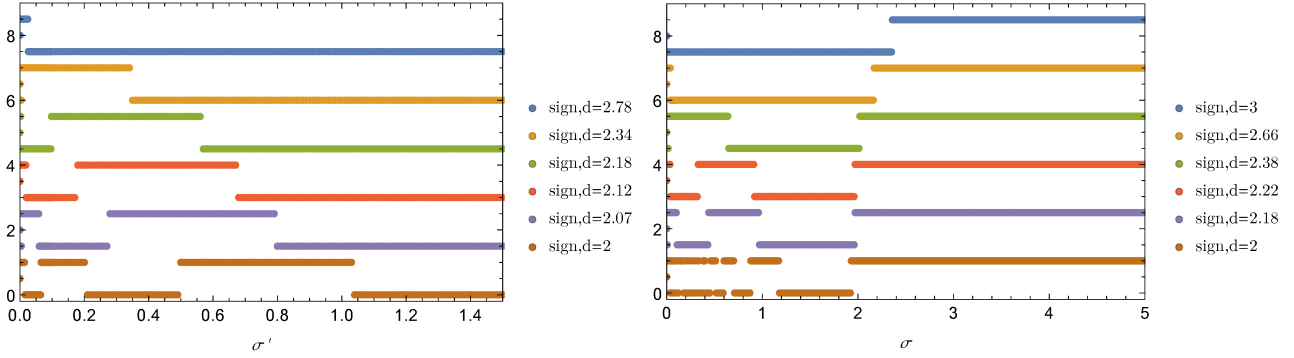


Figure 4.5.: We give the spike plots for different dimensions d . We only depict the change of sign of the scaling part to avoid overlappings in this plot. The plots are shifted by some constant value along the ordinate each. On the left hand side we give the different spike plots for fixed $\eta = 1/10$. On the right we want to see a wide range of models. Therefore we are using η_0 i.e. η evaluated at $\phi_0 = 0$ that is nearly zero for a near Gaussian solution. This allows us to also see models in $d = 2$ for very small η . This gives us the high number of jumps in the sign that can be observed for small σ .

4.3. Spikes from polynomials

As was pointed out in [137] one can find the fixed points by doing a polynomial expansion around $\phi = 0$ so that $W = a_n \phi^n$. We do so by producing a spike plot using an estimate for the radius of convergence. By adding the information given by the sign of the coefficients one can get a good estimate for the location of the nearest singularity. Some technical informations can be found in [138]. If the mentioned singularity is positioned on the real axis it prevents us from going to larger values in the field using the shooting method. We use a Domb-Sykes plot with the root criteria and extrapolating to $1/n = 0$. The estimate for the radius of convergence depends on the chosen initial conditions and the used truncation order.

We only investigate even superpotentials u , e.g. the Ising class or tetra-Ising class. In doing so one has only two free parameter. One is the chosen anomalous dimension and one the free parameter of the potential. This is completely analogue to the previously discussed shooting method scenario.

For reasons of convenience we actually use an expansion in $\rho = \phi^2/2$. This does not influence the results for the radius of convergence when one translates it appropriately into the coordinate system with ϕ . For the numerical approach we derived an implicit dependence of the higher

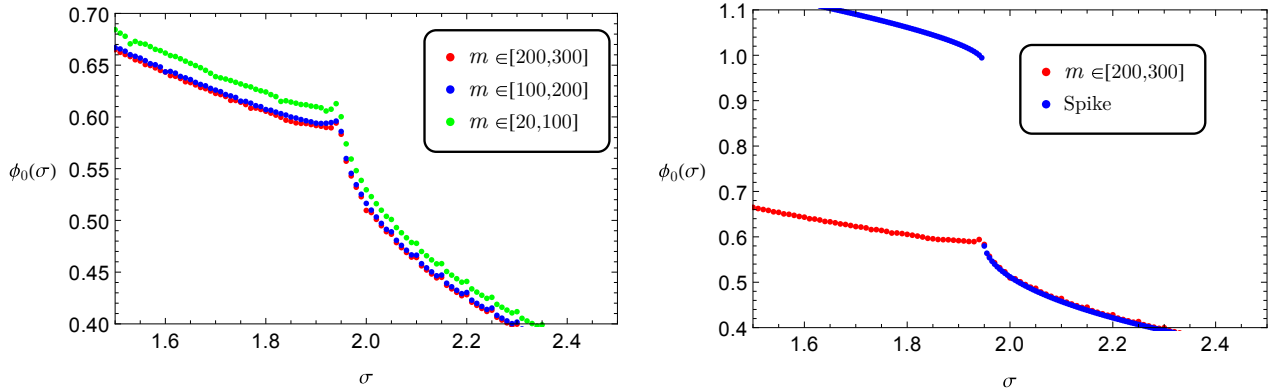


Figure 4.6.: We see the spike plot for the first critical supersymmetric models in $d = 2$ with η chosen as the LPA' value. On the left we compare different truncations. On the right is a comparison of the spike plot given by the shooting method with the one from the polynomial expansion. $\phi_0(\sigma)$ is determined by the estimate for the radius of convergence or in case of the shooting method as described before. Note the nice agreement on the right of the spike. This indicates that the singularity spotted by the polynomial expansion is the same as the one stopping the numerical integration.

order coefficients on the lower ones. We parametrize our spike plot in the same way as in the previous Secs. 4.1.2 and 4.1.3 and get Fig. 4.6. We can see that for a truncation order of ≈ 200 the extrapolation already seemed to have converged. In fact one already gets a much better estimate by only taking the coefficients $a_{50} \dots a_{100}$ (not depicted). Comparing the convergence radius values to the right of the spike with the one from the shooting method indicates that the singularities spotted by both methods coincide. Note that the singularity does not vanish as we go to the left of the spike. It is shifted into the complex plane as we see later on and is only moving slowly (Fig. 4.8). At the moment it remains unclear whether we are tracking the same singularity on both sides of the spike. It could be that we start to track a different singularity. Therefore we cannot conclude on the fate of the original singularity for decreasing σ by now. But there is still information we can exploit in order to learn more. We can try to look at the sign pattern of the coefficients to determine the angle in the complex plane at which the singularity is positioned.

Before doing so we look at an actual Domb-Sykes plot of the Ising model on the left of Fig. 4.7. We have suppressed the sign in this plot. To make up for this we give the sum of all signs normalized by the number of coefficients for a broad range of coefficients in the right plot of

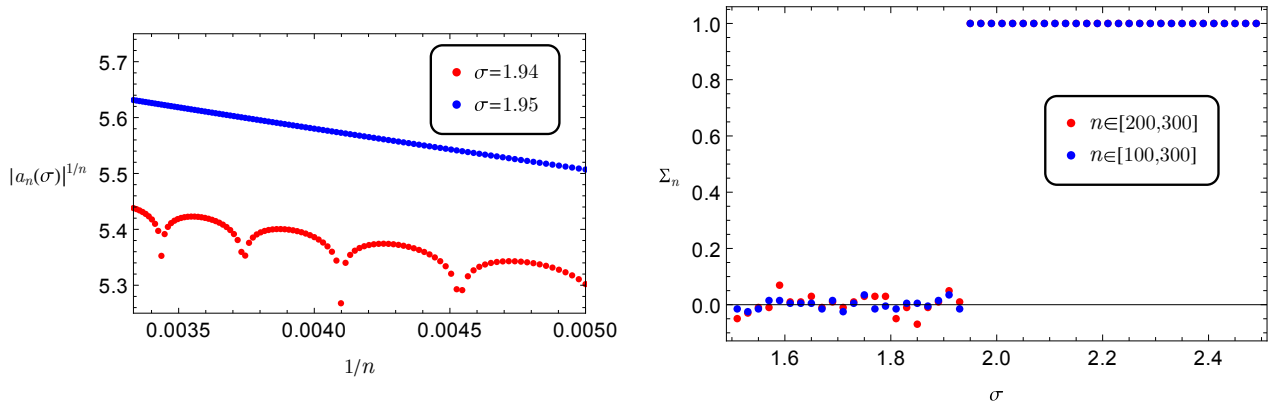


Figure 4.7.: We give a Domb-Sykes plot of the supersymmetric Ising model in $d = 2$ for two different values of σ . The critical value lies in between those two. Note the change of behavior. For $\sigma > \sigma_{\text{cr}}$ we obtain a straight line. This is a hint for a singularity positioned on the real ρ axis. To the left of the spike we have some structure indicating a periodicity and a sign change. This picture is supported by the plot on the right hand side. Plotted is the averaged sign of the expansion coefficients. We are taking the coefficients indicated by the interval for n into account. Down to σ_{cr} we have a constant sign and afterward we have an approximate average of 0.

the same figure.

First we focus on the right side of the spike. The sign of almost all coefficients is positive. This indicates that the singularity is positioned on the positive ρ axes and therefore also on the real ϕ axes. As we have already concluded both discussed singularities coincide. Now we are interested in the fate of the singularity when we go to the left of the spike. The sign is clearly not constant any more indicating that the singularity has moved into the complex ϕ plane. If it is moving continuously in σ the sign pattern changes slowly. We look at the length of a cycle with constant sign as a discrete function in σ in Fig. 4.8. We see a monotonous function with decreasing variation going further to the left of the spike. This is a good indication that we track the same singularity all the time.

We want to note that our ODE is real. This gives a mirror symmetry of complex conjugating. Thus, we expect to have non-real singularities that appear in complex conjugated pairs. In the plot, we have suppressed the singularity in the lower half of the complex plane. It remains unclear from the analysis done whether the singularity on the real axis is degenerate or merges with a second singularity. In the latter case it could be absent at the critical value. We do not explore any more into this direction. It does not seem to provide us with any further useful

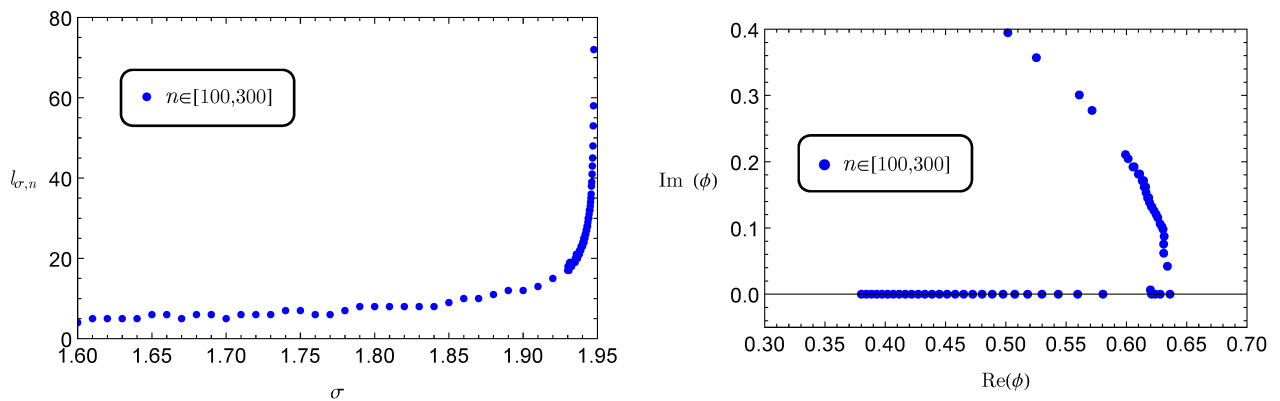


Figure 4.8.: We see a plot of the length of a cycle of coefficients with a constant sign on the left hand side. Combining this information with the radius of convergence we can give an estimate for the path of the singularity we have spotted in the complex plane. This is done on the right. We estimated the polar angle $\phi = \pi/l_{\sigma,n} - \delta_\phi$. Here we chose δ_ϕ such that the discretization error done by having only a maximum length of a cycle is subtracted. In this way the plotted singularity is starting on the real axis. Still the angles are elements of a discrete set $\phi \in \{\pi/n, n \in \mathbb{N}\}$. At the critical σ the singularity starts to move into the complex plane. We chose to plot only the singularity in the positive complex plane. Our problem is real and we expect to have only complex conjugated pairs of singularities that are not real.

information. It is noteworthy that the trajectory of the singularity may put a constraint on the rate of convergence of pseudospectral methods¹.

4.4. Critical exponents from different methods

The following discussion could also be made for a scalar Ising model. We do nonetheless work with the Wess-Zumino model in $d = 2, 3$ as we use the results in the following chapter⁵ about emergent supersymmetry.

Beside the search for a global solution or an expansion in polynomials around $\phi = 0$ there is also the possibility to expand around the physical minimum. In LPA' the anomalous dimension η is typically defined at this minimum. This allows for the inclusion of perturbations of η in a straightforward manner. Given the potential in terms of the expansion coefficients one can also express η in those and eliminate η from the flow equation. Solving the resulting system for the fixed point and linear perturbations around it effectively means that fluctuations in η where included in the linearized equation. So equation 4.1.10 turns effectively into

$$-\theta\delta u(\phi) = H(u, \eta, \partial_\phi)\delta u(\phi) + \delta\eta\partial_\eta(\partial_t u) \quad (4.4.1)$$

$$\begin{aligned} \delta\eta &= \eta(u + \delta u, u' + \delta u', u'' + \delta u'')|_{\phi_0 + \delta\phi_0} - \eta(u)|_{\phi_0} \\ &= \partial_{u''}\eta(\delta u'' + u'''\delta\phi_0) + \partial_{u'}\eta(\delta u' + u''\delta\phi_0) + \partial_u\eta(\delta u + u'\delta\phi_0) \end{aligned} \quad (4.4.2)$$

Solving in a polynomial truncation is a standard technique which we do not want to elaborate on. In the last chapter on the $O(N)$ model Sec. 6.3 more details are given. We just give the ansatz for even u

$$u(\rho) = \sum_{i=1}^{\text{trunc}} a_i(\rho - \rho_0)^i, \quad \delta u(\rho) = \sum_{i=1}^{\text{trunc}} (a_i + \delta a_i)(\rho - (\rho_0 + \delta\rho_0))^i - u(\rho)|_{\delta^1}, \quad \rho = \phi^2/2.$$

trunc is just a natural number giving the truncation order of the polynomial expansion. We give the critical exponents obtained using this method in Tab. 4.7². The flow equation used was $d = 3$ with $r_{2,1}$.

Comparing them to the Slac numbers without varying η shows a slight deviation. Especially the first non relevant eigenvalue shows a significant shift. We have to take into account that

¹As long as it is actually present for the global fixed-point solution.

²As we already know the fixed-point solution we used the value of the zero $\rho_0 = \phi_0^2/2$ and the first derivative at this zero $u'(\rho_0) = u'(\phi_0)/\phi_0$ as input for the polynomial expansion. Starting with these we compute the fixed-point values of the other a_i .

the Slac derivative does not satisfy (4.4.2) in the physical minimum. One problem is that the shift in the minimum $\delta\phi$ does not allow to use the functional eigenvalue solver proposed.

We therefore use another shooting method described before in Sec. 2.4.1.

All the numbers for the $d = 3$ and $r_{2,1}$ case are given in the mentioned Tab. 4.7. Note that the here used implementation of the shooting method is providing a trend on how the eigenvalues change by implementing $\Delta\eta$. $\Delta\eta$ is scaled down in the fluctuation equation by a factor in order to do so. The actual numbers implementing it to full extend are the same as the ones obtained within the polynomial approximation.

We want to point out that η in the LPA' truncation is typically far off from the one obtained by other methods. This is immanently seen when we look into the literature dealing with the scalar $O(1)$ model in $d = 2$ [139]. Therefore the equation obtained for η seems not too good³ and so also variations of it may or may not improve the obtained critical exponents. As long as all three methods give the same sign for all the eigenvalues and the critical ones are only slightly shifted we should be able to trust our qualitative picture.

We may start to investigate how different fluctuations look like depending on the used method. To do so we pick out the two most relevant fluctuations and give the plots of these in Fig. 4.9 and 4.10. We also insert the polynomial solution into the fluctuation ODE within its radius of convergence and look how good it fulfills it. This is shown in Fig. 4.11. As an error estimate for the shooting method we depict a dependence of the eigenvalues θ_1^+ and θ_2^+ w.r.t. the $\delta\eta$ input in Fig. 4.12. Firstly, we see a linear behavior coinciding with the fact that we are dealing with a linearized theory. Secondly, our error is in the range of percents.

For the sake of completeness we give in Tab. 4.8 the numbers for the Ising model in $d = 3$ and $d = 2$ for both regulators when possible. We see that for the odd critical exponents a stronger shift is possible as these eigenvalues are more strongly correlated to the anomalous dimension.

We also observe that including $\delta\eta$ is shifting the eigenvalues at most to smaller values for the examined fixed points. To show this was the main point of using the shooting method with a scaled $\Delta\eta$ term. Therefore we seem to overestimate the number of relevant directions at most using the Slac derivative method but not underestimate it. The latter being a catastrophic scenario, while the former just makes the fine tuning toward a fixed point much easier.

We discussed this topic at this point since we encounter a similar one in the next chapter.

³at least in LPA'

⁴The fixed-point solution was found via a pseudospectral method. The critical exponents were found in a polynomial ansatz as described in this section.

| | θ_1^+ | θ_2^+ | θ_3^+ |
|------------------------------|--------------|--------------|--------------|
| Slac | 1.413 | -0.382 | -2.681 |
| shoot $\Delta\eta = 0$ | 1.413 | -0.382 | -2.681 |
| shoot $\Delta\eta \neq 0$ | 1.379 | -0.393 | -2.682 |
| Polynom $\Delta\eta = 0$ | 1.413 | -0.382 | -2.681 |
| Polynom $\Delta\eta \neq 0$ | 1.385 | -0.765 | -2.658 |
| SUSY NNLO [130] ⁴ | 1.410 | -0.715 | -1.490 |

Table 4.7.: We see the different values of the even critical exponents computed with different methods. The first line gives the already presented results from the Slac derivative. The second line are the results from the shooting method without varying η . The third line includes a variation of η using the shooting method. The fourth and fifth line are in complete analogue the ones for the polynomial expansion. We expect the first, second, and fourth line to coincide. This is indeed the case. We also compare in the last line to the most recent values in the literature. The agreement is best with the polynomial ansatz as this method was used to compute the spectrum in the cited paper.

| | | | | | |
|---------------------------|--------------|--------------|--------------|--------------|--------------|
| $d = 3 \ n = 1$ | θ_1^+ | θ_2^+ | θ_3^+ | θ_1^- | θ_2^- |
| Slac | -1.413 | 0.382 | 2.681 | -0.587 | 1.476 |
| shoot $\Delta\eta \neq 0$ | -1.379 | 0.393 | 2.682 | -0.528 | 1.461 |
| $d = 3 \ n = 2$ | θ_1^+ | θ_2^+ | θ_3^+ | θ_1^- | θ_2^- |
| Slac | -1.416 | 0.377 | 2.620 | -0.584 | 1.450 |
| shoot $\Delta\eta \neq 0$ | -1.390 | 0.387 | 2.622 | -0.533 | 1.423 |
| $d = 2 \ n = 2$ Ising | θ_1^+ | θ_2^+ | θ_3^+ | θ_1^- | θ_2^- |
| Slac | -0.801 | 0.513 | 2.542 | -0.199 | 1.437 |

Table 4.8.: We give the eigenvalues after including the correction provided by $\Delta\eta$ and compare them with the previous ones. We see a trend that the relevant and near relevant eigenvalues tend to be corrected to smaller, i.e. less relevant, values.

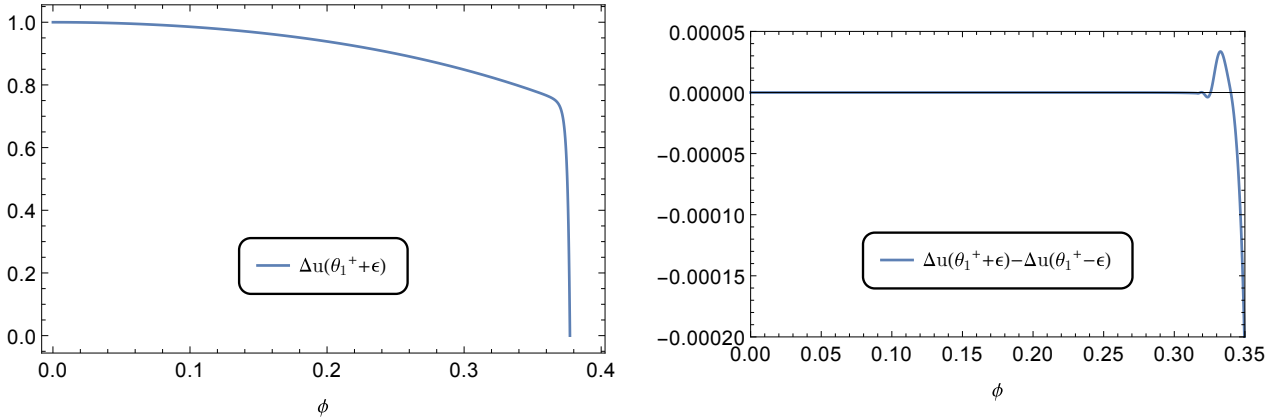


Figure 4.9.: We give the approximate eigenfunction belonging to the first eigenvalue $\theta_1^+ \approx -1.43$. On the left we see the shape of an approximate solution to the eigenvalue problem that diverges to minus ∞ . On the right we give the difference between a solution diverging to minus ∞ and one diverging to plus ∞ . As we can see we should have determined the correct solution up to $\phi \approx 0.3$. The ϵ is of order 10^{-9} and the solution are normalized to 1 at the origin. Here we fixed $\delta\eta$ as described in the discussion of the present shooting method.

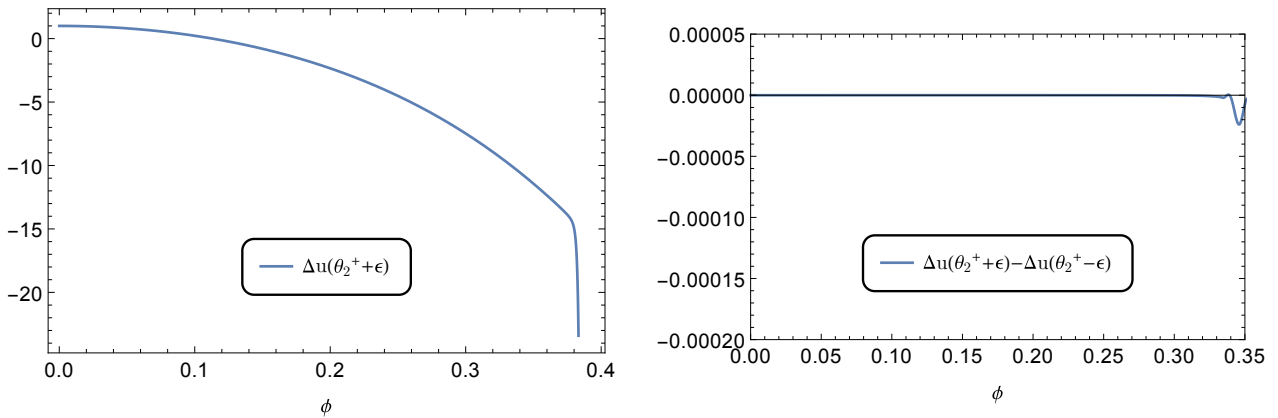


Figure 4.10.: We give the approximate eigenfunction belonging to the second eigenvalue $\theta_2^+ \approx 0.39$. To the left is again an approximate solution. The right figure shows the estimated error w.r.t. the correct solution to the eigenvalue problem for given $\delta\eta$.

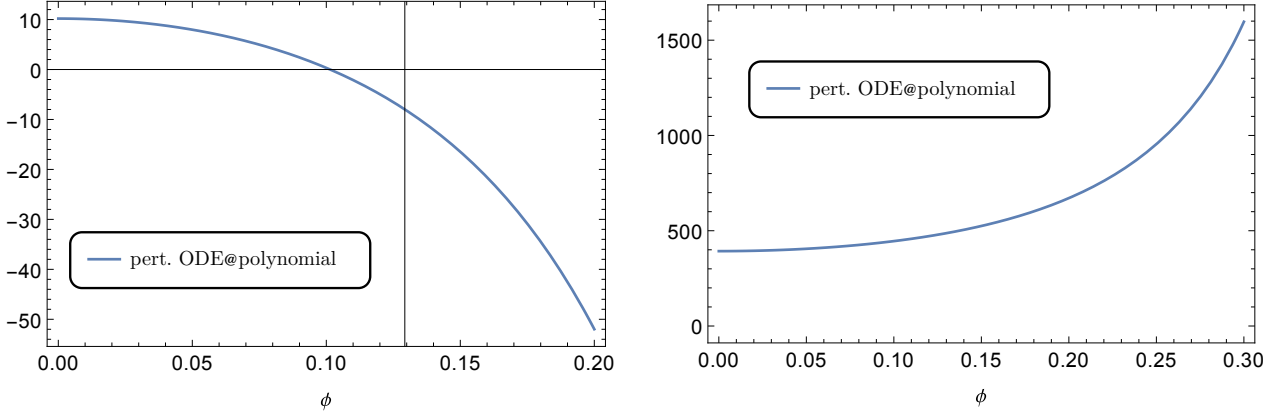


Figure 4.11.: We give the value of the fluctuation ODE when we insert the polynomial solution into it. On the left we give it for the fluctuation belonging to θ_1 and on the right the one for θ_2 .

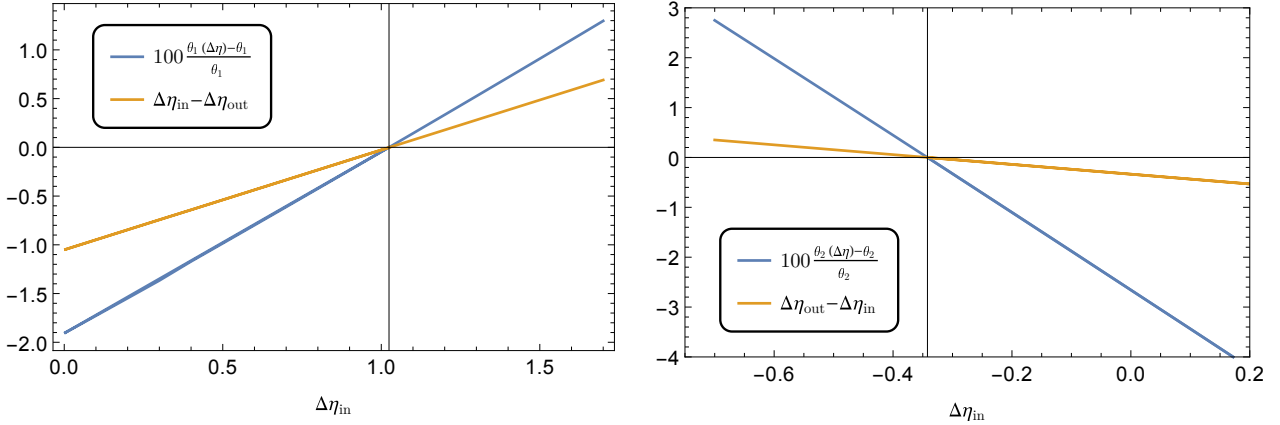


Figure 4.12.: The relative error in percent of the obtained eigenvalues for fixed $\Delta\eta_{\text{in}}$ w.r.t. these (Blue curve). We also give the dependence of the obtained $\Delta\eta_{\text{out}}$ computed in the new minimum with respect to the input parameter $\Delta\eta_{\text{in}}$ (Yellow curve). We see the normalized numbers times $\Delta\eta\Delta u(0)$. In the actual computations $\Delta u(0) = 10^{-6}$ was chosen. So we stay in the linearized regime. The results are given on the left for θ_1^+ and on the right for θ_2^+ of the $d = 3, n = 2$ case.

As a side mark note that in an NLO truncation one can choose $\eta = -\partial_t \log Z_k(0)$. Then in the scaling part $\delta\eta$ only shows up at $\phi = 0$. Given such a definition for η $\delta\phi$ vanishes and an inclusion of the perturbation in the Slac formalism is much easier.

4.5. Summary

In this chapter we introduced the Wess-Zumino model in $d = 2$ and $d = 3$ dimensions. We employed the spike plots to reliably obtain the fixed-point solutions. Using the Slac derivative we were able to compute the critical exponents to high precision within the given truncation. To do so we used the fact that only a finite region is necessary to compute these. This should be true for a large range of models which show a sign change in the function in front of the highest derivative of the potential term. We are using the fixed-point solution obtained in the $d = 3$ case for our further computations in the next chapter.

We showed that this Ising class solution can also be obtained using a polynomial expansion at the origin. The obtained parameter σ from the spike plot coincides with the one from the polynomial expansion. This gives us another indication that we obtained the correct fixed-point solution. Within the polynomial expansion we tracked the nearest singularity that stopped us from obtaining a global solution when we are to the right of a spike. This singularity moved out of the real axis just at the critical parameter.

At last we studied the difference in the numbers for the critical exponents when we vary η . We expanded in a polynomial truncation in the physical minimum and used a shooting method to obtain the critical exponents when we include $\Delta\eta$ in the fluctuation equation. We saw that we got the same numbers as from the Slac derivative when we artificially set $\Delta\eta = 0$ with both methods. Looking for a self consistent solution in $\Delta\eta$ we obtained the same numbers. We showed that the form of the fluctuations obtained with the polynomial expansion are worse compared to the ones from the shooting method. The latter ones naturally fulfilling the fluctuation ODE.

5. Emergent supersymmetry

5.1. Introduction

After we have discussed the $\mathcal{N} = 1$ Wess-Zumino model in some detail for $d = 3$ we want to turn to a class of more generic Yukawa models. The supersymmetric model is a subclass of these. We want to know whether the supersymmetric class is infrared attractive. In other words: Is the infrared physics of the Yukawa models dominated by the supersymmetric effective theory? This was hinted at in recent studies [140]. With regard to this we calculate the critical exponents and search for eigenfunctions with relevant critical exponents that are softly breaking supersymmetry in the terminology of [55]. By doing so we compute the universality class of this model. Some other work on this was done in the framework of conformal bootstrap [141, 142]. In the following we will describe our further proceedings within this chapter. We start with a general Yukawa model with one Majorana fermion and one real scalar field. We transform its Lagrangian into a part that is invariant under supersymmetry transformations and the soft breaking term. The fixed point of the supersymmetric part was already computed in the last chapter. Setting the additional part to zero our theory is protected from generating it again by supersymmetry. In a technical realization using the FRG we will also have to make sure our regulator respects supersymmetry. Then the flow is supersymmetric. Therefore we have already found a fixed point of the Yukawa model, i.e. the Wess-Zumino one. This can be accomplished by introducing an auxiliary field. As we are seeing in the actual computation later on, we can now parametrize the additional non-supersymmetric part in different ways. In order to avoid ambiguities in calculating our flow we have to fix these degrees of freedom. We can do so by choosing a certain truncation scheme or use a technique that is known as dynamical bosonization in the context of four-Fermi systems. The latter one is more consistent. Nonetheless we give also results for the former approach to see which level of truncation is necessary to get correct qualitative results. We note that in our case the bosonization is not absorbing fermionic degrees

of freedom in a field but rather bosonic ones.

In the end we have a spectrum that is the union of the spectrum of the Wess-Zumino model and additional contributions from the supersymmetry-breaking terms. We simply have to compute how many relevant critical exponents are present in the additional contribution to see how many explicit supersymmetry breaking fluctuations exist in the model. For instance, the vacuum energy provides a non-supersymmetric direction.

5.2. Rewriting the Yukawa model

In the following we rewrite the Yukawa model Lagrangian as described before

$$\mathcal{L}_Y = \mathcal{L}_{\text{susy}} + \mathcal{L}_{\text{rest}}. \quad (5.2.1)$$

The Lagrangian we start with is given by

$$\mathcal{L}_Y = -\frac{1}{2}\partial_\mu\phi\partial^\mu\phi + \frac{i}{2}\bar{\psi}\not{\partial}\psi + V(\phi) - \frac{1}{4}\lambda(\phi)\bar{\psi}\psi. \quad (5.2.2)$$

To make it look more supersymmetric we rewrite it as

$$\begin{aligned} \mathcal{L}_Y &= -\frac{1}{2}\partial_\mu\phi\partial^\mu\phi + \frac{i}{2}\bar{\psi}\not{\partial}\psi + W'(\phi)^2/2 - \frac{1}{4}W''(\phi)\bar{\psi}\psi + \tilde{V}(\phi) + V_0 + \frac{1}{4}h(\phi)\bar{\psi}\psi, \\ \mathcal{L}_{\text{rest}} &= \tilde{V}(\phi) + V_0 + \frac{1}{4}h(\phi)\bar{\psi}\psi, \quad \mathcal{L}_{\text{susy}} = -\frac{1}{2}\partial_\mu\phi\partial^\mu\phi + \frac{i}{2}\bar{\psi}\not{\partial}\psi + W'(\phi)^2/2 - \frac{1}{4}W''(\phi)\bar{\psi}\psi. \end{aligned}$$

V_0 is the vacuum energy. As we expect to have a bounded potential V we can subtract its minimum V_0 and end up with a potential whose minimum is zero, as we have seen in the Wess-Zumino model. We can write this as the square of an function $W' = \sqrt{2V - 2V_0}$. This function defines the supersymmetric part of the Yukawa term. The additional part is cast $h = W'' - \lambda$. We already see that we could have also gone the other way: i.e., Identify λ as W'' and then have some bosonic potential term left. Or do something in between. This freedom has to be dealt with later on.

As mentioned before we want a supersymmetric flow when we restrict ourself to $\mathcal{L}_{\text{susy}}$. Therefore, it is helpful to introduce an auxiliary field in the same way as before. As it enters only in a quadratic way

$$\mathcal{L}_{\text{susy,off}} = -\frac{1}{2}\partial_\mu\phi\partial^\mu\phi + \frac{i}{2}\bar{\psi}\not{\partial}\psi - \frac{1}{2}F^2 + FW'(\phi) - \frac{1}{4}W''(\phi)\bar{\psi}\psi, \quad (5.2.3)$$

we can integrate it out in a path integral formulation. Doing so shows that the off- and on-shell formulation provides us with the same physics. But now we can formulate a supersymmetric

invariant regulator that is quadratic in the fields. We end up with the following ansatz for the effective action

$$\Gamma_k = \frac{1}{2} \left(-(Z_k + Z_{k,\phi})(\partial_\mu \phi)^2 + (Z_k + Z_{k,\psi})i\bar{\psi}\not{\partial}\psi - Z_k F^2 \right) + \quad (5.2.4)$$

$$FW'_k(\phi) - \frac{1}{4}W''_k(\phi)\bar{\psi}\psi + V_{0,k}(\phi) + \frac{1}{4}h_k(\phi)\bar{\psi}\psi. \quad (5.2.5)$$

We have included different wavefunction renormalizations for the different kinetic terms. Also we generate a flow in F^0 at zero momentum which generates $V_{0,k}$. As we count the number of introduced potential terms we end up with three (W, V_0, h) while in the original formulation there were only two (V, λ) . We generated additional degrees of freedom along our reformulation compared to the Yukawa model. Where did this happen?

Let us look at our auxiliary field. Eliminating it using its equations of motion gives us the effective potential

$$V_{\text{bos}} = \frac{W'^2}{2Z} + V_0 = \frac{\tilde{W}'^2}{2Z} + V_{\text{bos}}(\phi_{\text{min}}). \quad (5.2.6)$$

Here $V_{\text{bos}}(\phi_{\text{min}})$ is the minimum of V_{bos} . So we could introduce a new \tilde{W} related to W and V_0 to amount for the additional degree of freedom. Now we can reintroduce an auxiliary field \tilde{F} and recast the effective potential in a form with a constant \tilde{F}^0 term. Doing the calculations shows that F and \tilde{F} are related by

$$\tilde{F} = F - \frac{W'}{2Z} + \sqrt{\frac{W'^2}{4Z} + V_0 - V(\phi_{\text{min}})}. \quad (5.2.7)$$

So a simple shift in the auxiliary field can absorb the generation of a field dependent V_0 . This is very similar to what happens in the dynamic bosonization procedure when dealing with a four-Fermi condensate [95]. There the flow of the coupling in front of the four-Fermi term is set to zero by absorbing it into the flow of a scalar that is representing the condensate which is a bosonic quantity. We follow the same path and go from F to F_k . We choose the flow of F_k in such a way that the flow of $V_{0,k}(\phi)$ is set to a constant. This constant does not enter the right hand side of the flow equation. Therefore we do not actually have to compute it. A fluctuation in this direction just gives us the fluctuation related to the vacuum energy.

In [95] the introduction of a k dependent field was done. Later on [64] it was worked out how to maintain a one-loop structure in the flow equation. The general form of the new flow equation

is given in terms of the old one for constant field plus some corrections

$$\partial_t \Gamma_k[\Phi_k] = \frac{1}{2} \text{STr} [(\Gamma^{(2)} + R_k)^{-1} \partial_t R_k] + \int (G_k \delta_{\Phi_k}) R_k \partial_t \Phi_k - \int \frac{\delta \Gamma_k[\Phi_k]}{\delta \Phi_k} \partial_t \Phi_k \quad (5.2.8)$$

$$= \partial_t \Gamma_k|_{\text{old}} + \int (G_k \delta_{\Phi_k}) R_k \partial_t \Phi_k - \int \frac{\delta \Gamma_k[\Phi_k]}{\delta \Phi_k} \partial_t \Phi_k. \quad (5.2.9)$$

We continue our analysis in the following steps being increasingly less approximate. We consider the model and just simply truncate V_0 to be a constant. Then we do not need any k dependent field. The same is true if we set h to zero and just stick with W'' for the Yukawa interaction. Afterwards we improve our truncation and set the flow of V_0 to a constant by introducing the k dependent F field. We change our flow equation only using the leading order term and therefore in principal lose the one-loop exact property. We neglect this and calculate as if it were still one-loop exact. Then we have a look at the model when we also include the last ingredient and have again a one-loop exact formulation. In all those cases we give the critical exponents. We already saw that there is a difference in those regarding varying η or not. Using the Slac derivative we do not need to calculate the anomalous dimension of the scalar field and the fermions and just use the one of the auxiliary field. This is possible as we are not varying η . When we vary η we have to also implement the different anomalous scaling of ϕ and ψ away from the supersymmetric hypersurface.

5.3. Setting V_0 to a constant

We start with the simple truncation setting V_0 to a constant. Using a very naive ansatz for the effective average action would lead us to such a truncation

$$\Gamma_k = \frac{1}{2} \left(-(Z_k + Z_{k,\phi}) (\partial_\mu \phi)^2 + (Z_k + Z_{k,\psi}) i \bar{\psi} \not{\partial} \psi - Z_k F^2 \right) + F W'_k(\phi) - \frac{1}{4} W''_k(\phi) \bar{\psi} \psi + \frac{1}{4} h_k(\phi) \bar{\psi} \psi.$$

As we mentioned before the constant to which V_0 was reduced does not enter the flow and we neglect it in the further study. We use the $d = 3$ Wess-Zumino fixed point computed before in the LPA' truncation.

As mentioned we neglect the perturbations in the anomalous dimensions and proceed with the Slac derivative to compute the critical exponents. We expect that our qualitative picture regarding the number of relevant supersymmetry breaking fluctuations is at most overcounted

| | | | | |
|----------------------|-----------------|-----------------|-----------------|-----------------|
| $\eta \approx 0.167$ | $\theta_{1,W'}$ | $\theta_{2,W'}$ | $\theta_{3,W'}$ | $\theta_{4,W'}$ |
| susy | 1.416 | -0.377 | -2.620 | -5.222 |
| | $\theta_{1,h}$ | $\theta_{2,h}$ | $\theta_{3,h}$ | $\theta_{4,h}$ |
| susy break | -0.445 | -2.704 | -5.309 | -8.230 |

Table 5.1.: We give the critical exponents in the truncation $V_0 = \text{const.}$ The first row contains the ones that lead at most to a spontaneous breaking of supersymmetry. The second row belongs to fluctuations that break it explicitly.

as discussed before. We only give the critical exponents that belong to the symmetry class of the model; therefore even fluctuations in W' and odd ones in h . All these numbers are summarized in Tab. 5.1. For completeness we also give the dimensionless quantities used to obtain the critical exponents:

$$\tilde{\phi} = k^{-\frac{1}{2}} Z^{-\frac{1}{2}} \phi, \quad (5.3.1)$$

$$\tilde{\psi} = k^{-1} Z^{-\frac{1}{2}} \psi, \quad (5.3.2)$$

$$u = k^{-3/2} Z^{-\frac{1}{2}} W', \quad (5.3.3)$$

$$\tilde{h} = k^{-1} Z h. \quad (5.3.4)$$

For the numerical computation it is useful to exploit the split of the spectrum in the old and the new one. As mentioned this is due to the fact that fluctuations in W' cannot generate ones in h . This gives a block diagonal form of a discretized fluctuation operator.

We observe that there is no relevant operator that explicitly breaks supersymmetry within this truncation. This gives us some motivation to go on with our study and turn to the next case.

5.4. Neglecting h

Another formulation that one can use is to neglect h and just stick with the W'' as the fermionic potential. Doing so leaves us with

$$\Gamma_k = \Gamma_k = \frac{1}{2} \left(-(Z_k + Z_{k,\phi})(\partial_\mu \phi)^2 + i(Z_k + Z_{k,\psi})\bar{\psi}\not{\partial}\psi - Z_k F^2 \right) + F(W'_k(\phi) + \mathcal{V}_k(\phi)) - \frac{1}{4} W''_k(\phi)\bar{\psi}\psi + V_{0,k}(\phi).$$

| | | | | |
|----------------------|--------------------------|--------------------------|--------------------------|--------------------------|
| $\eta \approx 0.167$ | $\theta_{1,W'}$ | $\theta_{2,W'}$ | $\theta_{3,W'}$ | $\theta_{4,W'}$ |
| susy | 1.416 | -0.377 | -2.620 | -5.222 |
| | $\theta_{1,\mathcal{V}}$ | $\theta_{2,\mathcal{V}}$ | $\theta_{3,\mathcal{V}}$ | $\theta_{4,\mathcal{V}}$ |
| susy break | 1.416 | -0.445 | -2.704 | -5.309 |
| | θ_{1,V_0} | θ_{2,V_0} | θ_{3,V_0} | θ_{4,V_0} |
| susy break | 3 | 1.584 | -0.450 | -2.879 |

Table 5.2.: We give the critical exponents in the truncation $h = 0$. The first row contains the ones that lead at most to a spontaneous breaking of supersymmetry. The second and third row belongs to fluctuations that break it explicitly. In the second one we used the formulation in \mathcal{V} and constant V_0 . In the last row are the results formulating it in $V_0(\phi)$ setting \mathcal{V} to zero.

We have added now two bosonic potential terms. We have the correction to the bosonic part of the superpotential \mathcal{V} and we have the standard potential term $V_0(\phi)$. Going on-shell gives us a simple relation between those two. So again one can set V_0 to a constant and stay with \mathcal{V} . We then obtain a spectrum that should be almost the same as the one in the previous section. We can see it in Tab. 5.2. Again for completeness we also provide the dimensionless formulation of the two additional potentials.

$$\mathcal{V} = k^{3/2} \sqrt{Z_V} \quad (5.4.1)$$

$$v_0 = k^3 v_0 \quad (5.4.2)$$

What do we observe in the actual numbers? Let us first look at the formulation in \mathcal{V} . We have one additional critical exponent. But this is exactly the one we already found for W' . In fact it is a constant fluctuation in \mathcal{V} . This is obvious as \mathcal{V} shares the same scaling part as W' . We discussed this fluctuation before when we discussed special fluctuations 4.1.1. As absorbing this one in W' does not change W'' it is not breaking supersymmetry explicitly.

Now let us turn toward the third row. We see two relevant exponents that both do not agree with the ones obtained before. Let us look at the first one $\theta_{1,V_0} = 3$. This one we already mentioned in the introduction. It is just the one belonging to the vacuum energy. We had it all the time when we treated V_0 as a constant but neglected it as uninteresting. While it breaks supersymmetry it provides us with no corrections to the correlators and propagators.

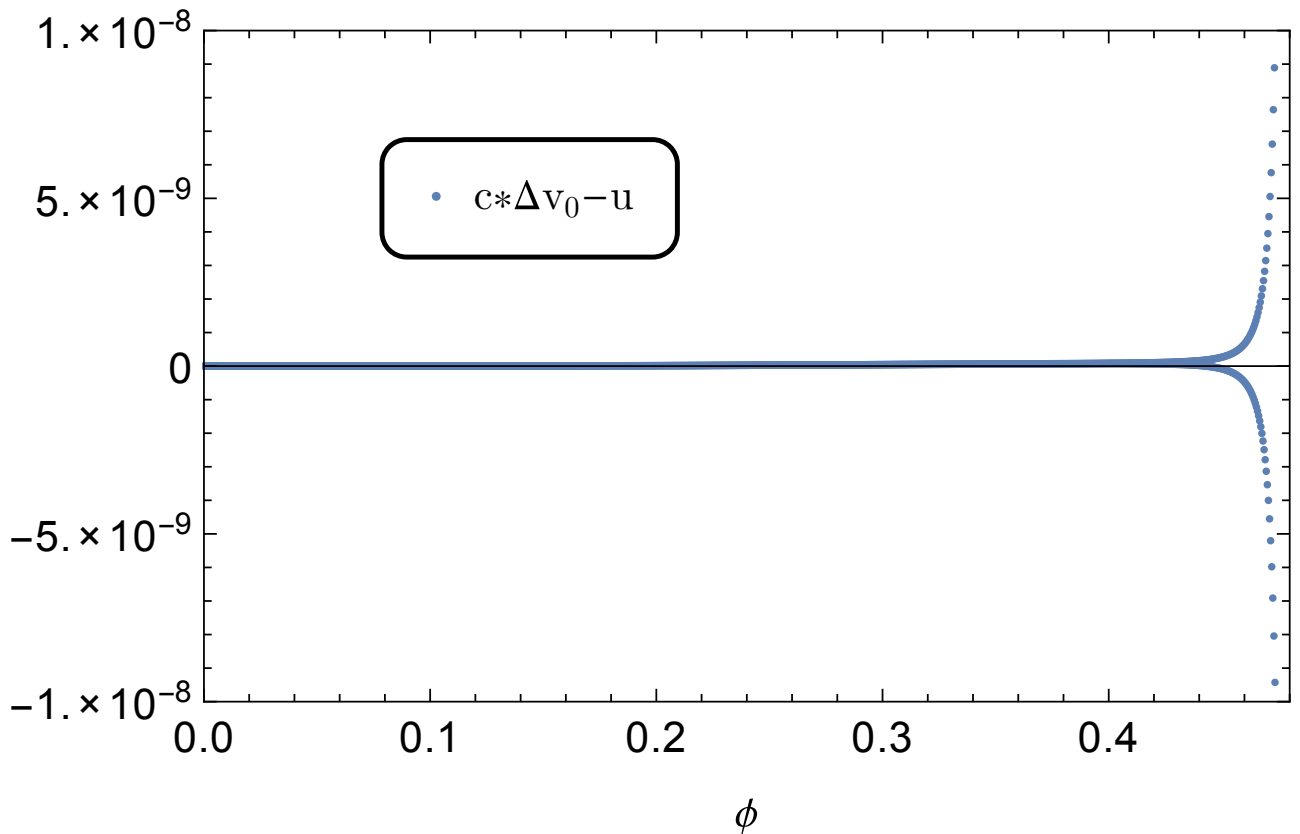


Figure 5.1.: We see the deviation of the computed fluctuation Δv_0 belonging to θ_{2,v_0} from the dimensionless fixed point potential u . We clearly see the coincidence suggesting that this is indeed again absorbable in $\Delta u = \text{const}$. Keep in mind that u was of the order 10^{-1} .

The second one is more interesting. We can simply verify that its value is $\theta_{2,v_0} = \theta_{1,v} + \eta$. This difference in one η was also mentioned earlier. We have used a different scaling relation in order to obtain the dimensionless quantities v and v_0 . This is now showing up. After realizing this we can now test whether the fluctuation belonging to θ_{2,v_0} looks like u (Fig. 5.1). Indeed this is the case.

5.5. Adaptive flow F_k

In the following two sections we use a k dependent auxiliary field. This provide us with a chance to turn the flow of V_0 into a field independent one. We use two different truncation methods in order to do so. Firstly, we use an easier but inexact formulation. Secondly, we turn toward the more complex situation.

Either way we have the following effective average action

$$\Gamma_k = \Gamma_k = \frac{1}{2} \left(-(Z_k + Z_{k,\phi})(\partial_\mu \phi)^2 + i(Z_k + Z_{k,\psi})\bar{\psi}\not{\partial}\psi - Z_k F_k^2 \right) + F_k W'_k(\phi) - \frac{1}{4} W''_k(\phi)\bar{\psi}\psi + \frac{1}{4} h_k(\phi)\bar{\psi}\psi.$$

5.5.1. Not one loop exact

We use the formula (5.2.9)

$$\partial_t \Gamma_k[\Phi_k] = \partial_t \Gamma_k|_{\text{old}} - \int \frac{\delta \Gamma_k}{\delta F_k} \partial_t F_k, \quad (5.5.1)$$

where we neglect the ϕ derivative term of $\partial_t F_k = -\alpha_k$. This gives us the following correction of the flow equations:

$$\begin{aligned} F^0 : \partial_t V_0 &= \partial_t V_0|_{\text{old}} + W' \alpha_k, \\ F^1 : \partial_t W' &= \partial_t W'|_{\text{old}} - Z(\phi_0) \alpha_k, \\ \bar{\psi}\psi : \partial_t (W'' - h) &= \partial_t (W'' - h)|_{\text{old}}. \end{aligned} \quad (5.5.2)$$

Here the old on the right hand side denotes the flow equations we obtained in the case of k independent fields i.e. the ones used in the previous section. As we want to eliminate the flow of V_0 up to a constant we can easily solve for α . We get

$$\alpha(\phi) = \frac{\partial_t V_0|_{\text{old}}(\phi) - \partial_t V_0|_{\text{old}}(\phi_{\text{NST}})}{W'(\phi)}. \quad (5.5.3)$$

Where ϕ_{NST} is defined as the zero of W' . We can immediately see, that W' should have only one zero or several zeros that have all the same value in the old flow of V_0 . Otherwise our transformation is singular. In the case of the Ising like fixed point solution this is fulfilled. As we can see the change in the flow of h is mediated by the change of the flow in W' but the Yukawa term altogether does not change.

We go to dimensionless quantities as introduced before in order to compute the spectrum. In the supersymmetric hypersurface $\partial_t V_0|_{\text{old}} = 0$ is true and we are back in the old case of the Wess-Zumino model. Therefore we expect again a split in the spectrum. The supersymmetric fluctuations are well known by now and are not further discussed. The fluctuations explicitly breaking supersymmetry give rise to a non-smooth fluctuation operator. We can easily see this when we look at

$$\partial_t V_0|_{\text{old}} = h(\phi) f(\phi, W''(\phi), W'''(\phi)) + (O)(h(\phi)^2).$$

Therefore the fluctuation of h depends on $h(\phi_{\text{NST}})$. As mentioned before such a behavior is not really suitable for the Slac formulation as we have a non smooth function. We thus give the eigenvalues neglecting this additional term using the Slac derivative and as a backup also the results using the shooting method employed already when dealing with $\delta\eta$. In a more involved truncation scheme we could also include the fluctuation with respect to the different η . Note that our introduced dimensionless quantities are then defined as

$$W' = k^{3/2}\sqrt{Z}u \quad \text{as} \quad W' \propto F_k Z, \quad (5.5.4)$$

$$h = k^1(Z_{k,\psi} + Z_k)\tilde{h}, \quad (5.5.5)$$

$$v_0 = k^3 v_0, \quad (5.5.6)$$

$$\eta_\phi = -\partial_t \log(Z + Z_\phi), \quad \eta_\psi = -\partial_t \log(Z + Z_\psi) \quad \eta = -\partial_t \log Z. \quad (5.5.7)$$

Therefore W'' does not have to have the same dimensional scaling as h although both give rise to the Yukawa interaction.

Before computing the eigenvalues we want to make a technical remark. The shape of the function

$$\partial_t \tilde{h} = \partial_t \tilde{h}|_{\text{old}} - \partial_\phi \alpha = \partial_t \tilde{h}|_{\text{old}} - \tilde{h}' \frac{f}{u} - \tilde{h} \frac{f'}{u} + (\tilde{h} - \tilde{h}(\phi_0)) \frac{f}{u^2}, \quad (5.5.8)$$

provides us with a singular term in the eigenvalue formulation at $\phi = \phi_0$ in the $\Delta \tilde{h}'$ and $\Delta \tilde{h}$ terms. It is useful to transform the perturbation equation to new quantities in the perturbation

$$\Delta \tilde{h} = u \Delta h + c, \quad c = \Delta \tilde{h}(\phi_0), \quad \text{as} \quad \tilde{h}^* = 0 \quad (5.5.9)$$

and then do a rescaling as prescribed in Sec. 2.4 in order to get rid of the first derivative of the perturbation. One ends up with fluctuations whose spectrum are determined by the fixed-point informations in the interval $(-\phi_0, \phi_0)$ when restricting oneself to perturbations that are connected to the origin. We provide the spectrum computed in the way mentioned for $c = 0$ using the Slac derivative. Further more we use the shooting method and include the constraint $c = \Delta \tilde{h}(\phi_0)$ and therefore $u \Delta h|_{\phi \rightarrow \phi_0^-} = 0$ in the described (eq. (5.5.9)) formulation. All those results can be found in Tab. 5.3.

In the case of the Slac derivative no additional relevant direction shows up. In Fig. 5.2 we give two fluctuation solutions times u for the lowest eigenvalue for given c and $r_{2,1}$. As we can see c is rather small but influences the eigenvalue significantly. Also the found solutions do diverge away from zero due to the choice of c . This happens before the divergence due to the

| | $\theta_{1,h}$ | $c(\theta_1)$ | $\theta_{2,h}$ | $c(\theta_2)$ | $\theta_{3,h}$ | $c(\theta_3)$ |
|----------------------------------|----------------|------------------|----------------|----------------|----------------|----------------|
| Slac $r_{2,1}$ | -0.202 | 0 | -0.506 | 0 | -0.897 | 0 |
| Slac $r_{2,2}$ | -0.295 | 0 | -0.747 | 0 | -0.1337 | 0 |
| Shoot with $u(\phi_0)$ $r_{2,1}$ | -0.1 | $-2.8 * 10^{-5}$ | -0.5 | $-6 * 10^{-7}$ | -0.8 | $-3 * 10^{-5}$ |

Table 5.3.: We see the results for the spectrum of the Yukawa potential h . The results for the two regulators in the case of the Slac derivative and in the case of the shooting methods are given. For the shooting method we also provide the chosen c . As we can see the given eigenvalues are also very regulator dependent. This is in stark contrast to the supersymmetric fluctuations.

wrongly chosen θ can show up. It could therefore be that there is no fluctuation with roughly the given eigenvalue that is consistent with the condition $u\Delta h|_{\phi \rightarrow \phi_0} = 0$. For this reason we are reluctant to make a definite statement about the eigenvalues from these calculations and do avoid giving too many figures. The same pattern emerges for the other regulator choice $r_{2,2}$. As we describe later on we have a good reason to think that no supersymmetry breaking relevant directions appears.

5.5.2. One loop exact

We are implementing the full equation (5.2.9) giving us the corrections

$$\begin{aligned}
F^0 : \partial_t V_0 &= \partial_t V_0|_{\text{old}} + W' \alpha_k - \alpha'_k \int dq \frac{q^2}{2\pi^2} \frac{r_2 Z W''}{q^2 (1+r_2)^2 Z^2 + (1+r_2) Z V'' + W''^2} \\
F^1 : \partial_t W' &= \partial_t W'|_{\text{old}} - Z(\phi_0) \alpha_k - \alpha'_k \int dq \frac{q^2}{2\pi^2} \frac{-r_2 (1+r_2) Z^2 W'' W'''}{(q^2 (1+r_2)^2 Z^2 + (1+r_2) Z V'' + W''^2)^2} \\
\bar{\psi} \psi : \partial_t (W'' - h) &= \partial_t (W'' - h)|_{\text{old}}.
\end{aligned} \tag{5.5.10}$$

As we can see we have to solve an ODE in the first F^0 term in order to avoid a flow of the V term. We would have again the freedom of including a parameter $W'(\phi_0)$ to leave a field independent flow for V . We saw in the last section that this proved troublesome and will therefore avoid this kind of modification. We will fix the freedom in α by demanding that in the supersymmetric hypersurface the flow of F_k is vanishing. In this way we will immediately end up with a splitted spectrum of supersymmetric fluctuations and those breaking it.

At this point it seems that we have avoided the earlier constraint that only one zero of W' is

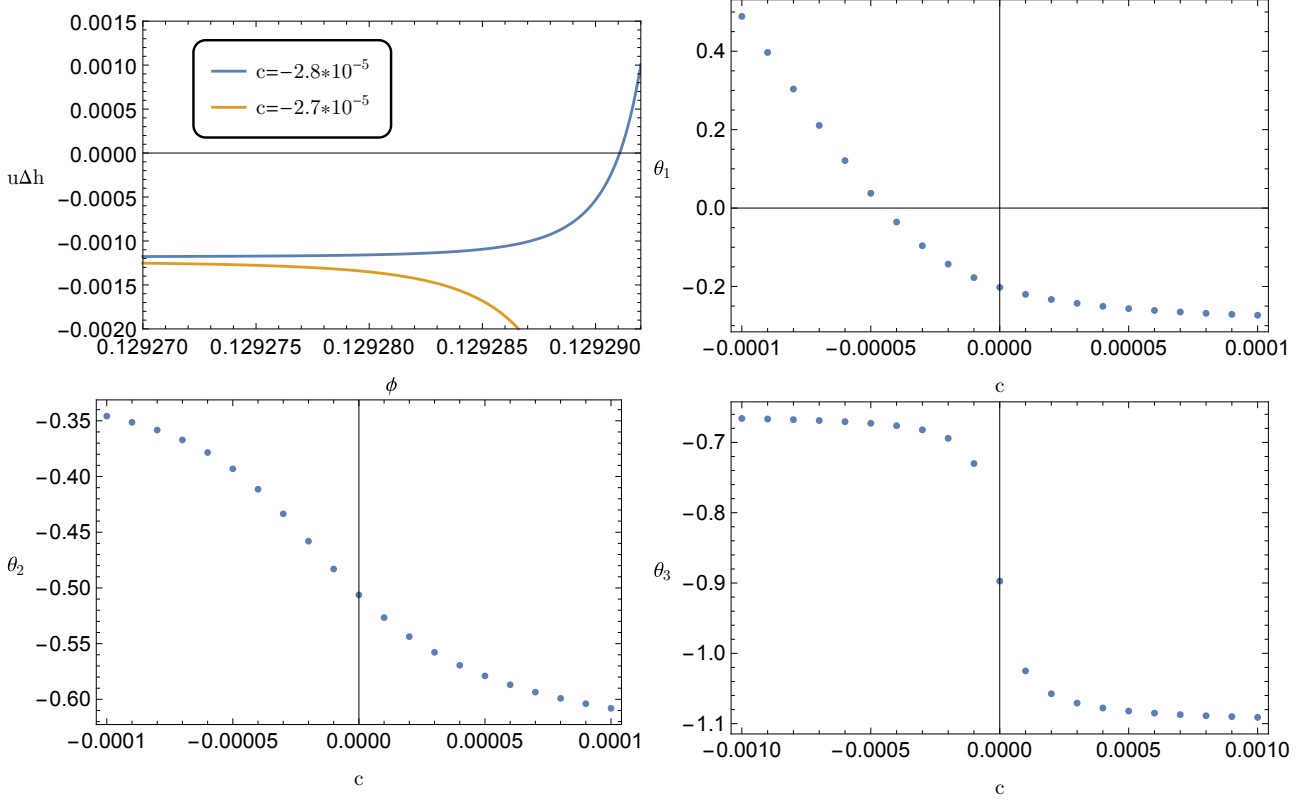


Figure 5.2.: In the upper row on the left we show two solutions for the fluctuation equation depending on the chosen c . We were looking for solutions going to zero in the limit $\phi \rightarrow 0.1292975$. The divergence away from zero shown in the plot is caused by the choice of c and not due to the fact that we are only using an approximate θ value as given in Fig. 4.9. We could not find a good convergence to zero. This may be related to our insufficient numerics or the absent of such a solution. The other three plots depict the strong dependence of the different eigenvalues on the choice of c . Especially the sign of c plays an important role.

allowed. When investigating the solution of the ODE for α we can see that this is in fact not true for the given system. The coefficient of α' is scaling with W'' and therefore this quantity should have only one zero¹. In the Ising class it is located at $\phi = 0$. Thus we conclude that a fixed point with one zero in W' for semipositive ϕ is valid. Therefore we restrict ourself to the analysis of the Ising class as was done throughout this whole section. We are using the same dimensionless quantities as before eq. (5.5.7) and neglect again the fluctuations in η . We give the calculated spectrum using the Slac derivative in Tab. 5.4 for both regulators.

¹This is no proof but the system seems overconstrained and there is no obvious reason why the fixed point solution should be of a form that allows for a solution to this system

| | $\theta_{1,h}$ | $\theta_{2,h}$ |
|----------------|----------------|----------------|
| Slac $r_{2,1}$ | -2.72 | -5.11 |
| Slac $r_{2,2}$ | 1.06 | -4.92 |

Table 5.4.: We give the results for the first two critical exponents for the explicit supersymmetry breaking term. While the second one shows a decent agreement for the two regulator choices the first one is far off. Our numerical results are not too good but the eigenfunction belonging to the result $r_{2,2}$ has too many knots, i.e. 3, in order to be the correct first odd excited state. For the regulator $r_{2,1}$ it shows only one knot. We therefore do trust the Result $\theta_1 = -2.72$ a lot more than the result that would indicate it to be relevant.

We see a drastic change in the spectrum. The reason for the bad performance of our numerics is not entirely clear. We relate it to the fact that the solution for α involves an exponential of an integral and this term is non analytical at $\phi = 0$. This gives our used numerics a hard time to deal with it.

Due to this, one might be suspicious regarding the obtained critical exponents. Let us compare our findings to recently obtained ones in the literature in Tab. 5.5. We also include the critical exponents of the supersymmetric fluctuations and provide the ones obtained by varying η . What we do see is that the supersymmetric fluctuations provide us already with those fluctuations given in this paper [56]. We therefore conclude that the supersymmetry breaking critical exponents are small. This is exactly what we see when putting the negative one found in the $r_{2,2}$ part aside². The problem of finding a correct c in the previous section 5.5.1 may be related to this fact.

We want to elaborate a bit on the fact that we think that the comparison with the literature already shows that the soft breaking terms should have small critical exponents. The two most relevant critical exponents found in the general Yukawa model [56] are the same ones found in the supersymmetric case when we employ a polynomial truncation scheme. Therefore the fluctuations belonging to those two in the Yukawa theory are ones that are will not leave

²We want to emphasize that in principle the regulator $r_{2,2}$ is better suited for increasing the truncation but is not as optimal as $r_{2,1}$ w.r.t. the gap criteria. We therefore do trust the $r_{2,1}$ results more. Especially as they are also more easily to handle numerically.

| | θ_1 | θ_2 |
|-----------------|------------|------------|
| FRG Yukawa [56] | 1.443 | -0.796 |
| FRG Susy pol | 1.385 | -0.765 |
| FRG Susy Slac | 1.413 | -0.382 |
| FRG Susy shoot | 1.379 | -0.393 |

Table 5.5.: We compare a recent result from the literature with our findings of Tab. 4.7. A comparison with other methods can be found there. As we can see the two most relevant fluctuations found in the Yukawa system have eigenvalues that match the ones of supersymmetric fluctuations. We conclude that the fluctuations breaking supersymmetry explicitly have smaller critical exponents as the given ones.

the supersymmetric hypersurface if a supersymmetric invariant regulator is employed. This means the supersymmetry breaking term will have a critical exponent that is less than the ones given and therefore less than -0.8 . We think that this is a justified upper limit for explicit supersymmetry breaking critical exponents.

5.6. Summary

Let us summarize the findings of this chapter. We treated the mentioned Yukawa system in a way that is closely related to the supersymmetric formulation of the $\mathcal{N} = 1$ Wess-Zumino model. We found that the spectrum is always splitted in fluctuations letting us stay in the supersymmetric hypersurface and those explicitly breaking supersymmetry. We gave a formalism to compute the critical exponents belonging to the breaking of supersymmetry. The comparison with the literature and the results indicate that the breaking fluctuations are strongly irrelevant. Therefore a system near criticality should quickly approach the supersymmetric hypersurface. This should show up in an experiment [55].

The obtained results show that the inclusion of a scale dependent auxiliary field may be necessary to see the correct eigenvalues. On the negative side the method including the field redefinition is numerically demanding. Using the one called not one loop exact provided us with solutions for fluctuations we could not resolve whether they are artifacts of the method or not. The complete inclusion of the scale dependence showed much stronger suppression of the

supersymmetry breaking fluctuation but also an additional relevant one in case of the usage of the regulator $r_{2,2}$. At this point we are therefore not sure how reliable those numbers are. An improvement in the numerics may be advised. A next step would be to include the fluctuations in the different η in order to take this effect into account. As we have seen this can provide a significant shift. We must leave this problem open for further research.

6. The $O(N)$ model

In this chapter we want to discuss the $O(N)$ model in three dimensions. The model consists of N copies of the $d = 3$ Wess-Zumino model with an additional $O(N)$ symmetry connecting the superfields Φ_i of each model. This model was studied before in the large N limit using other methods than the flow equation, e.g. [96, 143–146]. In [147] a negative outlook for the possibility of spontaneous supersymmetry breaking was given within a perturbative regime. We summarize shortly the results that were found in [97] and [98] discussing the model in the large N limit using the flow equation. As a next step we use a polynomial ansatz to find some finite N solutions. We do so in different truncations starting with the LPA and working our way up to NLO. The limits N going to one and infinity will be studied in detail. After this extensive use of the polynomial method the next step will be the employment of the shooting method to extend our polynomial solutions to a larger domain. Firstly we start at the origin; Secondly in the minimum found with the polynomial methods. We are restricting ourselves for this to an LPA' truncation with an uniform wavefunction renormalization. As the obtained picture will not be as self consistent as we would hope it to be we will return to the sketchbook and rethink our chosen ansatz. We then give some arguments what is probably going on. To strengthen this argument we also start from the already known $N = 1$ solution and using the $O(N)$ flow equations go to higher N .

6.1. Formulation of the theory

Our most general ansatz for the effective average action is

$$\Gamma_k = \int dz \left[-\frac{Z}{2} (\bar{D}\Phi_i D\Phi_i) - \frac{Y}{16} (\bar{D}(\Phi_i\Phi_i) D(\Phi_i\Phi_i)) + W(\Phi_i\Phi_i/2) \right]. \quad (6.1.1)$$

We use the already in eq. (3.2.4) introduced superfield Φ as well as the other superspace ingredients in order to formulate an $O(N)$ invariant theory. The index i distinguishes between

the N copies of the Wess-Zumino model and is summed over ranging from 1 to N . By integrating out the Grassmannian variables in Φ we get

$$\Gamma_k = \int d^d x (\mathcal{L}_{k,\text{Bos}} + \mathcal{L}_{k,\text{Ferm}}), \quad (6.1.2)$$

$$\mathcal{L}_{k,\text{Bos}} = -\frac{Z}{2} [(\partial_\mu \phi_i)^2 + F^2] - \frac{Y}{4} [(\partial_\mu \rho)^2 + (F_i \phi_i)^2] + F_i \phi_i W' \quad (6.1.3)$$

$$\mathcal{L}_{k,\text{Ferm}} = i\frac{Z}{2} \bar{\psi}_i \not{\partial} \psi_i + i\frac{Y}{4} \phi_j \bar{\psi}_j \not{\partial} (\psi_i \phi_i) - \frac{1}{4} (W' \bar{\psi}_i \psi_i + W'' (\phi_i \bar{\psi}_i \psi_j \phi_j)) \quad (6.1.4)$$

We have the already known superpotential $W(\rho)$, a wave function renormalization $Z(\rho)$ for the transversal modes, and an additional contribution to the wave function renormalization of the radial mode $Y(\rho)$. We also use the $O(N)$ invariant $\rho = \phi_i^2/2$. It can be useful to choose a preferred direction for the field, e.g. $\rho = \phi_1^2/2$. In order to obtain the flow equations for W , Z , and Y we use the standard techniques already used for the bosonic $O(N)$ model [57] in a superspace formulation. In LPA' the flow of W is given by

$$\partial_t W = \int_0^\infty dq \frac{\dot{r}_2}{(2\pi)^3} \left(\frac{N-1}{2} \frac{-W'(\rho)}{W'(\rho)^2 + q^2 \tilde{h}^2} + \frac{1}{2} \frac{-\tilde{W}'(\rho)}{\tilde{W}'(\rho)^2 + q^2 \tilde{h}^2} \right), \quad (6.1.5)$$

$$h = Z(1 + r_2), \quad \tilde{h} = Z(1 + r_2 + \rho \frac{Y}{Z}), \quad \tilde{W}'(\rho) = W'(\rho) + 2\rho W''(\rho). \quad (6.1.6)$$

We have again the two regulator choices $r_{2,1}$ and $r_{2,2}$ at hand as we are not leaving the NLO truncation. Also note the mirror symmetry $W \rightarrow -W$.

We identify the effective bosonic potential V_{Bos} by eliminating the auxiliary fields F_i ,

$$0 = F_i \partial_{F_i} \mathcal{L} = -Z F_i^2 + W'(\rho) \phi_i F_i - \frac{1}{2} Y (F_i \phi_i)^2, \quad (6.1.7)$$

$$0 = \phi_i \partial_{F_i} \mathcal{L} = -Z F_i \phi_i + W'(\rho) \phi_i^2 - \frac{1}{2} Y F_i \phi_i \phi_j^2, \quad (6.1.8)$$

$$\Rightarrow V_{\text{Bos}} = \frac{\rho W'(\rho)^2}{Z + \rho Y}. \quad (6.1.9)$$

We would like to highlight the difference to the bosonic model. The flow of Y does not necessarily go to zero for increasing N in contrast to the one of Z ¹. This means that LPA will not be exact when calculating the flow of the effective potential instead of the one of the superpotential. Therefore, the limit $N \rightarrow \infty$ and $N = \infty$ do not have to coincide. Note that in $N = \infty$ the Y term is absent as a result of only taking transversal directions into account.

¹This is due to the fact that $N - 1$ transversal modes can propagate in the loop and this cancels the $1/N$ suppression of the loop. This is in contrast to the one longitudinal mode propagating in the loop for Z .

6.2. The large N results

In [98] the above given equation was solved for $N = \infty$ and therefore $Z = 1, Y = 0$. This means LPA gives already exact results. A continuum of solutions was found with a spectrum consisting of one relevant and one marginal eigenvalue while the rest is irrelevant,

$$\theta_i = 1 - i, \quad i = 0, 1, 2, \dots \quad (6.2.1)$$

The solutions were analytically determined using the method of characteristics. The results for the phase structure are in good agreement with the ones found by employing a variation ansatz [148]. The observed fixed-point solutions has the interesting property that the potential has always a zero at the same dimensionless ρ value. Furthermore, there are solutions whose domain was limited in ρ . Some were even double valued in a positive ρ region. Moreover, some solutions were not defined for small positive ρ . This was called the strong coupling regime as the first derivative of the effective potential diverged for a positive ρ value.

The interesting questions when dealing with the finite N solutions are the following: Will the finite N correction turn the marginal eigenvalue into an irrelevant one? Does a single solution emerge from the limit $N \rightarrow \infty$? Will it be in the strong coupling regime? Is it possible to find a continuous function in N to connect the $N = 1$ Wilson-Fisher case with one $N = \infty$ case?

In the following sections we will provide answers to these questions. We start our investigations with the polynomial expansion around the minimum.

6.3. Polynomial expansions around the minimum

We provide at this point some technical details. These are not essential for the following sections but may nonetheless be helpful for a deeper understanding. So a reader may skip ahead if interested mainly in the results.

In order to do a fixed point analysis we have to introduce dimensionless quantities,

$$\tilde{\rho} = \frac{8\pi^2 Z}{Nk} \rho, \quad (6.3.1)$$

$$u = \frac{1}{k\sqrt{Z}} W', \quad (6.3.2)$$

$$\eta = -\partial_t \log(Z), \quad (6.3.3)$$

$$\tilde{\eta} = -\partial_t \log(Z + \rho Y), \quad (6.3.4)$$

$$y = \frac{kN}{8\pi^2 Z^2} Y. \quad (6.3.5)$$

The numerical constant $\frac{1}{8\pi^2}$ given above is for the case $r_{2,1}$. The constant is chosen such that for both regulators the large N minimum is positioned at $\tilde{\rho} = 1$. In the following notations we drop the $\tilde{\cdot}$ on the $O(N)$ invariant $\tilde{\rho}$. Both the $N=1$ case and the $N=\infty$ case suggest the existence of a fixed point solution with one minimum, for positive ρ , of the effective potential. This minimum is given as a zero of the superpotential. Therefore, we make the truncated ansatz

$$u(\rho, t) = \sum_{i=1}^I a_i(t) (\rho - \rho_0(t))^i. \quad (6.3.6)$$

The fixed-point equation will only be fulfilled up to a certain order. As the expanded equation of order n depends on the couplings a_{n+1} and a_{n+2} we have to make an ansatz for these. One way is to set them to zero for $n = I^2$ or use some additional input, e.g. as done before in Sec. 4.4. If not stated otherwise we use the former approach in this section. The spectrum is calculated by rewriting the time dependent coefficients,

$$a_i(t) = a_i^* + \epsilon \delta a_i(t) e^{-\theta t}, \quad i = 0, 1, 2, \dots, \quad a_0(t) = \rho_0(t), \quad (6.3.7)$$

and expanding the equation up to linear order in ϵ . Here a_i^* are the fixed point values

Let us turn toward the different truncation levels.

6.3.1. The case of LPA

As LPA is exact for $N = \infty$ we start with this truncation and investigate the large N results.

In this truncation the flow equation for u using $r_{2,1}$ reads

$$\partial_t u = -u + \rho u' - \frac{N-1}{N} \frac{1-u^2}{(1+u^2)^2} u' - \frac{1}{N} \frac{1-(u+2\rho u')}{(1+(u+2\rho u')^2)^2} (3u' + 2\rho u''). \quad (6.3.8)$$

Inserting our polynomial ansatz we find a special set of solutions with

$$\rho_0^* = \frac{N-1}{N}, \quad a_1^* = -\frac{1}{2\rho_0^*}, \quad a_2^* = \frac{3}{2} \frac{1}{4\rho_0^{*2}}. \quad (6.3.9)$$

The higher order coefficients a_i will now start to appear at order $(\rho - \rho_0)^i$. Therefore increasing the truncation $I \rightarrow I+1$ will not change the fixed-point coefficients a_0^*, \dots, a_I^* . As thus the flow of a_i does not depend on the flow of a_{i+n} also the stability matrix is block diagonal. In fact, the actual computation shows that it has upper-diagonal form. Therefore the coefficients can easily be read off. Computational details can be found in [149].

²This is essentially the stated ansatz for u .

The eigenvalues are given as

$$\theta_i = (1 - i) + (i + 1)i \frac{N - 1 \mp \sqrt{(N + 17)(N - 1)}}{6\rho_0^* N}, \quad i \in \mathbb{N} \cup \{0\}. \quad (6.3.10)$$

We have two sets of eigenvalues. The one with only positive and therefore relevant eigenvalues is given by the plus sign. The other one has only one relevant direction. The origin of this is a freedom of choice in the parameter a_3^* . Those giving only one relevant direction will appear in the large N limit. The other one scales with N and therefore diverges. This means that defining the expansion point and the first and second derivative is not sufficient to determine the fixed-point solution. We conclude that we are expanding the ODE around a somewhat singular point. This might also prove to be challenging when fine tuning to criticality. A typical UV Lagrangian with a ϕ^4 potential would not be able to distinguish between those two fixed points. We give a short example at the end of the section. At this point let us concentrate on the solution with only one relevant direction.

As promised we compare our fixed-point solution and its spectrum with the solutions for $N = 1$ in Sec. 4.1.2 and $N = \infty$ in Sec. 6.2. We see that our critical exponents in eq. (6.3.10) behave in leading order of an $1/N$ expansion in the same way as the large N ones, see eq. (6.2.1). We furthermore observe that the finite N corrections shift the marginal fluctuation into an irrelevant one. There is nonetheless no correction to the sole positive eigenvalue. The only found solution with one relevant direction connecting the $N = \infty$ solution to the finite N is given by eq. (6.3.9) at $N = \infty$. We do not expect to find a consistent solution with more than one relevant direction. The reason is that the dimensional analysis done in Sec. 4.2 still holds true for the potential³.

On the other hand we have a hard time going to $N = 1$. As ρ_0^* approaches zero and a_1^* diverges according to eq. (6.3.9). We reexamine the $N = 1 + \epsilon$ case in Sec. 6.5.

One may distrust the results obtained for the $r_{2,1}$ regulator as we expand around a somewhat singular point. Therefore, we list the results for the regulator $r_{2,2}$ in comparison to the ones of $r_{2,1}$ in Tab. 6.1. The decoupling of the higher coefficients does not happen and therefore we give the results for different N as examples. Still the same pattern emerges.

We also promised to show a plot of the flow near the fixed point and the problem related to the fact that another repulsive fixed point is close to it. Limiting ourselves to a ϕ^6 UV effective potential our superpotential u has to be of order ρ 6.1.9. We restrict our potential to a constant

³We will have a closer look into this at a later stage.

⁴We have to compare the absolute error to one as this is the typical order of the critical exponents

| | θ_1 | θ_2 | θ_3 | ρ_0^* | a_1^* | a_2^* |
|------------------|------------|------------|------------|------------|---------|---------|
| N=100, $r_{2,1}$ | 1 | -0.029 | -1.1 | 0.99 | -0.505 | 0.383 |
| N=100, $r_{2,2}$ | 1.0 | -0.051 | -1.1 | 0.99 | -0.741 | 0.709 |
| N=10, $r_{2,1}$ | 1 | -0.24 | -1.7 | 0.9 | -0.56 | 0.46 |
| N=10, $r_{2,2}$ | 0.98 | -0.32 | -1.9 | 0.90 | -0.82 | 0.81 |
| N=3, $r_{2,1}$ | 1 | -0.72 | -3.2 | 0.67 | -0.75 | 0.84 |
| N=3, $r_{2,2}$ | 0.97 | -0.77 | -3.1 | 0.67 | -1.12 | 1.4 |

Table 6.1.: We compare the results for the critical exponents and the first three couplings for the two regulators $r_{2,1}$ and $r_{2,2}$. The Results are given for small N=3, medium N=10, and large N=100. For the regulator $r_{2,2}$ we used a truncation level $I = 12$ at which the given critical exponents have converged to the given values (two significant figures). As we can see the critical exponents show a reasonable agreement⁴. We can see that the first critical exponent does get finite N corrections when choosing the $r_{2,2}$ regulator while these are absent for the $r_{2,1}$ regulator. Due to our choice of dimensionless quantities the ρ_0^* values are also in good agreement. The other two couplings show no agreement as these are no universal quantities and thus regulator dependent.

plus a linear term in ρ . Taking this ansatz and plotting the flow diagram in the (ρ_0, a_1) plane, Fig. 6.1, we see that we have two relevant directions near the projection of the fixed point instead of one. This is related to the fact that the repulsive fixed point is more influential in this plane than the attractive one.

Although this seems a bit discouraging it is still true that one can find initial values in such a way that the trajectory is close to the discussed fixed point. Especially one can still find a separatrix between the broken and the unbroken phase within a polynomial flow at LPA level. But not all initial points on this line will have a trajectory bringing them close to the fixed point with one relevant direction. Therefore the phase transition is not necessarily governed by it.

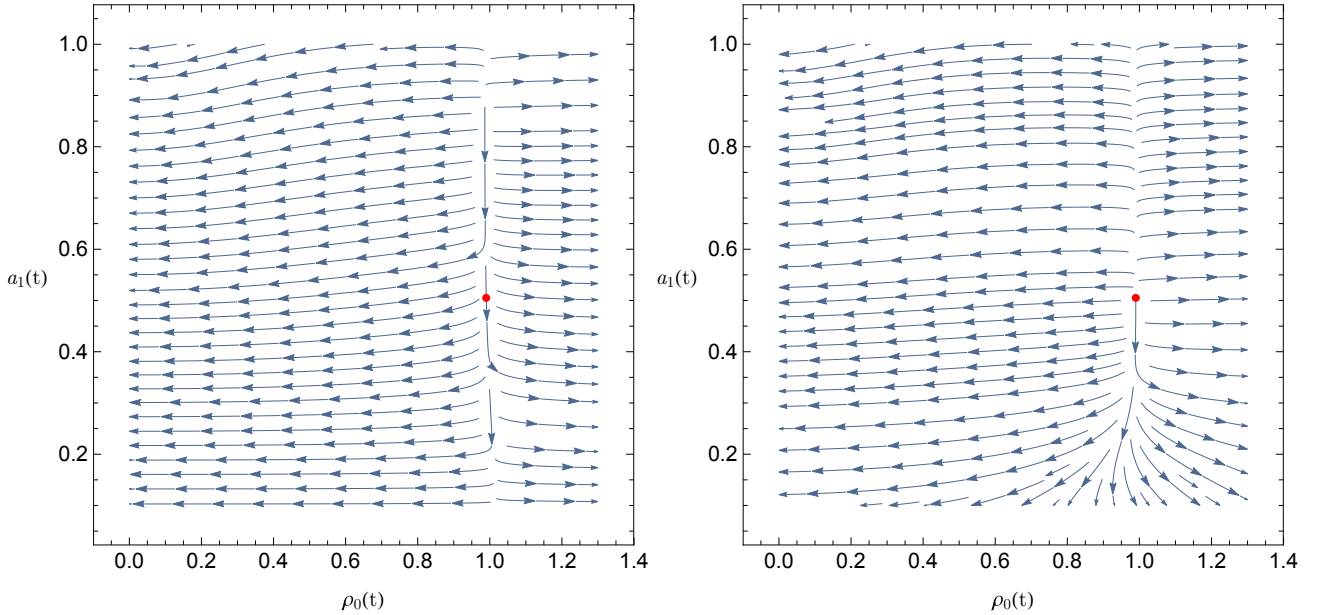


Figure 6.1.: On the left is a simple flow diagram in the (ρ_0, a_1) plane for $N=100$ with all other couplings set to zero. This is the flow of a ϕ^6 action in the UV. Near the projection of the fixed point (Red) $(99/100, 99/200)$ we see no trace of an irrelevant direction. Including a term quadratic in ρ in the potential and setting this coupling to its fixed-point value a_2^* does not moderate the problem. This can be seen on the right.

6.3.2. The case of LPA'

In this section we will introduce a uniform wave function renormalization Z and neglect the correction Y . The aim is to investigate the stability of our derivative expansion and look for some finite N corrections when dealing with $r_{2,1}$. The η equation in this truncation can be found in the appendix and the flow of the potential is given below eq.(6.4.1).

Including the wavefunction renormalization presents two major changes. The first one is that the decoupling of the flow of the coefficients from the higher order coefficients does not take place any more. Therefore the truncation scheme employed will influence our results. The second problem is that setting the highest coefficients to zero does not allow us to find a valid fixed-point solution⁵. We avoid this problem by setting the two highest coefficients to the LPA values times a constant (α) and vary this constant. In Fig. 6.2 we give the dependency of our lower order coefficients on the choice of the constant. One can see that the results get less sensitive for a large range of values of this constant with increasing truncation order I . The same is true for the critical exponents as is also depicted in the same figure.

⁵At least we were not able to do so for a wide range of truncations and initial data.

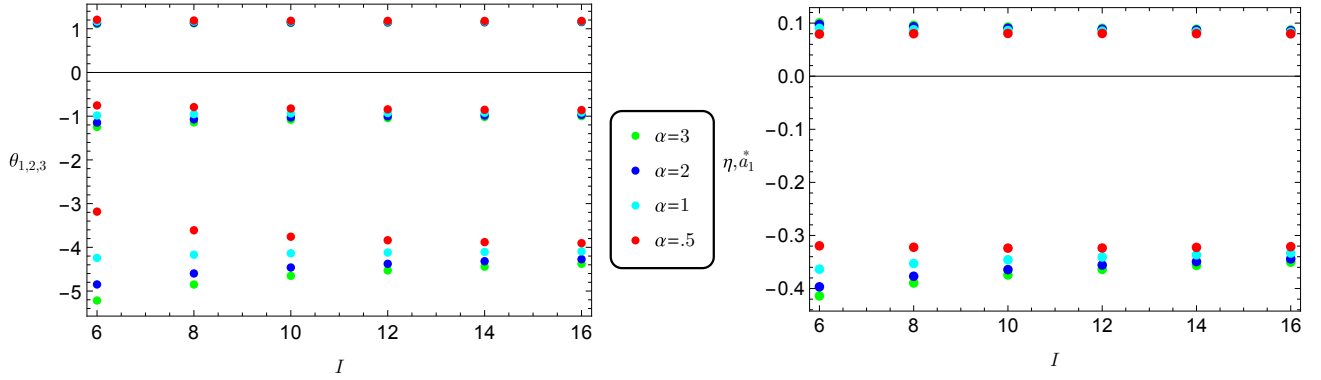


Figure 6.2.: We see the dependency of the calculated critical exponents (left hand side) and the anomalous dimension (positive values on the right hand side) as well as the first coupling (also on the right hand side). The plot shows different values for α with which the couplings $a_{I+1,\text{LPA}}$ and $a_{I+1,\text{LPA}}$ were multiplied and used as an input for the system of equations for the lower order coefficients. As we can see the results are converging in I regardless of the chosen input α to the same result. The choice of α with the fastest convergence seems to be in between $\alpha = 1$ and $\alpha = 0.5$.

In Fig. 6.3 we follow the trajectory of the first coupling as well as η w.r.t. N in the LPA' case. We note that we end up in the weak coupling, nearly Gaussian, regime in case of the LPA' case in contrast to the LPA. As this classification had some impact on the physical masses present in the large N system we will have to go on and clarify this issue.

As for the case of small N , LPA' is also not able to go to $N=1$. Also the results for small N are not very stable. Furthermore the anomalous dimension is quite large for $d = 3$ as depicted in Fig 6.3 on the left. We would expect $\eta \leq 2/10$ as found for the $N = 1$ case, see Tab. 4.1.

6.3.3. NLO truncation

A study of this model up to NLO level ($W(\rho), Z(\rho), Y(\rho)$) within a polynomial expansion was done. The results were always discouraging. Two typical problems are:

- The fixed-point solution as a function of N ceases to exist for small N . This behavior seems quite generic for NLO truncations. Typically this happened around $N \approx 3$. Using the $r_{2,2}$ regulator this already occurred in LPA for $N = 2$.
- The number of relevant directions changed for increasing N from one to two. No other

⁶We cannot exclude its existence but were not able to track it by decreasing N . Thus we think it absent.

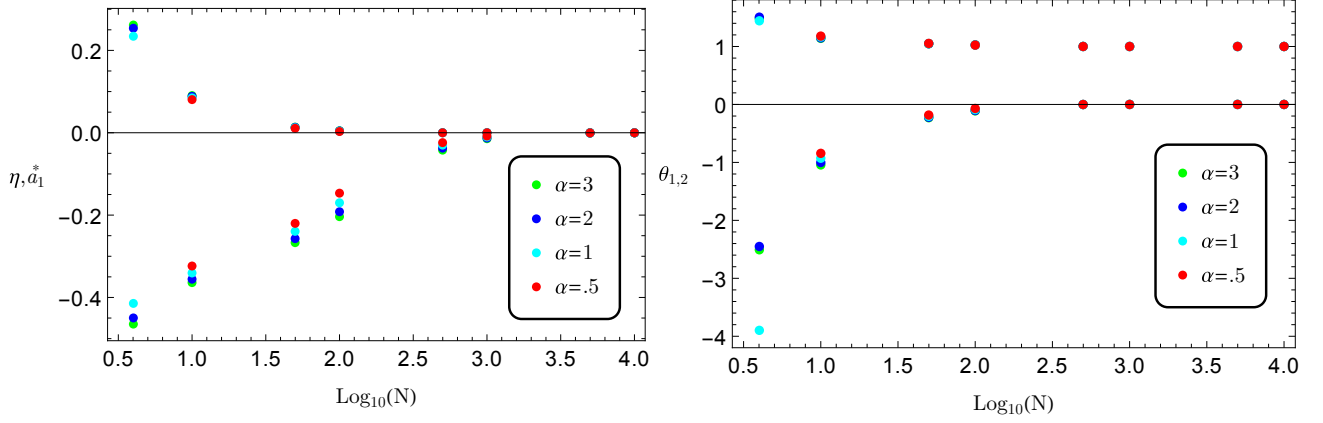


Figure 6.3.: We see on the left hand side the dependency of η (positive values) and a_1^* in an polynomial truncation $I=14$. We set a_{13}^* and a_{14}^* to the LPA values times α . It can be clearly seen how the solution tends to the Gaussian one for large N . We can also see that for small $N(= 4)$ the values are not as stable as one would expect. Especially, also the first two critical exponents given on the right hand side have not settled w.r.t. α . The solution with $\alpha = .5$ was not found for $I = 14$ and $N = 4^6$.

solution with one relevant direction showed up at such an N .

All these problems and the fact that no coherent picture emerges motivates us to look into a global approach toward this problem.

6.4. The shooting method

6.4.1. Starting at $\rho = 0$

We proceed as in the former chapters and start at $\rho = 0$ and try to find a global solution. To do so we use a spike plot and limit ourselves to LPA'. The input parameter chosen is $u(0)$.

$$\partial_t u = -(1 - \eta)u + (1 + \eta)\rho u' - \left(1 - \frac{\eta}{3}\right) \frac{N-1}{N} \frac{1-u^2}{(1+u^2)^2} u' \quad (6.4.1)$$

$$- \left(1 - \frac{\eta}{3}\right) \frac{1}{N} \frac{1 - (u + 2\rho u')^2}{(1 + (u + 2\rho u')^2)^2} (3\rho u' + 2\rho u'') \\ = \mathcal{S} - \mathcal{G}(3\rho u' + 2\rho u'') \quad (6.4.2)$$

We note that at $\rho = 0$ the choice of $u(0)$ already determines a single solution.

If one is interested in a fixed-point solution with one minimum the range of $u(0)$ is limited, $u(0) \in (0, 1)$. Negative values mirror the positive ones and larger values provide us with a

global solution that has no minimum as it is ever-growing. This can easily be seen by setting u' to zero and $u = 1 + c$. Then u'' is strictly positive for every c .

From our discussion in Sec. 2.3 we expect that our spike is determined by the zero of the right hand side of the first line (\mathcal{S}) and the zero of \mathcal{G} . In Fig. 6.4 we give for two different η and two different N the values of $\mathcal{S}(\rho_{\max})$, $\mathcal{G}(\rho_{\max})$, and ρ_{\max} , the endpoint value. As we can see there is no spike and therefore we do not expect any global solution. A similar spike plot was given in the case of the Wess-Zumino model when starting with an odd superpotential u_{WZ} in Fig. 4.2.

Still, one could argue that a fixed-point solution that is non-existent for a finite range of ρ will influence the IR physics as in dimensionful quantities this range shrinks to zero going to smaller k . Also in the large N case some fixed-point solutions showed such a gap and were related to the solution of flow equations with reasonable UV starting potentials. In order to investigate this issue further we will shoot from a finite ρ value.

6.4.2. Starting at $\rho > 0$

As we have a lot of degrees of freedom when starting at $\rho > 0$ let us constraint ourselves a bit. As we want to enforce the existence of one minimum we choose $u(\rho_0) = 0$. We have two remaining parameters $u'(\rho_0)$ and ρ_0 . The anomalous dimension will be determined in the minimum and can be calculated from the chosen parameters. As we do not expect to find global solutions we search for implicit solutions of the form $\rho(u)$. This is inspired by the exact solutions found in the large N limit. In Fig. 6.5 we give an example of such a fixed-point solution. As we can see the function $u(\rho)$ is double valued while $\rho(u)$ is single valued. We only allow for those solutions that do not end in a singularity for both positive and negative u .

In Fig. 6.5 we provide the parameter space for which solutions of the above given type exist. For a well-posed fixed-point problem these should be quantized. Instead, we see a continuum of solutions. The reason is that we have lost our quantization-condition $\mathcal{G} = 0 \rightarrow \mathcal{S} = 0$. We observe that the admitted region shrinks to a line for increasing N . This line is a part of the continuum of solutions found in the large N case. We note that the weak coupling regime is excluded. Therefore the LPA' polynomial expansion gives us a solution that is not compatible with the constraint for fixed-point solutions. Note that our polynomial expansion did not provide us with such a plethora of solutions. This is partly due to the fact that we looked for solutions with one relevant direction. The number of relevant directions is not examined for

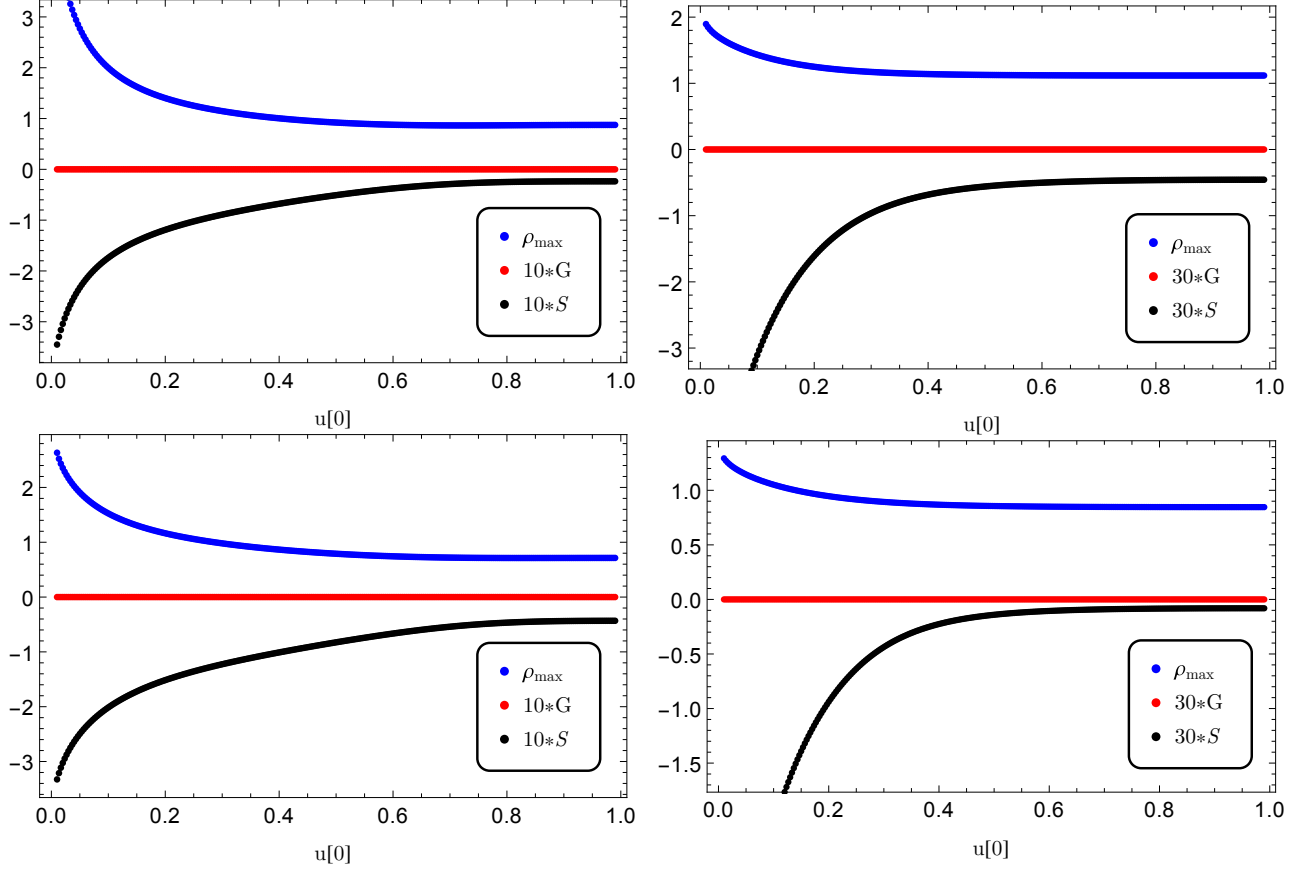


Figure 6.4.: We see different spike plots (Blue curves) combined with a plot of \mathcal{G} and \mathcal{S} at the endpoints of the numeric integration. On the left are the cases with $N=10$ and on the right the ones with $N=100$. In the upper row $\eta = 1/10$ was chosen while in the lower one $\eta = 0$. As we can see we never have any spike and we also have the singularity due to the zero in \mathcal{G} without any sign change in \mathcal{S} .

the given numerical solutions.

6.5. N close to one

By now we have found a lot of indications that the model does not have a valid Wilson-Fisher fixed point. Let us examine why this may be the case. We investigated in Sec. 4.2 the number of critical models for a given type of potentials w.r.t. the dimension d . We saw that for $d = 3$ only a ϕ^4 coupling was relevant. When examining the effective potential formulated in this section we found (eq. (6.1.9))

$$V_{\text{bos}} \propto \rho W'(\rho)^2. \quad (6.5.1)$$

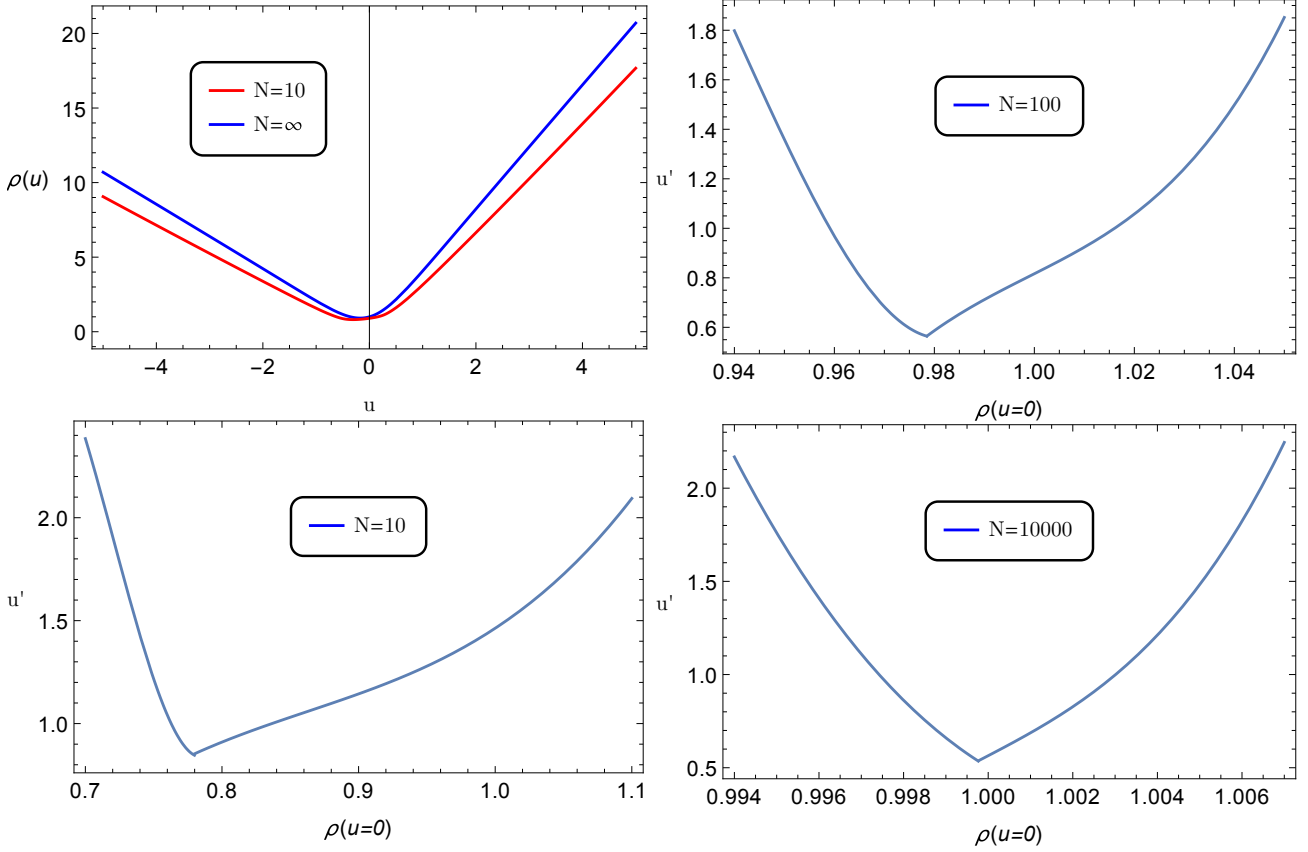


Figure 6.5.: In the upper left corner we see an example solution $\rho(u)$ for $N = 10$ (Blue). Its shape is similar to the fixed point solutions found in the $N = \infty$ case (Red). The other three plots depict the approximate parameter region $a_1 = u'(\rho(u = 0))$ and $\rho(u = 0)$ for which solutions of the plotted type exist. The region within the given curve is allowed. We see a continuum of solution. The range of a_1 is limited from below.

This effective potential will have no ρ^2 coupling for $C^{(2)}(\mathbb{R}^+)$ potentials W' . Therefore we are missing the essential ingredient for the discussion of a phase transition. Even allowing for a diverging W'' in the last section did not lift this problem. We were not able to find a solution.

On the other hand, we know a valid solution for $N = 1$. So it may be a good idea to reformulate the obtained flow equation in such a way that we end up with the old flow equation of the Wess-Zumino model for $N = 1$.

Doing so involves a singular transformation in order to lift the zero at $\rho = 0$ of the effective potential.

$$\tilde{u}(\phi) = \phi u(\phi^2/2), \quad \phi = \sqrt{2\rho}. \quad (6.5.2)$$

Here we have introduced a scalar ϕ that carries no $O(N)$ vector indices. After this transfor-

mation the fixed point equation of \tilde{u} looks like

$$0 = -\frac{3-\eta}{2}\tilde{u} + \frac{1+\eta}{2}\tilde{u}'(\phi)\phi + \frac{1}{N}\frac{3-\eta}{3}\frac{\tilde{u}'(\phi)^2-1}{(\tilde{u}'(\phi)^2+1)^2}\tilde{u}''(\phi) + \frac{N-1}{N}\frac{3-\eta}{3}\frac{\phi^2-\tilde{u}(\phi)^2}{(\phi^2+\tilde{u}(\phi)^2)^2}(\tilde{u}(\phi)-\tilde{u}'(\phi)\phi).$$

We can now easily reproduce the spike plot of the $N = 1$ case. As N appears as a parameter in our formulation we may increase it continuously to higher values and observe how the spike plot changes. This is depicted in Fig. 6.6. We see that the spike disappears for $N \rightarrow 2$. As we do not have a sign change in \mathcal{S} we again will not be able to continue our solution to larger field values. For this reason it was not possible to connect the $N = 1$ solution with the $N \geq 2$ solutions.

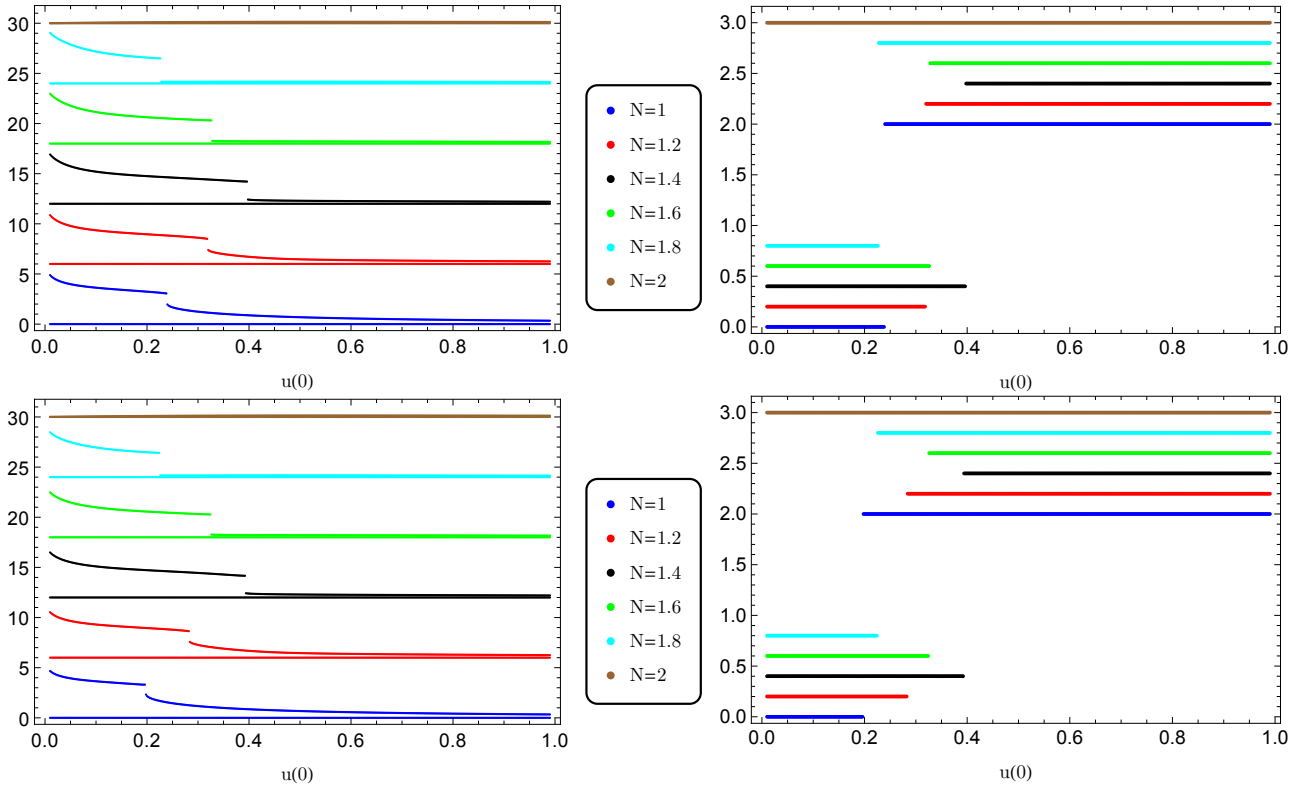


Figure 6.6.: We provide the spike plot with the endpoints of the numerical integration plus an N depend constant on the left hand side. On the right is the sign of \mathcal{S} depicted which is also shifted by an N dependent constant. The upper row is for $\eta = 0$ while the lower one is for $\eta = 1/10$. For the reason of better readability we added a baseline in the same color on the left hand side. The difference between baseline and spikeplot is the maximum ϕ to which we could integrate. Note that for increasing N the influence of η is diminishing.

The reason why the spike seems to exactly vanish for $N = 2$ is not obvious. Although this may be an interesting question we do not want to pursue it⁷. We note the shrinking domain of the solutions to the right hand side of the spike indicating a decreasing domain of the solutions we are interested in.

Let us instead turn toward the effective potential and Yukawa coupling we have realized by employing the given reformulation of our flow equation. As we have formulated the dimensionless effective potential in the form

$$v_{\text{Bos}} = \frac{\tilde{u}^2}{2}, \quad (6.5.3)$$

well known from the previous chapters, the Yukawa term from eq. 6.1.4

$$V_{\text{Yuk}} = -\frac{1}{4} (u(\rho)\bar{\psi}_i\psi_i + u'(\rho)(\phi_i\bar{\psi}_i\psi_j\phi_j)), \quad (6.5.4)$$

now reads

$$V_{\text{Yuk}} = -\frac{1}{4} \left(\frac{\tilde{u}(\phi)}{\phi} \bar{\psi}_i\psi_i + \frac{\tilde{u}'(\phi)}{\phi^2} - \frac{\tilde{u}(\phi)}{\phi^3} (\phi_i\bar{\psi}_i\psi_j\phi_j) \right). \quad (6.5.5)$$

A divergence at $\phi = 0$ arises for every $N > 1$ as long as $u'(0) \neq 0$. Thus making field configurations with $\phi \approx 0$ and $\psi \neq 0$ very costly in terms of the action. Note that this is also true for those solutions with a turnaround. There u' diverges and field configurations are again costly.

6.6. $d < 3$

As a last part we want to briefly explore the theory for $d < 3$. As we know that we cannot expect any nontrivial solutions for $d = 2$ and $N > 2$ let us focus on dimensions close to 3. Those theories may emerge as effective theories [153]. We are interested in these theories as $d = 3$ is the critical dimension for a ϕ^6 coupling as argued in Sec. 4.2. If the problem is really as simple as that we are looking at the problem in the wrong dimension we should be able to observe fixed points for $d < 3$.

⁷Looking into this no simple argument was found. We want to point out that in the scalar case at exactly $N = 2$ the higher critical models vanished in $d = 2$ in the sense of the reference noting this, i.e. [150, 151]. So an equal number of transversal and longitudinal degrees of freedom seems to be very special. See also Kosterlitz-Thouless transition [152].

We use a different constant factor⁸ for the definition of the dimensionless renormalized $O(N)$ invariant $\tilde{\rho}$ and end up with the flow equation

$$\dot{u} = - \left(\frac{d-1}{2} + \eta \right) u + (d-2+\eta)\rho u' - \left(\frac{2}{d-2} - \eta \frac{2}{d(d-1)} \right) \times \\ \left(\frac{N-1}{N} \frac{1-u^2}{(1+u^2)^2} + \frac{1}{N} \frac{1-(u+2\rho u')^2}{(1+(u+2\rho u')^2)^2} (3u' + 2\rho u'') \right).$$

The usage of $r_{2,1}$ limits the number of dimensions: $d > 2$.

We provide the spike plot for two values of d and four different N in Fig. 6.7 and Fig. 6.8. We chose $\eta = 0$ in these plots. As we can see there are now spikes indicating a valid fixed point. This is as we suspected. On the other hand for large N a second spike arises. The origin of this change of behavior can be traced back to the transversal modes contributing to the function \mathcal{S} . These modes seem to destroy the fixed point for large values of N . As the necessary number N for which the spike vanishes is decreasing for diminishing d this reminds us somewhat of the Mermin-Wagner theorem [154]. Note the contrast to the scalar $O(N)$ model [151] in which the higher critical models do not vanish in the above given sense⁹.

In Fig. 6.9 we plot solutions for both sides of the two spikes. As we can see the behavior is quite similar. We note that the value ρ_{\max} is not nearly vanishing as it was in Fig. 6.6. Also the found solutions have already a zero crossing and therefore the minimum of the effective potential lies within the region in which we compute the spectrum, see Sec.2.4.

⁸formerly $8\pi^2$ for $r_{2,1}$, now also d dependent

⁹There the critical exponent of the correlation length diverged at $d = 2$ starting at $N = 2$.

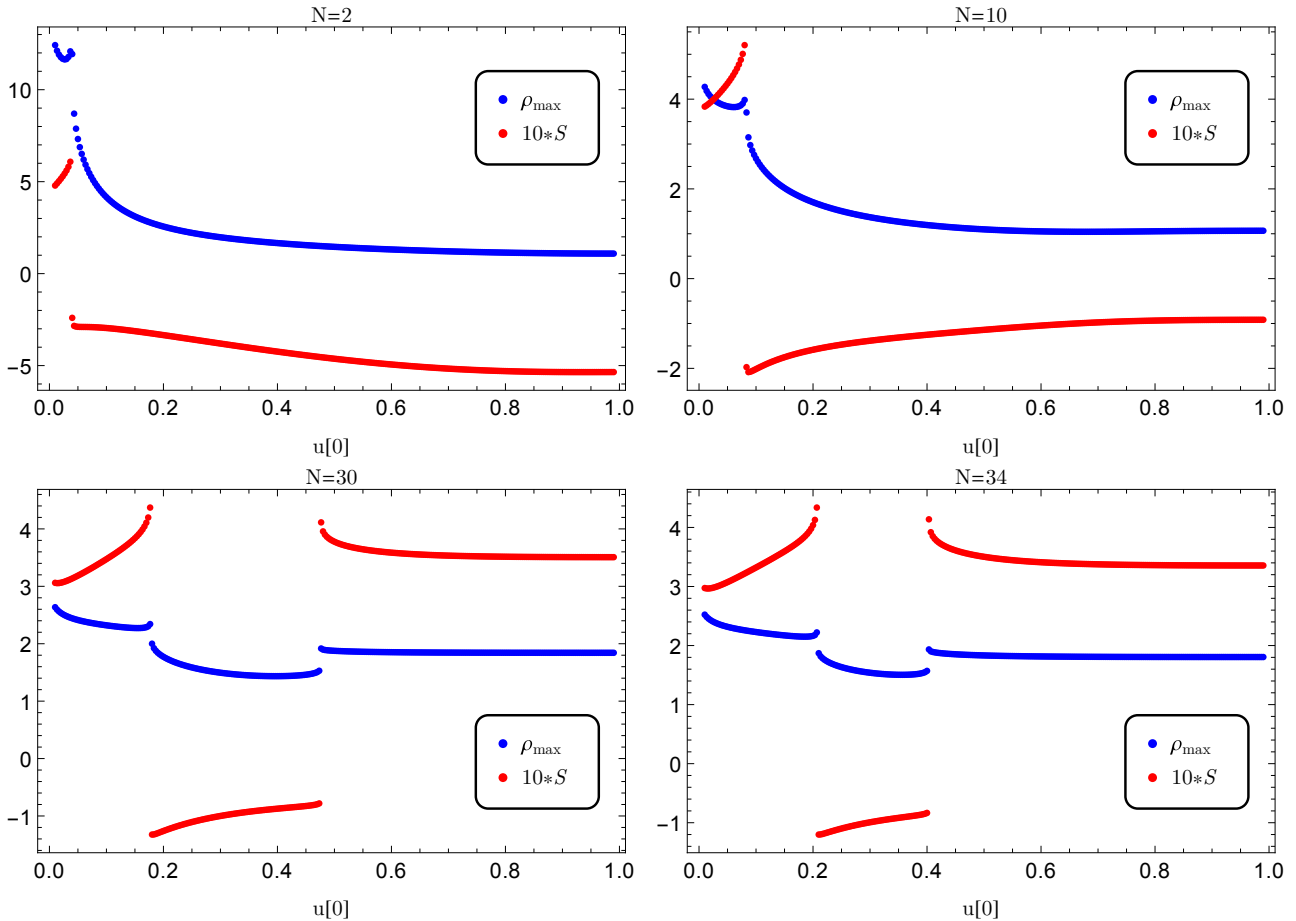


Figure 6.7.: We provide four different spike plots along with the values of the function \mathcal{S} at the endpoints. The dimension is $d = 2.9$. As we can see there is a pronounced spike for $d < 3$ as long as N is not too large. For large N a second spike appears. This change of behavior is related to the increasing part of the transversal modes in the function \mathcal{S} .

6.7. summary

Let us summarize our findings in this chapter. We looked at the $O(N)$ model and searched for fixed-point solutions within different truncations. Although we were able to find solutions for $2 \leq N \leq \infty$, these solutions did not fulfill our expectations. The polynomial ansatz provided us with quantized solutions. These seem not to converge at the investigated truncation level of the derivative expansion. Furthermore we found that these solutions could not be analytically continued to arbitrary small positive ρ . To see this we used a shooting method. We even found that the solutions were not quantized when shooting from zero. We realized that the problem may be related to the way our theory is formulated as no smooth transition to the

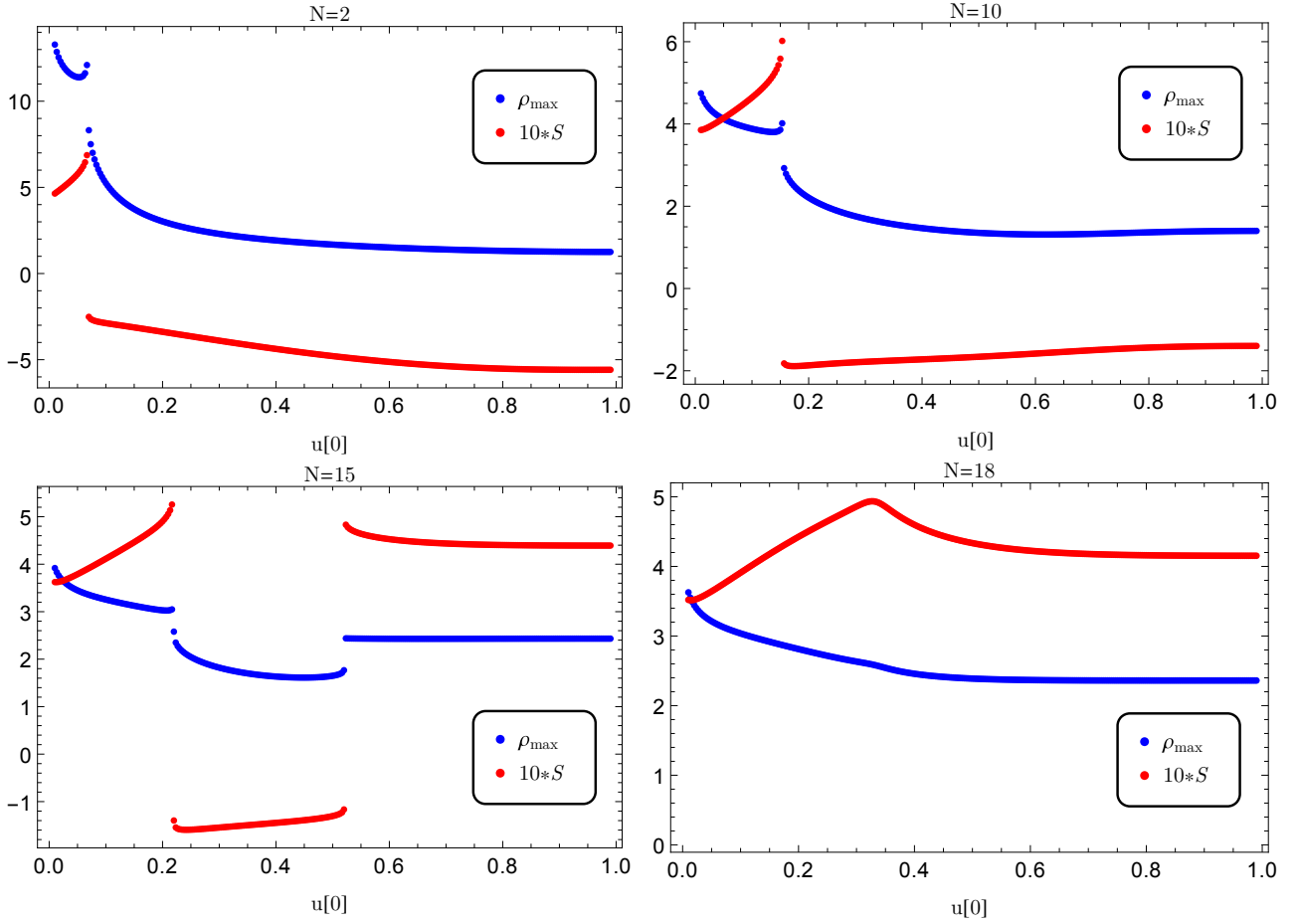


Figure 6.8.: As in Fig. 6.7, we show the spike plot along with \mathcal{S} at the endpoint of the integration. This time $d = 2.8$. As we can see the appearance of the second spike occurs for smaller N . We also depict the case in which the range between the two spikes has vanished ($N = 18$). One can see a remnant of the two merged spikes in the peak of the function \mathcal{S} .

known $N = 1$ solution was possible. We reformulated the theory in order to mimic the $N = 1$ case and extended to $N > 1$. We observed that the fixed-point solutions vanish for $N \geq 2$. For $1 < N < 2$ the range of existence was shrinking with N . We conclude that the problem is ill posed in $d = 3$. This confirms perturbative studies in [147]. The absence of a valid fixed points solution goes also hand in hand with the findings in [145]. For $d < 3$ valid fixed-point solutions could be found depending on N . This strengthens our point that the formulation of the model is such that $d = 3$ is the critical dimension at which a fixed point arises.

What have we learnt from this study from a methodological point of view? It is at some point necessary to go to higher truncations in the derivative expansion to confirm the existence or absence of a fixed point. Also, the shooting method seems to be more reliable when looking

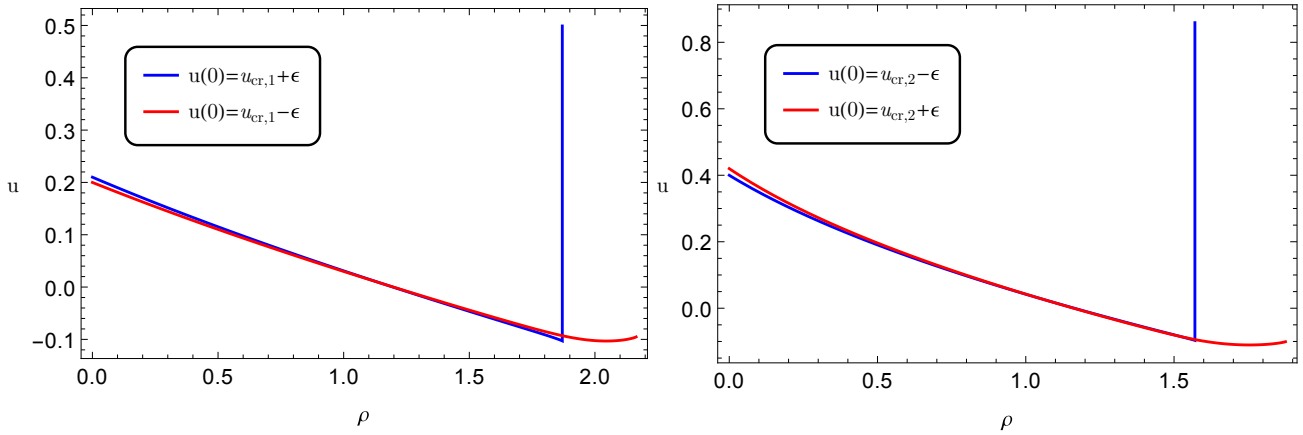


Figure 6.9.: We depict the different numerical solutions found for $N = 34$ and $d = 2.9$. On the left hand side we chose values close to the first spike $u_{cr,1} \approx 0.2$ and on the right for the second spike $u_{cr,2} \approx 0.4$. The Blue curves are the ones providing us with solutions we would consider as the correct fixed-point solutions as they stay concave. The vertical line indicates the endpoint of the numerical integration for those. The red ones are solutions from the other side of their respective spike.

for global solutions. This is one reason why we used it mainly in the previous chapters.

7. Conclusion

In the scope of this work we covered different topics. Let us remind ourselves of our main goals and to what extent we reached those. Our first goal was to reexamine the derivative expansion for a supersymmetric theory. We dedicated the first half, Sec. 3.3, of the chapter 3 toward this goal. We used a toy model of quantum mechanics which can be solved exactly. Thus, we had a reference frame for our results. We saw that our derivative expansion converged toward the exact results as long as tunneling effects were not too strong. We suspected that this was due to the effect that we did not include non-local terms.

In the second half of this chapter, Sec. 3.4, we investigated the formulation of flows in the case of spontaneously broken supersymmetry. We pointed out that the projection scheme in powers of F is not justified in the broken phase. Instead one has to use an expansion point F_0 . This was necessary to keep a positive mass in the propagator. Using this formulation we produced good estimates for the ground state energies.

Our next goal was to test methods which are well established in the framework of scalar field theories to find fixed points and their spectrum in the supersymmetric case. Our testing ground was the Wess-Zumino model with $\mathcal{N} = 1$ supercharges in $d = 2, 3$. We tested for fixed points using the shooting method and found those solutions that were already found in polynomial expansions, Sec. 4.1. Beforehand we gave some reasoning why the shooting method should provide us with the correct results, Sec. 2.3. We showed that the polynomial expansion around zero does allow to find the fixed point of the Ising model, Sec. 4.3. Furthermore, we gave the spectrum. We demonstrated how different implementations of the anomalous dimension in the calculation of the spectrum influenced the critical exponents, Sec. 4.4. An important message we took away was the tendency to decrease the first two critical exponents when varying η compared to the case in which η is kept fixed as an input parameter.

After contemplating these methodological problems we turned toward the interesting question of emergent supersymmetry, Sec. 5. We used a Yukawa model with a field content matching

those of the on-shell Wess-Zumino model. We asked ourselves how relevant are explicitly supersymmetry breaking fluctuations; or equivalently: How stable is supersymmetry in such general systems? To this end we provided a reformulation of the Yukawa system by introducing an auxiliary field which we ultimately chose scale dependent 5.2. While our numerics were not as stable as we hoped for them to be we are still convinced that the supersymmetry breaking terms are irrelevant and probably even strongly suppressed. We used results from the literature to strengthen this argument, Tab. 5.5. We think further work is still fruitful in this direction. An inclusion of the fluctuation of the anomalous dimension could provide a clearer picture concerning the critical exponents of the explicitly supersymmetry breaking fluctuations.

We want to make a remark on the used technique of employing a scale dependent auxiliary field. To the knowledge of the author the technique of absorbing the flow of a whole potential in the one of a scale dependent field was not implemented before. This procedure could prove helpful in other models.

With this positive findings we turned our attention toward the supersymmetric linear $O(N)$ model in $d = 3$, Chap. 6. We wanted to investigate the finite N case as the literature was very sparse on this topic. We hoped to connect the results from the large N analysis with the ones from $N=1$. In order to do so we employed both, the shooting method as well as the polynomial expansion. No coherent fixed point picture emerged and we started to question whether the problem is well-posed. We realized that the original formulation has the critical dimension $d = 3$ coinciding with the chosen spacetime dimension. We therefore tried a reformulation in Sec. 6.5. We could then reproduce the $N = 1$ results but failed to find a fixed point solution for $N \geq 2$. In order to examine the statement that the critical dimension of our original formulation was $d = 3$ we went to dimensions smaller than three, Sec. 6.6. There we found a fixed point solution for not too large N . We concluded that indeed the problem is ill-posed. It would be interesting to do the finite N analysis in the path-integral formulation used in [96, 144] and see what happens there.

A. Appendix

A.1. Shooting Example

We give an example of the shooting method that is in order to obtain the critical exponents in the case of a problem described in 2.4.1. Take the familiar harmonic oscillator $u'' - \phi^2 u = \theta u$. The eigenvalues belonging to even solutions are $-1, -5, -9, \dots$. We modify the problem to

$$u'' - \phi^2 u + u(1) = \theta u. \quad (\text{A.1.1})$$

We take $u(1)$ as a constant c and end up with

$$u'' - \phi^2 u + c = \theta(c)u. \quad (\text{A.1.2})$$

We use the shooting method to look for polynomial solutions of u giving us the $\theta(c)$ as described before. In Fig. A.1 we provide a series of steps that lead us iteratively to our θ guesses for a given c .

We start with $c_1 = 0$. As we know the first eigenvalue to be -1 we start with $\theta_+ = 1$ and $\theta_- = -3$. Undergoing our bisection method we end up with $\theta(0) = -1$ as expected. The solutions close to θ will give us a good estimate on $u(1)|_{c=0}$. We take $u(1)|_{c=0}$ as the estimate for our next c and redo our analysis. We have now two data points and can do a linear interpolation and look for a zero in $(u(1)|_c) - c$. We use this value of c . In Tab. A.1 we give consecutive values of c , $(u(1)|_c) - c$ and $\theta(c)$. We see a quick convergence in the numbers.

A.2. Superspace formulation

In order to obtain our flow equations we are using a superspace formulation with the superfield Φ . We will sketch how to derive the flow equations for the NNLO truncation. At the end we will also give the flow equations of the Wess-Zumino model and the emergent supersymmetry case.

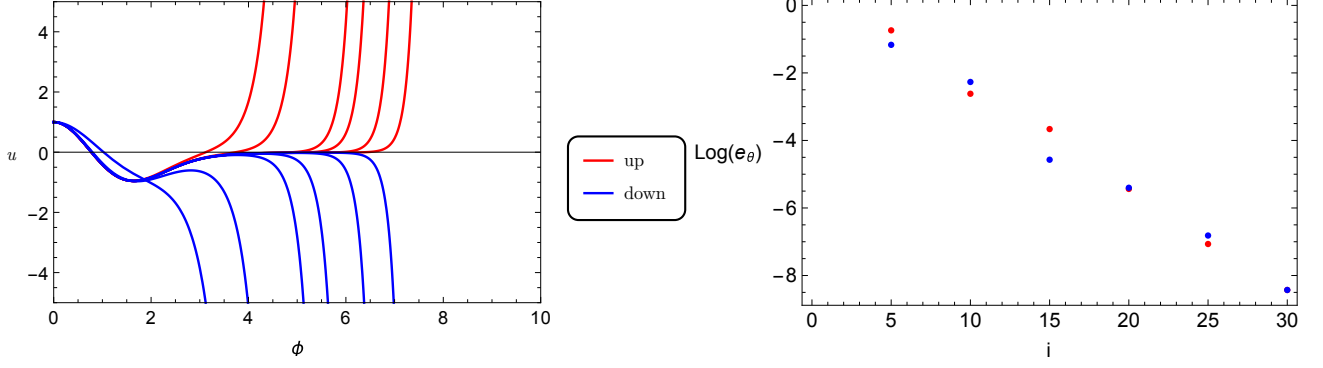


Figure A.1.: On the left we give the numerical solutions for different input θ s. The blue solutions are the ones that go to $-\infty$ and underestimate θ . The red ones on the other hand go to ∞ and overestimate θ . We give the solutions for the iterations steps $i = 5, 10, 15, 20, 25, 30$. As we can see both solutions agree to high precision on an increasing interval. In the region in which they almost agree we have a good approximation of the correct fluctuation. On the right we give the logarithm of the input θ and the estimate for θ after 30 iterations for both the up and the down case, i.e. $\text{Log}(e_\theta) = \log_{10}(\theta_\pm(i) - \theta_{\text{end}})$. In this example we chose a bisection method and therefore the increase in precision is exponential. In fact every step provides us with an increase by the factor two. The computation shown is for the best guess of c for the second even eigenvalue, see Tab. A.1.

As described it is useful to write down the effective average action in terms of superfields so that a consistent derivative expansion can be formulated. In the simple case of a model depending on only one superfield the flow equation can easily be formulated as

$$\partial_t \Gamma_k = \text{STr} \left((\Gamma_k^{(2)} - R_k)^{-1} * \partial_t R_k \right), \Gamma_k^{(2)}(p', p'', \theta', \theta'') = \frac{\delta}{\delta \Phi(p'', \theta'')} \frac{\delta}{\delta \Phi(p', \theta')} \Gamma_k, \quad (\text{A.2.1})$$

$$\text{with } \frac{\delta \Phi(p, \theta)}{\delta \Phi(p', \theta')} = \delta(\theta - \theta') \delta(p - p'), \quad (\text{A.2.2})$$

$$\text{and } (A * B)(p, p', \theta, \theta') = \int d\theta'' d\bar{\theta}'' dp'' A(p, p'', \theta, \theta'') B(p'', p', \theta'', \theta'). \quad (\text{A.2.3})$$

$$\text{STr} A(p, p', \theta, \theta') = \int d\theta d\bar{\theta} d\theta' d\bar{\theta}' \delta(\theta - \theta') dp dp' \delta(p - p') A(p, p', \theta, \theta') \quad (\text{A.2.4})$$

We have not taken the derivatives w.r.t. the component fields but are using the Grassmannian variables θ . In the off-shell formulation we have as many bosonic field degrees of freedom as fermionic ones. Also we have as many degrees of freedom in $(\bar{\theta}, \theta)$ as in the fermionic sector. Therefore a particular combination $(\bar{\theta}, \theta, \theta', \theta'')$ encodes the same information as is present in a matrix formulation of $\Gamma^{(2)}$ using the component fields. In fact we can translate both cases and

| θ_1 | | | θ_2 | | |
|------------|------------|-------------|------------|------------|-------------|
| c | $u(1) - c$ | $\theta(c)$ | c | $u(1) - c$ | $\theta(c)$ |
| 0 | 0.607 | -1 | 0 | -0.607 | -5 |
| 0.607 | 0.070 | -0.195 | -0.607 | 0.32 | -4.47 |
| 0.686 | -0.002 | -0.096 | -0.397 | -0.011 | -4.68 |
| 0.683 | 0.0006 | -0.099 | -0.404 | -0.0002 | -4.68 |

Table A.1.: We provide the iteration steps toward the eigenvalues of the given problem. We do so for the first and second even eigenvalue.

can use the formulation in the Grassmann variables also for non-supersymmetric theories.

By using this formulation the calculations look exactly like the ones in the bosonic case. In order to project out the flow equations it is useful to use the component fields after doing the algebra on the right hand side. For example after going to a constant field approximations we have in the QM model at NNLO

$$\Gamma_k = \int dz \left(iW - \frac{1}{2} Z\Phi K\Phi + \frac{i}{4} Y_1 K^2\Phi + \frac{i}{4} Y_2 (K\Phi)^2 \right), \quad (\text{A.2.5})$$

$$\partial_t \Gamma_k |_{\Phi=\text{const}, \psi=0} = \frac{Z}{2} F^2 + iFW' + \frac{i}{4} Y_2' F^3. \quad (\text{A.2.6})$$

We compute the polynomial expansion of the right hand side of the flow equation around $F = 0$ and identify both sides up to third order in F . As a supersymmetric theory lacks a term $F^0(\bar{\psi}\psi)^0$ this should be also absent on the right hand side. If the computation is done correctly this is the part at which the fermionic contributions should cancel the bosonic ones. As we can see it is possible to project out easily three of the four functions we are interested in by setting the fields to constant ones. For the computation of the last one we can still use the auxiliary field. As $K^2 = \partial^2$ we could try to project onto $p^2 F$ to obtain the flow of Y_1 . As only the quantity $X = Y_2 + Y_1'$ enters the flows we project onto this one. The p^2 projection is done in analogue to the bosonic case by taking the second functional derivative of both sides of the flow equation w.r.t. $\Phi(p, \theta''')$ and $\Phi(-p, \theta''')$. One has to pick the correct term in (θ''', θ''') .

Calculating the terms without any spacetime derivatives yields the following flow equations:

$$\begin{aligned}
\partial_t \Gamma_k = & \int d^d q \dot{r}_2 \left[\frac{1}{2R_2 + 3iFY_2'} 2 \left(1 - \frac{64q^2(R_2 + iFY_2')(2R_2 + 3iFY_2')}{(2R_2 + 3iFY_2')^2} \right) \right] \\
& \left[\frac{2\dot{r}_2(4q^2(2R_2 + 3iFY_2')^2 - (4R_1 + 2q^2X - 4iFZ' + 3F^2Y_2'') +}{4(4(R_1^2 + q^2R_2^2) + 4q^2R_2X + q^4X^2) + 8iF(-4R_1Z' + q^2(4R_2Y_2' + R_2X' - 2XZ') + 2R_2W''')} \right. \\
& \cdots \frac{8\dot{r}_1(4R_1 + 2q^2X - 4iFZ' + 3F^2Y_2'')}{+4F^2(-3q^2Y_2'(Y_2' + X') - 4Z'^2 + 6R_1Y_2'' + 3q^2XY_2'' + 2R_2Z'' - 6Y_2'W''')} \\
& \left. \cdots \frac{+4iF^3(-6Z'Y_2'' + 3Y_2'Z'' + R_2Y_2''') + F^4(9Y_2''^2 - 6Y_2'Y_2''')}{16(4R_1 + 2q^2Y_4 - 2iFZ' + F^2Y_2'')} \right] \\
& - \frac{16(4R_1 + 2q^2Y_4 - 2iFZ' + F^2Y_2'')}{(4R_1 + 2q^2Y_4 - 2iFZ' + F^2Y_2'')^2 + 32q^2(R_2 + iFY_2')^2}, \tag{A.2.7}
\end{aligned}$$

$$R_2 = (Z(\phi_0)r_2 + Z(\phi)), \quad R_1 = r_1 + W''(\phi), \quad X = Y_1' + Y_2 \tag{A.2.8}$$

We spare ourselves the flow of X . It is not insightful and the way to obtain it is given. As mentioned the flow equations are the same ones as in the Wess-Zumino model due to a rescaling in the effective average action.

In the case of the emergent supersymmetry calculations we obtain the flow of V as the F^0 term and the flow of $H = W'' - h$ as the $\bar{\psi}\psi$ term. This gives us at nearly LPA' level the following flow equations:

$$\partial_t W' = \int_0^\infty dq \frac{q^2 \dot{r}_2 (q^2 R^2 - W''^2) W'''}{4\pi^2 (q^2 R^2 + RV'' + W''^2)^2} \tag{A.2.9}$$

$$\partial_t V = - \int_0^\infty dq \frac{q^2 \dot{r}_2 (-H^2(2q^2 R + V'') + q^2 R(RV'' + 2W''^2))}{4\pi^2 (q^2 R^2 + H^2)(q^2 R^2 + RV'' + W''^2)} \tag{A.2.10}$$

$$\begin{aligned}
\partial_t H = & - \int_0^\infty dq \left[\frac{q^2 \dot{r}_2 ((q^2 R^2 + H^2)^2 H''(-q^2 R^2 + W''^2) + 2HH''(q^2 R^2(H^2 + R(3q^2 R + 2V''))))}{4\pi^2 (q^2 R^2 + H^2)^2 (R(q^2 R + V'') + W''^2)^2} \right. \\
& \left. \times \frac{(q^2 R^2 - H^2) W''^2}{1} \right] \tag{A.2.11}
\end{aligned}$$

$$R = Z(1 + r_2), \quad H = W'' - h. \tag{A.2.12}$$

We have not considered different wave function renormalizations at this stage. As we know that the fixed point is supersymmetric these will only show up in the analysis of the spectrum and not in the calculation of the fixed point.

Bibliography

- [1] B. Sakita. Supermultiplets of elementary particles. *Phys. Rev.*, 136: B1756–B1760, Dec 1964. doi: 10.1103/PhysRev.136.B1756. URL <http://link.aps.org/doi/10.1103/PhysRev.136.B1756>.
- [2] Steven Weinberg. Comments on relativistic supermultiplet theories. *Phys. Rev.*, 139:B597–B601, Aug 1965. doi: 10.1103/PhysRev.139.B597. URL <http://link.aps.org/doi/10.1103/PhysRev.139.B597>.
- [3] Sidney Coleman and Jeffrey Mandula. All possible symmetries of the s matrix. *Phys. Rev.*, 159:1251–1256, Jul 1967. doi: 10.1103/PhysRev.159.1251. URL <http://link.aps.org/doi/10.1103/PhysRev.159.1251>.
- [4] Rudolf Haag, Jan T. Lopuszanski, and Martin Sohnius. All possible generators of supersymmetries of the s -matrix. *Nuclear Physics B*, 88(2):257 – 274, 1975. ISSN 0550-3213. doi: [http://dx.doi.org/10.1016/0550-3213\(75\)90279-5](http://dx.doi.org/10.1016/0550-3213(75)90279-5). URL <http://www.sciencedirect.com/science/article/pii/0550321375902795>.
- [5] J. Wess and B. Zumino. Supergauge Transformations in Four-Dimensions. *Nucl. Phys.*, B70:39–50, 1974. doi: 10.1016/0550-3213(74)90355-1.
- [6] J. Wess and B. Zumino. A lagrangian model invariant under supergauge transformations. *Physics Letters B*, 49(1):52 – 54, 1974. ISSN 0370-2693. doi: [http://dx.doi.org/10.1016/0370-2693\(74\)90578-4](http://dx.doi.org/10.1016/0370-2693(74)90578-4). URL <http://www.sciencedirect.com/science/article/pii/0370269374905784>.
- [7] G. Veneziano. Construction of a crossing - symmetric, Regge behaved amplitude for linearly rising trajectories. *Nuovo Cim.*, A57:190–197, 1968. doi: 10.1007/BF02824451.

- [8] Yoichiro Nambu. Quark model and the factorization of the Veneziano amplitude. In *International Conference on Symmetries and Quark Models, Wayne State U., Detroit Detroit, Mich., USA, June 18-20, 1969*, pages 269–278, 1997.
- [9] Katrin Becker, Melanie Becker, and John H. Schwarz. *String Theory and M-Theory: A Modern Introduction*. Cambridge University Press, 2007. ISBN 0521860695.
- [10] F. Gliozzi, Joel Scherk, and David I. Olive. Supersymmetry, Supergravity Theories and the Dual Spinor Model. *Nucl. Phys.*, B122:253–290, 1977. doi: 10.1016/0550-3213(77)90206-1.
- [11] Jean-Loup Gervais and B. Sakita. Field Theory Interpretation of Supergauges in Dual Models. *Nucl. Phys.*, B34:632–639, 1971. doi: 10.1016/0550-3213(71)90351-8.
- [12] Vardan Khachatryan et al. Search for new physics in final states with two opposite-sign, same-flavor leptons, jets, and missing transverse momentum in pp collisions at $\sqrt{s} = 13$ TeV. *Submitted to: JHEP*, 2016.
- [13] Vardan Khachatryan et al. Search for supersymmetry in pp collisions at $\sqrt{s} = 13$ TeV in the single-lepton final state using the sum of masses of large-radius jets. *Submitted to: JHEP*, 2016.
- [14] Vardan Khachatryan et al. Search for supersymmetry with photons in pp collisions at $\sqrt{s} = 8$ TeV. *Phys. Rev.*, D92(7):072006, 2015. doi: 10.1103/PhysRevD.92.072006.
- [15] Serguei Chatrchyan et al. Search for supersymmetry in events with a lepton, a photon, and large missing transverse energy in pp collisions at $\sqrt{s} = 7$ TeV. *JHEP*, 06:093, 2011. doi: 10.1007/JHEP06(2011)093.
- [16] Georges Aad et al. Search for supersymmetry at $\sqrt{s} = 13$ TeV in final states with jets and two same-sign leptons or three leptons with the ATLAS detector. *Eur. Phys. J.*, C76(5):259, 2016. doi: 10.1140/epjc/s10052-016-4095-8.
- [17] Morad Aaboud et al. Search for heavy long-lived charged R -hadrons with the ATLAS detector in 3.2 fb^{-1} of proton–proton collision data at $\sqrt{s} = 13$ TeV. *Phys. Lett.*, B760:647–665, 2016. doi: 10.1016/j.physletb.2016.07.042.

- [18] P. J. E. Peebles. Large scale background temperature and mass fluctuations due to scale invariant primeval perturbations. *Astrophys. J.*, 263:L1–L5, 1982. doi: 10.1086/183911.
- [19] D. N. Spergel et al. First year Wilkinson Microwave Anisotropy Probe (WMAP) observations: Determination of cosmological parameters. *Astrophys. J. Suppl.*, 148:175–194, 2003. doi: 10.1086/377226.
- [20] D. N. Spergel et al. Wilkinson Microwave Anisotropy Probe (WMAP) three year results: implications for cosmology. *Astrophys. J. Suppl.*, 170:377, 2007. doi: 10.1086/513700.
- [21] E. Komatsu et al. Seven-Year Wilkinson Microwave Anisotropy Probe (WMAP) Observations: Cosmological Interpretation. *Astrophys. J. Suppl.*, 192:18, 2011. doi: 10.1088/0067-0049/192/2/18.
- [22] P. A. R. Ade et al. Planck 2013 results. XVI. Cosmological parameters. *Astron. Astrophys.*, 571:A16, 2014. doi: 10.1051/0004-6361/201321591.
- [23] P. A. R. Ade et al. Planck 2015 results. XIII. Cosmological parameters. 2015.
- [24] Riccardo Catena and Chris Kouvaris. Direct Detection of Dark Matter Bound to the Earth. 2016.
- [25] Eric Cotner and Alexander Kusenko. Astrophysical constraints on dark-matter Q-balls in the presence of baryon-violating operators. 2016.
- [26] P. A. R. Ade et al. Planck 2015 results. XIV. Dark energy and modified gravity. 2015.
- [27] P. Gondolo, G. Gelmini, and E. Roulet. Cornering the supersymmetry preferred dark matter candidate: The Neutralino. *Nucl. Phys. Proc. Suppl.*, 14B:251–258, 1990. doi: 10.1016/0920-5632(90)90386-9. [,251(1989)].
- [28] Gerard Jungman, Marc Kamionkowski, and Kim Griest. Supersymmetric dark matter. *Phys. Rept.*, 267:195–373, 1996. doi: 10.1016/0370-1573(95)00058-5.
- [29] Morad Aaboud et al. Dark matter interpretations of ATLAS searches for the electroweak production of supersymmetric particles in $\sqrt{s} = 8$ TeV proton-proton collisions. 2016.
- [30] Glennys R. Farrar and Pierre Fayet. Phenomenology of the production, decay, and detection of new hadronic states associated with supersymmetry. *Physics Letters B*, 76(5):

- 575 – 579, 1978. ISSN 0370-2693. doi: [http://dx.doi.org/10.1016/0370-2693\(78\)90858-4](http://dx.doi.org/10.1016/0370-2693(78)90858-4).
URL <http://www.sciencedirect.com/science/article/pii/0370269378908584>.
- [31] Savas Dimopoulos and Howard Georgi. Softly broken supersymmetry and $su(5)$. *Nuclear Physics B*, 193(1):150 – 162, 1981. ISSN 0550-3213. doi: [http://dx.doi.org/10.1016/0550-3213\(81\)90522-8](http://dx.doi.org/10.1016/0550-3213(81)90522-8). URL <http://www.sciencedirect.com/science/article/pii/0550321381905228>.
- [32] N. Sakai and Tsutomu Yanagida. Proton decay in a class of supersymmetric grand unified models. *Nuclear Physics B*, 197(3):533 – 542, 1982. ISSN 0550-3213. doi: [http://dx.doi.org/10.1016/0550-3213\(82\)90457-6](http://dx.doi.org/10.1016/0550-3213(82)90457-6). URL <http://www.sciencedirect.com/science/article/pii/0550321382904576>.
- [33] H. Georgi and S. L. Glashow. Unity of All Elementary Particle Forces. *Phys. Rev. Lett.*, 32:438–441, 1974. doi: 10.1103/PhysRevLett.32.438.
- [34] Stuart Raby. SUSY GUT Model Building. *Eur. Phys. J.*, C59:223–247, 2009. doi: 10.1140/epjc/s10052-008-0736-x.
- [35] T. E. Clark, Tzee-Ke Kuo, and N. Nakagawa. A $SO(10)$ SUPERSYMMETRIC GRAND UNIFIED THEORY. *Phys. Lett.*, B115:26–28, 1982. doi: 10.1016/0370-2693(82)90507-X.
- [36] Radovan Dermisek, Arash Mafi, and Stuart Raby. SUSY GUTs under siege: Proton decay. *Phys. Rev.*, D63:035001, 2001. doi: 10.1103/PhysRevD.63.035001.
- [37] H. S. Goh, R. N. Mohapatra, S. Nasri, and Siew-Phang Ng. Proton decay in a minimal SUSY $SO(10)$ model for neutrino mixings. *Phys. Lett.*, B587:105–116, 2004. doi: 10.1016/j.physletb.2004.02.063.
- [38] K. S. Babu, Jogesh C. Pati, and Zurab Tavartkiladze. Constraining Proton Lifetime in $SO(10)$ with Stabilized Doublet-Triplet Splitting. *JHEP*, 06:084, 2010. doi: 10.1007/JHEP06(2010)084.
- [39] Paul Langacker. Grand Unified Theories and Proton Decay. *Phys. Rept.*, 72:185, 1981. doi: 10.1016/0370-1573(81)90059-4.
- [40] Pran Nath and Pavel Fileviez Perez. Proton stability in grand unified theories, in strings and in branes. *Phys. Rept.*, 441:191–317, 2007. doi: 10.1016/j.physrep.2007.02.010.

- [41] K. Abe et al. Letter of Intent: The Hyper-Kamiokande Experiment — Detector Design and Physics Potential —. 2011.
- [42] Nima Arkani-Hamed and Savvas Dimopoulos. Supersymmetric unification without low energy supersymmetry and signatures for fine-tuning at the LHC. *JHEP*, 06:073, 2005. doi: 10.1088/1126-6708/2005/06/073.
- [43] M. Drees and Jong Soo Kim. Minimal natural supersymmetry after the LHC8. *Phys. Rev.*, D93(9):095005, 2016. doi: 10.1103/PhysRevD.93.095005.
- [44] Nima Arkani-Hamed, Raffaele Tito D’Agnolo, Matthew Low, and David Pinner. Unification and New Particles at the LHC. 2016.
- [45] David B. Kaplan, Emmanuel Katz, and Mithat Unsal. Supersymmetry on a spatial lattice. *JHEP*, 05:037, 2003. doi: 10.1088/1126-6708/2003/05/037.
- [46] Simon Catterall, David B. Kaplan, and Mithat Unsal. Exact lattice supersymmetry. *Phys. Rept.*, 484:71–130, 2009. doi: 10.1016/j.physrep.2009.09.001.
- [47] Georg Bergner and Simon Catterall. Supersymmetry on the lattice. *Int. J. Mod. Phys.*, A31(22):1643005, 2016. doi: 10.1142/S0217751X16430053.
- [48] Keisuke Asaka, Alessandro D’Adda, Noboru Kawamoto, and Yoshi Kondo. Exact lattice supersymmetry at the quantum level for $N = 2$ Wess-Zumino models in 1- and 2-dimensions. *Int. J. Mod. Phys.*, A31(23):1650125, 2016. doi: 10.1142/S0217751X16501256.
- [49] M. Heinrich, M. A. Miri, S. Stuetzer, S. Nolte, A. Szameit, and D. N. Christodoulides. Supersymmetric photonics: From mode converters to a new class of transformation optics. In *Proceedings, 9th International Congress on Advanced Electromagnetic Materials in Microwaves and Optics: Oxford, UK, September 7-12, 2015*, pages 103–105, 2015. doi: 10.1109/MetaMaterials.2015.7342537.
- [50] Daniel Friedan, Zong-an Qiu, and Stephen H. Shenker. Superconformal Invariance in Two-Dimensions and the Tricritical Ising Model. *Phys. Lett.*, B151:37–43, 1985. doi: 10.1016/0370-2693(85)90819-6.

- [51] Z. A. Qiu. Supersymmetry, Two-dimensional Critical Phenomena and the Tricritical Ising Model. *Nucl. Phys.*, B270:205–234, 1986. doi: 10.1016/0550-3213(86)90553-5.
- [52] Sung-Sik Lee. Emergence of supersymmetry at a critical point of a lattice model. *Phys. Rev.*, B76:075103, 2007. doi: 10.1103/PhysRevB.76.075103.
- [53] S.-S. Lee. Emergence of supersymmetry at a critical point of a lattice model. 76(7): 075103, August 2007. doi: 10.1103/PhysRevB.76.075103.
- [54] Hidenori Sonoda. Phase structure of a three-dimensional Yukawa model. *Prog. Theor. Phys.*, 126:57–80, 2011. doi: 10.1143/PTP.126.57.
- [55] Tarun Grover, D. N. Sheng, and Ashvin Vishwanath. Emergent Space-Time Supersymmetry at the Boundary of a Topological Phase. *Science*, 344(6181):280–283, 2014. doi: 10.1126/science.1248253.
- [56] Gian Paolo Vacca and Luca Zambelli. Multimeson Yukawa interactions at criticality. *Phys. Rev.*, D91(12):125003, 2015. doi: 10.1103/PhysRevD.91.125003.
- [57] Christof Wetterich. Exact evolution equation for the effective potential. *Phys. Lett.*, B301:90–94, 1993. doi: 10.1016/0370-2693(93)90726-X.
- [58] Tim R. Morris. The Exact renormalization group and approximate solutions. *Int. J. Mod. Phys.*, A9:2411–2450, 1994. doi: 10.1142/S0217751X94000972.
- [59] F. J. Dyson. The s matrix in quantum electrodynamics. *Phys. Rev.*, 75:1736–1755, Jun 1949. doi: 10.1103/PhysRev.75.1736. URL <http://link.aps.org/doi/10.1103/PhysRev.75.1736>.
- [60] Julian Schwinger. On the greenâs functions of quantized fields. ii. *Proceedings of the National Academy of Sciences*, 37(7):455–459, 1951. doi: 10.1073/pnas.37.7.455. URL <http://www.pnas.org/content/37/7/455.short>.
- [61] Reinhard Alkofer and Lorenz von Smekal. The infrared behaviour of {QCD} green’s functions: Confinement, dynamical symmetry breaking, and hadrons as relativistic bound states. *Physics Reports*, 353(5â6):281 – 465, 2001. ISSN 0370-1573. doi: [http://dx.doi.org/10.1016/S0370-1573\(01\)00010-2](http://dx.doi.org/10.1016/S0370-1573(01)00010-2). URL <http://www.sciencedirect.com/science/article/pii/S0370157301000102>.

- [62] Joseph Polchinski. Renormalization and effective lagrangians. *Nuclear Physics B*, 231(2): 269 – 295, 1984. ISSN 0550-3213. doi: [http://dx.doi.org/10.1016/0550-3213\(84\)90287-6](http://dx.doi.org/10.1016/0550-3213(84)90287-6). URL <http://www.sciencedirect.com/science/article/pii/0550321384902876>.
- [63] C. Bervillier. The Wilson-Polchinski exact renormalization group equation. *Phys. Lett.*, A332:93–100, 2004. doi: 10.1016/j.physleta.2004.09.037.
- [64] Jan M. Pawłowski. Aspects of the functional renormalisation group. *Annals Phys.*, 322: 2831–2915, 2007. doi: 10.1016/j.aop.2007.01.007.
- [65] Christof Wetterich. Effective quark interactions from QCD. 1995.
- [66] Jens Braun, Holger Gies, and Jan M. Pawłowski. Quark Confinement from Color Confinement. *Phys. Lett.*, B684:262–267, 2010. doi: 10.1016/j.physletb.2010.01.009.
- [67] Jan M. Pawłowski. Equation of state and phase diagram of strongly interacting matter. *Nuclear Physics A*, 931:113 – 124, 2014. ISSN 0375-9474. doi: <http://dx.doi.org/10.1016/j.nuclphysa.2014.09.074>. URL <http://www.sciencedirect.com/science/article/pii/S0375947414004564>. {QUARK} {MATTER} 2014XXIV {INTERNATIONAL} {CONFERENCE} {ON} {ULTRARELATIVISTIC} NUCLEUS-NUCLEUS {COLLISIONS}.
- [68] Jens Braun, Leonard Fister, Jan M. Pawłowski, and Fabian Rennecke. From Quarks and Gluons to Hadrons: Chiral Symmetry Breaking in Dynamical QCD. *Phys. Rev.*, D94(3): 034016, 2016. doi: 10.1103/PhysRevD.94.034016.
- [69] Wei-jie Fu, Jan M. Pawłowski, Fabian Rennecke, and Bernd-Jochen Schaefer. Baryon number fluctuations at finite temperature and density. 2016.
- [70] Takeru Yokota, Teiji Kunihiro, and Kenji Morita. Functional renormalization group analysis of the soft mode at the QCD critical point. 2016. doi: 10.1093/ptep/ptw062.
- [71] M. Reuter. Nonperturbative evolution equation for quantum gravity. *Phys. Rev.*, D57: 971–985, 1998. doi: 10.1103/PhysRevD.57.971.
- [72] Djamel Dou and Roberto Percacci. The running gravitational couplings. *Class. Quant. Grav.*, 15:3449–3468, 1998. doi: 10.1088/0264-9381/15/11/011.

- [73] O. Lauscher and M. Reuter. Flow equation of quantum Einstein gravity in a higher derivative truncation. *Phys. Rev.*, D66:025026, 2002. doi: 10.1103/PhysRevD.66.025026.
- [74] Max Niedermaier and Martin Reuter. The Asymptotic Safety Scenario in Quantum Gravity. *Living Rev. Rel.*, 9:5–173, 2006. doi: 10.12942/lrr-2006-5.
- [75] Alessandro Codello, Roberto Percacci, and Christoph Rahmede. Ultraviolet properties of f(R)-gravity. *Int. J. Mod. Phys.*, A23:143–150, 2008. doi: 10.1142/S0217751X08038135.
- [76] Ivan Donkin and Jan M. Pawłowski. The phase diagram of quantum gravity from diffeomorphism-invariant RG-flows. 2012.
- [77] Pietro DonÑ , Astrid Eichhorn, and Roberto Percacci. Matter matters in asymptotically safe quantum gravity. *Phys. Rev.*, D89(8):084035, 2014. doi: 10.1103/PhysRevD.89.084035.
- [78] Daniel F. Litim and Francesco Sannino. Asymptotic safety guaranteed. *JHEP*, 12:178, 2014. doi: 10.1007/JHEP12(2014)178.
- [79] Nobuyoshi Ohta, Roberto Percacci, and Gian Paolo Vacca. Renormalization Group Equation and scaling solutions for f(R) gravity in exponential parametrization. *Eur. Phys. J.*, C76(2):46, 2016. doi: 10.1140/epjc/s10052-016-3895-1.
- [80] Alessandro Codello and Rajeev Kumar Jain. Covariant Effective Field Theory of Gravity I: Formalism and Curvature expansion. 2015.
- [81] Alessandro Codello and Rajeev Kumar Jain. Covariant Effective Field Theory of Gravity II: Cosmological Implications. 2015.
- [82] Holger Gies, Clemens Gneiting, and RenÑ© Sondenheimer. Higgs Mass Bounds from Renormalization Flow for a simple Yukawa model. *Phys. Rev.*, D89(4):045012, 2014. doi: 10.1103/PhysRevD.89.045012.
- [83] Julia Borchardt, Holger Gies, and RenÑ© Sondenheimer. Global flow of the Higgs potential in a Yukawa model. *Eur. Phys. J.*, C76(8):472, 2016. doi: 10.1140/epjc/s10052-016-4300-9.

- [84] Friedrich Gehring, Holger Gies, and Lukas Janssen. Fixed-point structure of low-dimensional relativistic fermion field theories: Universality classes and emergent symmetry. *Phys. Rev.*, D92(8):085046, 2015. doi: 10.1103/PhysRevD.92.085046.
- [85] Franziska Synatschke, Georg Bergner, Holger Gies, and Andreas Wipf. Flow Equation for Supersymmetric Quantum Mechanics. *JHEP*, 03:028, 2009. doi: 10.1088/1126-6708/2009/03/028.
- [86] Sven Falkenberg and Bodo Geyer. Effective average action in N=1 superYang-Mills theory. *Phys. Rev.*, D58:085004, 1998. doi: 10.1103/PhysRevD.58.085004.
- [87] Kazunari Shima and Motomu Tsuda. On Wess-Zumino gauge. *Phys. Lett.*, B666:410–414, 2008. doi: 10.1016/j.physletb.2008.07.077.
- [88] Franziska Synatschke, Jens Braun, and Andreas Wipf. N=1 Wess Zumino Model in d=3 at zero and finite temperature. *Phys. Rev.*, D81:125001, 2010. doi: 10.1103/PhysRevD.81.125001.
- [89] N. Tetradis and C. Wetterich. Critical exponents from effective average action. *Nucl. Phys.*, B422:541–592, 1994. doi: 10.1016/0550-3213(94)90446-4.
- [90] Tim R. Morris. Derivative expansion of the exact renormalization group. *Phys. Lett.*, B329:241–248, 1994. doi: 10.1016/0370-2693(94)90767-6.
- [91] Tim R. Morris and John F. Tighe. Convergence of derivative expansions of the renormalization group. *JHEP*, 08:007, 1999. doi: 10.1088/1126-6708/1999/08/007.
- [92] Leonie Canet, Bertrand Delamotte, Dominique Mouhanna, and Julien Vidal. Nonperturbative renormalization group approach to the Ising model: A Derivative expansion at order partial**4. *Phys. Rev.*, B68:064421, 2003. doi: 10.1103/PhysRevB.68.064421.
- [93] Daniel F. Litim and Dario Zappala. Ising exponents from the functional renormalisation group. *Phys. Rev.*, D83:085009, 2011. doi: 10.1103/PhysRevD.83.085009.
- [94] C. Bervillier, B. Boisseau, and H. Giacomini. Analytical approximation schemes for solving exact renormalization group equations in the local potential approximation. *Nucl. Phys.*, B789:525–551, 2008. doi: 10.1016/j.nuclphysb.2007.07.005.

- [95] Holger Gies and Christof Wetterich. Renormalization flow of bound states. *Phys. Rev.*, D65:065001, 2002. doi: 10.1103/PhysRevD.65.065001.
- [96] Moshe Moshe and Jean Zinn-Justin. Quantum field theory in the large N limit: A Review. *Phys. Rept.*, 385:69–228, 2003. doi: 10.1016/S0370-1573(03)00263-1.
- [97] Daniel F. Litim, Marianne C. Mastaler, Franziska Synatschke-Czerwonka, and Andreas Wipf. Critical behavior of supersymmetric $O(N)$ models in the large- N limit. *Phys. Rev.*, D84:125009, 2011. doi: 10.1103/PhysRevD.84.125009.
- [98] Marianne Heilmann, Daniel F. Litim, Franziska Synatschke-Czerwonka, and Andreas Wipf. Phases of supersymmetric $O(N)$ theories. *Phys. Rev.*, D86:105006, 2012. doi: 10.1103/PhysRevD.86.105006.
- [99] Kenneth G. Wilson. THE RENORMALIZATION GROUP AND CRITICAL PHENOMENA. 1. RENORMALIZATION GROUP AND THE KADANOFF SCALING PICTURE. 1971.
- [100] Tim R. Morris. On truncations of the exact renormalization group. *Phys. Lett.*, B334: 355–362, 1994. doi: 10.1016/0370-2693(94)90700-5.
- [101] Juergen Berges, Nikolaos Tetradis, and Christof Wetterich. Nonperturbative renormalization flow in quantum field theory and statistical physics. *Phys. Rept.*, 363:223–386, 2002. doi: 10.1016/S0370-1573(01)00098-9.
- [102] M. Reuter and C. Wetterich. Effective average action for gauge theories and exact evolution equations. *Nucl. Phys.*, B417:181–214, 1994. doi: 10.1016/0550-3213(94)90543-6.
- [103] Holger Gies, Joerg Jaeckel, Jan M. Pawłowski, and Christof Wetterich. Do instantons like a colorful background? *Eur. Phys. J.*, C49:997–1010, 2007. doi: 10.1140/epjc/s10052-006-0178-2.
- [104] Daniel Becker and Martin Reuter. En route to Background Independence: Broken split-symmetry, and how to restore it with bi-metric average actions. *Annals Phys.*, 350: 225–301, 2014. doi: 10.1016/j.aop.2014.07.023.
- [105] Robert Bluhm. Explicit versus Spontaneous Diffeomorphism Breaking in Gravity. *Phys. Rev.*, D91(6):065034, 2015. doi: 10.1103/PhysRevD.91.065034.

- [106] Mahmoud Safari and Gian Paolo Vacca. Covariant and single-field effective action with the background-field formalism. 2016.
- [107] J. C. Ward. An identity in quantum electrodynamics. *Phys. Rev.*, 78:182–182, Apr 1950. doi: 10.1103/PhysRev.78.182. URL <http://link.aps.org/doi/10.1103/PhysRev.78.182>.
- [108] Y. Takahashi. On the generalized Ward identity. *Nuovo Cim.*, 6:371, 1957. doi: 10.1007/BF02832514.
- [109] Ulrich Ellwanger. Flow equations and brs invariance for yang-mills theories. *Physics Letters B*, 335(3):364 – 370, 1994. ISSN 0370-2693. doi: [http://dx.doi.org/10.1016/0370-2693\(94\)90365-4](http://dx.doi.org/10.1016/0370-2693(94)90365-4). URL <http://www.sciencedirect.com/science/article/pii/0370269394903654>.
- [110] Yuji Igarashi, Katsumi Itoh, and Jan M. Pawłowski. Functional flows in QED and the modified Ward-Takahashi identity. 2016.
- [111] Mahmoud Safari. Splitting Ward identity. *Eur. Phys. J.*, C76(4):201, 2016. doi: 10.1140/epjc/s10052-016-4036-6.
- [112] Richard D. Ball, Peter E. Haagensen, I. Latorre, Jose, and Enrique Moreno. Scheme independence and the exact renormalization group. *Phys. Lett.*, B347:80–88, 1995. doi: 10.1016/0370-2693(95)00025-G.
- [113] Daniel F. Litim. Mind the gap. *Int. J. Mod. Phys.*, A16:2081–2088, 2001. doi: 10.1142/S0217751X01004748.
- [114] Daniel F. Litim. Critical exponents from optimized renormalization group flows. *Nucl. Phys.*, B631:128–158, 2002. doi: 10.1016/S0550-3213(02)00186-4.
- [115] Leonie Canet, Bertrand Delamotte, Dominique Mouhanna, and Julien Vidal. Optimization of the derivative expansion in the nonperturbative renormalization group. *Phys. Rev.*, D67:065004, 2003. doi: 10.1103/PhysRevD.67.065004.
- [116] J. Berges, N. Tetradis, and C. Wetterich. Critical equation of state from the average action. *Phys. Rev. Lett.*, 77:873–876, 1996. doi: 10.1103/PhysRevLett.77.873.

- [117] S. J. Gates, Marcus T. Grisaru, M. Rocek, and W. Siegel. Superspace Or One Thousand and One Lessons in Supersymmetry. *Front. Phys.*, 58:1–548, 1983.
- [118] L. O’Raifeartaigh. Mass differences and lie algebras of finite order. *Phys. Rev. Lett.*, 14:575–577, Apr 1965. doi: 10.1103/PhysRevLett.14.575. URL <http://link.aps.org/doi/10.1103/PhysRevLett.14.575>.
- [119] R. Grimm, M. Sohnius, and J. Wess. Extended supersymmetry and gauge theories. *Nuclear Physics B*, 133(2):275 – 284, 1978. ISSN 0550-3213. doi: [http://dx.doi.org/10.1016/0550-3213\(78\)90303-6](http://dx.doi.org/10.1016/0550-3213(78)90303-6). URL <http://www.sciencedirect.com/science/article/pii/0550321378903036>.
- [120] Alexander Ostrowski. Über verfahren von steffensen und householder zur konvergenzverbesserung von iterationen. *Zeitschrift für angewandte Mathematik und Physik ZAMP*, 7(3):218–229, 1956. ISSN 1420-9039. doi: 10.1007/BF02044467. URL <http://dx.doi.org/10.1007/BF02044467>.
- [121] WILLIAM H. PRESS. *NUMERICAL RECIPES*. CAMBRIDGE UNIVERSITY PRESS, 2007. ISBN 0521880688.
- [122] Alessandro Codello. Scaling Solutions in Continuous Dimension. *J. Phys.*, A45:465006, 2012. doi: 10.1088/1751-8113/45/46/465006.
- [123] Roberto Percacci and Gian Paolo Vacca. Are there scaling solutions in the $O(N)$ -models for large N in $d > 4$? *Phys. Rev.*, D90:107702, 2014. doi: 10.1103/PhysRevD.90.107702.
- [124] Sidney D. Drell, Marvin Weinstein, and Shimon Yankielowicz. Strong-coupling field theory. i. variational approach to φ^4 theory. *Phys. Rev. D*, 14:487–516, Jul 1976. doi: 10.1103/PhysRevD.14.487. URL <http://link.aps.org/doi/10.1103/PhysRevD.14.487>.
- [125] A. Kirchberg, J. D. Lange, and A. Wipf. From the Dirac operator to Wess-Zumino models on spatial lattices. *Annals Phys.*, 316:357–392, 2005. doi: 10.1016/j.aop.2004.09.002.
- [126] Georg Bergner, Tobias Kaestner, Sebastian Uhlmann, and Andreas Wipf. Low-dimensional Supersymmetric Lattice Models. *Annals Phys.*, 323:946–988, 2008. doi: 10.1016/j.aop.2007.06.010.

- [127] T. R. Morris. Properties of derivative expansion approximations to the renormalization group. *Int. J. Mod. Phys.*, B12:1343–1354, 1998. doi: 10.1142/S0217979298000752.
- [128] Tobias Hellwig, Andreas Wipf, and Omar Zanusso. Scaling and superscaling solutions from the functional renormalization group. *Phys. Rev.*, D92(8):085027, 2015. doi: 10.1103/PhysRevD.92.085027.
- [129] Holger Gies, Franziska Synatschke, and Andreas Wipf. Supersymmetry breaking as a quantum phase transition. *Phys. Rev.*, D80:101701, 2009. doi: 10.1103/PhysRevD.80.101701.
- [130] Marianne Heilmann, Tobias Hellwig, Benjamin Knorr, Marcus Ansorg, and Andreas Wipf. Convergence of Derivative Expansion in Supersymmetric Functional RG Flows. *JHEP*, 02:109, 2015. doi: 10.1007/JHEP02(2015)109.
- [131] D. Zappala. Improving the renormalization group approach to the quantum mechanical double well potential. *Phys. Lett.*, A290:35–40, 2001. doi: 10.1016/S0375-9601(01)00642-9.
- [132] A. Satz, A. Codello, and F. D. Mazzitelli. Low energy Quantum Gravity from the Effective Average Action. *Phys. Rev.*, D82:084011, 2010. doi: 10.1103/PhysRevD.82.084011.
- [133] Franziska Synatschke, Holger Gies, and Andreas Wipf. Phase Diagram and Fixed-Point Structure of two dimensional $N=1$ Wess-Zumino Models. *Phys. Rev.*, D80:085007, 2009. doi: 10.1103/PhysRevD.80.085007.
- [134] Franziska Synatschke, Holger Gies, and Andreas Wipf. The Phase Diagram for Wess-Zumino Models. *AIP Conf. Proc.*, 1200:1097–1100, 2010. doi: 10.1063/1.3327547.
- [135] Luca Iliesiu, Filip Kos, David Poland, Silviu S. Pufu, David Simmons-Duffin, and Ran Yacoby. Bootstrapping 3D Fermions. *JHEP*, 03:120, 2016. doi: 10.1007/JHEP03(2016)120.
- [136] Philippe Francesco, Pierre Mathieu, and David SÃ©nÃ©chal. *Conformal Field Theory (Graduate Texts in Contemporary Physics)*. Springer, 1999. ISBN 038794785X.
- [137] Daniel F. Litim and Edouard Marchais. Critical $O(N)$ models in the complex field plane. 2016.

- [138] E. J. Hinch. *Perturbation Methods (Cambridge Texts in Applied Mathematics)*. Cambridge University Press, 1991. ISBN 9780521378970.
- [139] Tim R. Morris. The Renormalization group and two-dimensional multicritical effective scalar field theory. *Phys. Lett.*, B345:139–148, 1995. doi: 10.1016/0370-2693(94)01603-A.
- [140] Pedro R. S. Gomes. Aspects of Emergent Symmetries. *Int. J. Mod. Phys.*, A31(10): 1630009, 2016. doi: 10.1142/S0217751X1630009X.
- [141] Denis Bashkirov. Bootstrapping the $\mathcal{N} = 1$ SCFT in three dimensions. 2013.
- [142] Lin Fei, Simone Giombi, Igor R. Klebanov, and Grigory Tarnopolsky. Yukawa CFTs and Emergent Supersymmetry. 2016.
- [143] William A. Bardeen, Kiyoshi Higashijima, and Moshe Moshe. Spontaneous Breaking of Scale Invariance in a Supersymmetric Model. *Nucl. Phys.*, B250:437–449, 1985. doi: 10.1016/0550-3213(85)90490-0.
- [144] Ragnheidur Gudmundsdottir and Gunnar Rydneil. On a supersymmetric version of $(\phi^2)_3^3$ theory. *Nuclear Physics B*, 254:593 – 602, 1985. ISSN 0550-3213. doi: [http://dx.doi.org/10.1016/0550-3213\(85\)90236-6](http://dx.doi.org/10.1016/0550-3213(85)90236-6). URL <http://www.sciencedirect.com/science/article/pii/0550321385902366>.
- [145] Yoshimi Matsubara, Tsuneo Suzuki, Hisashi Yamamoto, and Ichiro Yotsuyanagi. ON A PHASE WITH SPONTANEOUSLY BROKEN SCALE INVARIANCE IN THREE-DIMENSIONAL O(N) MODELS. *Prog. Theor. Phys.*, 78:760, 1987. doi: 10.1143/PTP.78.760.
- [146] John F. Dawson, Bogdan Mihaila, Per Berglund, and Fred Cooper. Supersymmetric approximations to the 3d supersymmetric $o(n)$ model. *Phys. Rev. D*, 73:016007, Jan 2006. doi: 10.1103/PhysRevD.73.016007. URL <http://link.aps.org/doi/10.1103/PhysRevD.73.016007>.
- [147] A. C. Lehum. D=(2+1) O(N) Wess-Zumino model in a large N limit. *Phys. Rev.*, D84: 107701, 2011. doi: 10.1103/PhysRevD.84.107701.
- [148] J. Feinberg, M. Moshe, Michael Smolkin, and J. Zinn-Justin. Spontaneous breaking of scale invariance and supersymmetric models at finite temperature. *Int. J. Mod. Phys.*, A20:4475–4483, 2005. doi: 10.1142/S0217751X05028090.

- [149] T. Hellwig. Master Thesis. 2012.
- [150] Alessandro Codello and G. D’Odorico. O(N)-Universality Classes and the Mermin-Wagner Theorem. *Phys. Rev. Lett.*, 110:141601, 2013. doi: 10.1103/PhysRevLett.110.141601.
- [151] Alessandro Codello, Nicolo Defenu, and Giulio D’Odorico. Critical exponents of O(N) models in fractional dimensions. *Phys. Rev.*, D91(10):105003, 2015. doi: 10.1103/PhysRevD.91.105003.
- [152] D. J. Resnick, J. C. Garland, J. T. Boyd, S. Shoemaker, and R. S. Newrock. Kosterlitz-thouless transition in proximity-coupled superconducting arrays. *Phys. Rev. Lett.*, 47:1542–1545, Nov 1981. doi: 10.1103/PhysRevLett.47.1542. URL <http://link.aps.org/doi/10.1103/PhysRevLett.47.1542>.
- [153] Nicolo Defenu, Andrea Trombettoni, and Alessandro Codello. Fixed-point structure and effective fractional dimensionality for O(N) models with long-range interactions. *Phys. Rev.*, E92(5):052113, 2015. doi: 10.1103/PhysRevE.92.052113.
- [154] N. D. Mermin and H. Wagner. Absence of ferromagnetism or antiferromagnetism in one-dimensional or two-dimensional isotropic Heisenberg models. *Phys. Rev. Lett.*, 17:1133–1136, 1966. doi: 10.1103/PhysRevLett.17.1133.

Persönliche Angaben

Geburt **03.12.1986**, *Lutherstadt Eisleben*.
Familienstand **ledig**.

Ausbildung

Schule

1993–1997 **Grundschule**, *Grundschule am Hirtenborn, Helbra*.
1997–2006 **Gymnasium**, *Georg-Cantor-Gymnasium, Halle(Saale)*.
07/2006 **allgemeine Hochschulreife**.

Akademische Ausbildung und beruflicher Werdegang

08-09/2006 **Praktikum**, *IVH Halle*, Vermessungsgehilfe.
2006–2007 **Grundwehrdienst**, *Luftwaffe(LwAR 1 Goslar, TSLw 3 Fassberg)*.
07-09/2007 **Praktikum**, *IVH Halle*, Vermessungsgehilfe.
2007-2010 **Student**, *FSU Jena*, B.Sc. Physik.
23.09.2010 **Abschluss**, *FSU Jena*, B.Sc. Physik, 1.3.
2010–2012 **Student**, *FSU Jena*, M.Sc. Physik.
24.09.2012 **Abschluss**, *FSU Jena*, M.Sc. Physik, 1.1.
seit 2012 **Promotionsstudent**, *FSU Jena*, Physik.
seit 2012 **Wissenschaftlicher Mitarbeiter**, *FSU Jena*, Seminarleitung für Vorlesungen der theoretischen Physik.
2009-2012 **Übungsleiter**, *FSU Jena*, Analysis 1-3, insgesamt 5 Semester.
2011 **Ferienjob**, *IVH Halle*, Vermessungsgehilfe.

Sprachkenntnisse

Englisch **gute Kenntnisse** *Berufspraxis*
Spanisch **Grundkenntnisse A2** *3 Semester Hochschulkurs Spanisch A1/A2*

Wissenschaftliche Arbeit

Veröffentlichungen

- 2015 **Paper**, Marianne Heilmann, Tobias Hellwig, Benjamin Knorr, Marcus Ansorg, and Andreas Wipf. Convergence of Derivative Expansion in Supersymmetric Functional RG Flows. *JHEP*, 02:109, 2015. doi: 10.1007/JHEP02(2015)109.
- 2015 **Paper**, Tobias Hellwig, Andreas Wipf, and Omar Zanusso. Scaling and superscaling solutions from the functional renormalization group. *Phys. Rev.*, D92(8):085027, 2015. doi: 10.1103/PhysRevD.92.085027.

Vorträge, Konferenzen und Schulen

- 2012 **Vortrag**, *Monitoring Workshop GRK Graz und Jena*, Graz, Supersymmetric $O(N)$ theories.
- 2012 **Konferenz**, *SIFT Workshop*, Jena.
- 2013 **Vortrag**, *DPG Tagung FB: Mathematische Physik*, Jena, Supersymmetric $O(N)$ theories.
- 2013 **Schule**, *String-Steilkurs*, Hamburg.
- 2013 **Schule**, *Saalburg Sommerschule*, Wolfersdorf.
- 2013 **Vortrag**, *Monitoring Workshop GRK Graz und Jena*, Jena, An FRG approach to supersymmetric QM.
- 2013 **Konferenz**, *SIFT Workshop*, Jena.
- 2014 **Vortrag**, *Annual Meeting GRK*, Oppurg, An FRG approach to supersymmetric QM.
- 2014 **Schule**, *Saalburg Sommerschule*, Wolfersdorf.
- 2014 **Vortrag**, *ERG Lefkada*, Lefkada, Spontaneous breaking of SuSy in a QM system.
- 2014 **Vortrag**, *Monitoring Workshop GRK Graz und Jena*, Graz, Spontaneous breaking of SuSy in a QM system.
- 2015 **Vortrag**, *Monitoring Workshop GRK Graz und Jena*, Jena, Spikes and what they point out in the FRG.
- 2015 **Konferenz**, *SIFT Workshop*, Jena, Poster: Susy FRG a summary.
- 2016 **Konferenz**, *Annual Meeting GRK*, Oppurg.
- 2016 **Vortrag**, *DPG Tagung FB: Mathematische Physik*, Hamburg, Spikes and what they point out in the FRG.

Qualifikationen

Fortbildungen

- 2015 **Leadership Skills**, *Graduiertenakademie Jena*, Peter Wagner.
- 2016 **Erfolg im und als Team**, *Graduiertenakademie Jena*, Peter Wagner.
- 2016 **BWL Kompaktkurs**, *Graduiertenakademie Jena*, Torsten Mietko.

Sonstiges

- Hobbys **Schach**, *Spieler in der Oberliga seit 2008*, Elo Sept. 2016: 2193.
- 2006 **Schach**, *3. Platz bei der inoffiziellen europäischen Meisterschaft 206 in Pardubice in der Wertungsklasse U2200*.

Jena, 7. September 2016

Ehrenwörtliche Erklärung

Ich erkläre hiermit ehrenwörtlich, dass ich die vorliegende Arbeit selbstständig, ohne unzulässige Hilfe Dritter und ohne Benutzung anderer als der angegebenen Hilfsmittel und Literatur angefertigt habe. Die aus anderen Quellen direkt oder indirekt übernommenen Daten und Konzepte sind unter Angabe der Quelle gekennzeichnet.

Bei der Auswahl und Auswertung folgenden Materials haben mir die nachstehend aufgeführten Personen in der jeweils beschriebenen Weise unentgeltlich geholfen:

1. Andreas Wipf, Betreuung der Arbeit über die gesamte Promotion als betreuender Hochschullehrer. Siehe auch [128, 130].
2. Marianne Heilmann, Kooperationspartnerin bei Arbeiten die in die Kapitel 3 und 6 einfließen. Siehe auch [98, 130].
3. Omar Zanusso, Kooperationspartner bei Arbeiten die in die Kapitel 2, 4 und 5 einfließen. Siehe auch [128].
4. Benjamin Knorr, Kooperationspartner bei Arbeiten die in das Kapitel 3 einfließen. Siehe auch [130].

Weitere Personen waren an der inhaltlich-materiellen Erstellung der vorliegenden Arbeit nicht beteiligt. Insbesondere habe ich hierfür nicht die entgeltliche Hilfe von Vermittlungs- bzw. Beratungsdiensten (Promotionsberater oder andere Personen) in Anspruch genommen. Niemand hat von mir unmittelbar oder mittelbar geldwerte Leistungen für Arbeiten erhalten, die im Zusammenhang mit dem Inhalt der vorgelegten Dissertation stehen.

Die Arbeit wurde bisher weder im In- noch im Ausland in gleicher oder ähnlicher Form einer anderen Prüfungsbehörde vorgelegt.

Die geltende Promotionsordnung der Physikalisch-Astronomischen Fakultät ist mir bekannt.

Ich versichere ehrenwörtlich, dass ich nach bestem Wissen die reine Wahrheit gesagt und nichts verschwiegen habe.

Ort, Datum

Unterschrift des Verfassers

Danksagung

Zum Entstehen dieser Arbeit haben viele Personen ihren Beitrag geleistet. Zuvorderst möchte ich meinem Betreuer Prof. Dr. Andreas Wipf für die umfangreiche und gute Betreuung danken. Ohne seine Denkanstöße wären erhebliche Teile dieser Arbeit so nicht entstanden.

Meine Mitdoktoranden und Mitarbeitern am TPI gilt mein weiterer Dank. Besonders hervorheben möchte ich Rene Sondenheimer, der sowohl für fachlich anregende Gespräche bereitstand, und sich auch opferte Korrektur zu lesen. Fachliche Inspiration konnte ich mir des Weiteren in Gesprächen mit Julia Borchardt, Marianne Heilmann, Stefan Lippoldt, Benjamin Knorr, Luca Zambelli, Omar Zanusso und Prof. Dr. Gies holen.

Auch außerhalb Jenas konnte ich fachliche Unterstützung finden. So möchte ich mich bei Lukas Janssen, Georg Bergner, Prof. Dr. Litim sowie Prof. Dr. Pawlowski für hilfreiche Kommentare und Eingebungen bedanken.

Weiterer Dank gilt meiner Familie die mich während meiner langen Studienzeit stets unterstützt hat. Vielen Dank an meine Mutter Petra, meinen Vater Lutz und meine Schwester Karin sowie ihre Familie: Andreas, Lilia, Emil und Ole.